Jour. Sci. Hiroshima Univ., Ser. C, Vol. 10, No. 2, 267-332 (1995)

Structural evolution of multiple ductile shear zone system in the Ryoke belt, Kinki Province

By

Nobuo SAKAKIBARA

with 6 tables and 62 figures

(received, November 18, 1994)

Abstract: The ductile shear zones which developed in the Kinki Province of the low P/T Ryoke metamorphic belt, are mainly divided into the Ryoke southern marginal shear zone (RSMSZ) and Ryoke inner shear zone (RISZ). The RSMSZ is located at relatively lower structural level than the RISZ. The RSMSZ in the Kayumi district is regarded as subhorizontal ductile shear zone with westward directed sense of shear. The mylonitization related to the formation of the RSMSZ occurred at the temperature conditions of 470-350 °C (LT, low temperature to MT, medium temperature) during 83-60 Ma. The stretching direction which is represented by the mylonitic lineation is mostly oriented to EW. Strain analysis suggests that in the RSMSZ a NS directed stretching presumably occurred before the LT and MT mylonitization. On the other hand, in the RISZ (the Kasagi, Oikawa, Hakusan-Joryu and Takehara district) the mylonitization characterized by NS stretching occurred at 350-600 °C (LT to HT). A top to the southward directed sense of shear dominates for the LT and MT mylonitization in the RISZ. The HT mylonitization occurred under coaxial plane strain regime.

The temporal change of stretching direction from NS to EW in the RSMSZ appears to coincide with the change of subduction direction of the oceanic plate from NS to EW at ca. 85 Ma, suggested by the deformation temperature and mineral isotopic age in the RSMSZ. However, the kinematic data suggest that during the LT and MT mylonitization, the stretching directions were spatially partitioned into NS in the RISZ and EW in the RSMSZ. The partitioning of stretching direction is different in the different structural level in the continental crust. The spatial variation of stress field, which is indicated by dyke-orientations in the Ryoke metamorphic belt may be responsible for the spatial partitioning of stretching direction (heterogeneous flow).

CONTENTS

I. Introduction

Shear zones in the upper and lower crust of continents and island arcs play the important roles as deformation-buffer zones (e.g. Passchier 1986), accommodating the crustal thinning (extension) and thickening (shortening). In island arcs, oceanic plates subduct, high P/T metamorphism occurs and acidic magmatism with low P/T metamorphism takes place with development of large-scaled shear zones. The syntectonic intrusions of granitoids into the crustal fracture zones enhance the crustal exhumation and thickening, referred as "Surge tectonics" (Hollister and Crawford 1986). After the intrusions, these granitoids suffer ductile and/or brittle deformation at various temperatures throughout the cooling stages. The microstructures of minerals (quartz, plagioclase, K-feldspar, biotite, amphibole etc.) which compose the granitoids vary as a function of the deformation temperature, stress and strain rate (e.g. Tullis & Yund 1977, Hobbs 1985, Simpson 1985, Schmid & Casey 1986, Gapais 1989, Hirth & Tullis 1992, Fitz Gerald & Stünitz 1993). The microstructural analyses from previous reports indicate that ductile (and/or semi-brittle) shear zones (mylonite zone) formed at various temperatures within one metamorphic terrane with or without the intrusion of the granitoids (e.g. Krohe & Eisbacher 1988, Corsini *et al.* 1991). Therefore, deformational histories (P-T-d path) have been clarified, and correlation between metamorphism and tectonics have been discussed.

The accommodation patterns of crustal thinning and thickening depend on the pre-existing anisotropy (geometry of pre-existing fracture zones), spatial variation in temperature and spatial distribution of the various rock materials with various mechanical properties, and stress state and its variation in time and space. These factors correlate each other with feed-back effects and vary with time, and result in the complicated structural distribution pattern and strain and/or stress partitioning. Most of the previous studies on ductile shear zones have been focused on kinematic analyses such as the sense of shear (e.g. Platt & Behrmann 1986), non-coaxiality (kinematic vorticity number) (e.g. Ratschbacher *et al.* 1991), finite strain value and its direction (e.g. Hudleston 1983, Coward & Kim 1981), three dimensional shape of finite strain (k-value) (e.g. Siddans 1983, Law *et al.* 1984, Gapais *et al.* 1987) and its strain path (e.g. Lacassin & van den Driessche 1983). Shear strain magnitude within many of shear zones heterogeneously increases toward the center of shear zone. Such shear zones are referred to as heterogeneous shear zone (e.g. Ramsay 1980). Mechanisms of shear strain localization (presumably caused by shear instability) leads to the formation of heterogeneous shear zone, which could include geometric softening (Dillamore *et al.* 1979, Takeshita & Wenk 1988), structural softening (Sellars 1978), strain softening (Poirier 1980), strain-rate softening (Poirier 1980), changes in deformation mechanism (White 1976, Schmid et al. 1977), reaction softening (White & Knipe 1978), pore fluid effects (Fyfe *et al.* 1978, Rutter 1972), shear heating (Brun & Cobbold 1980, White *et al.* 1980) and others. Recently, interesting attempt was made by Knipe (1990), indicating pressure-temperature-qualitative strain rate (deformation mechanism)-time paths in the Moine Thrust zone. Such analysis is important for clarifying effects of temperature and pressure on the heterogeneous shear zone development.

Dynamic analyses of plastically deformed rocks (e.g. angles between c-axis and deformation lamella, reversal method for microboudinage, dynamically recrystallized grain

size, dislocation density etc.) have been made in order to clarify principle stress direction and stress magnitude (e.g. Christie and Ord 1980, Ferguson & Lloyd 1982, Dietrich & Song 1984), based on experimental and theoretical works (Turner 1953, Heard & Carter 1968, Goetze 1975, Twiss 1977, Koch & Christie 1981, Lloyd *et al.* 1982, Masuda & Kuriyama 1988). However, some authors suggest that it is necessary to carefully interpreting the results on these analyses (Ord & Christie 1984, Drury *et al.* 1985, Knipe 1989). Recently, two dimensional theoretical studies linking dynamics to kinematics are developed by Weijermars (1991, 1992), although the natural studies are rare (e.g. Castro 1986, Weijamars 1993). The theme on development of the ductile shear zones should be investigated in detail in future.

Mechanisms of granite emplacement should be clarified in order to understand the tectonic evolution of low P/T type metamorphic terranes accompanied by felsic magmatism. Since 1982, Hutton (1982) and co-workers showed the various tectonic setting for the emplacement of the granitoids and suggested that the style of the emplacement (e.g. forceful or permitted) depends on the ratio of the rate of buoyant uprise of magma to that of tectonic cavity opening (e.g. Hutton 1982, 1988a & b, Hutton *et al.* 1990). This aspect is associated with of the problem on if the granite emplacement is syntectonic or not. Some criteria for the inference of syntectonic emplacement based on foliation patterns, finite strain magnitude and the variation of three dimensional strain within (and/or around) pluton have been proposed (Brun & Pons 1981, Paterson *et al.* 1989, Schmeling *et al.* 1988, Guglielmo 1993).

The Ryoke southern marginal shear zone has been well investigated by many authors with reference to the macro to micro-structures (see Ohtomo 1993 for references). It has been regarded as subhorizontal ductile shear zones with the westward directed sense of shear (e.g. Ohtomo 1987, Yamamoto & Masuda 1987, Sakakibara *et al.* 1989, Yamamoto 1994).

Up to the present, in the inner zone of the Ryoke belt of Kinki province ductile shear zone have been not fully investigated, with exception of a brief description of the microstructures (Inoue 1980, Hayama *et al.* 1982). Recently, the present author has investigated some ductile shear zones in the inner region of Kinki Province. In this paper, the author will describe and discuss the structure of the older Ryoke granitic rocks based on both the distribution of different lithology and the orientation and its spatial variation of foliation and lineation. Furthermore, the microstructures of various minerals are investigated with petrographic microscope and electron microprobe in order to infer the kinematic information (sense of shear, deformation temperature and three dimensional shape of finite strain) in the RSMSZ of the Kayumi district and the Ryoke inner shear zone (RISZ) of the Kasagi, Oikawa, Hakusan-Joryu district, Takehara district (Fig. 1). These multiple shear zones in the Ryoke belt of the Kinki province was developed with spatial partitioning of stretching direction, although temporal changing of stretching direction was occurred in the RSMSZ. These partitioning are central for unraveling tectonics of the whole Ryoke metamorphic terrane and southwest Japan. Tectonic processes of RSMSZ and RISZ will be discussed in last chapter, in connection with tectonics of the Ryoke metamorphic terrane.

II. Research history

A. Ryoke southern marginal shear zone

First, rocks of the RSMSZ have been recognized as peculiar rocks along MTL in the Kashio district by Harada (1890), referring to as "Kashio gneiss". Afterwards, Since Sugiyama (1939) referred to these rocks as "Kashio mylonite", the RSMSZ has been discussed by many authors with reference to the tectonic implication and classification of the mylonitic rocks (protoclastic or cataclastic) (e.g. Kobayashi 1941, Hayama *et al.* 1963, Hayama & Yamada 1973, Yoshida & Masaoka 1973). These workers assume that the development of the protoclastically mylonitized rocks are related with the formation of MTL. However, these works were not based on kinematic and micro structural analyses.

The first quantitative microstructural analysis on the mylonitic rocks of the RSMSZ has been made by Echigo and Kimura (1973) in the Kayumi district. They suggest that the maximum compression axis (σ_1) during the mylonitization is nearly perpendicular to the mylonitic foliation, because asymmetric pressure shadow is not observed. On the other hand, Hara and Yokoyama (1974) suggested that based on the strain configuration and strain magnitude in the Deai district from the analyses of foliation trajectory, spatial variation in recrystallized grain size of quartz and quartz c-axis fabric, the RSMSZ is a heterogeneous strike slip ductile shear zone of sinistral sense, characterized by the high angle bulk shear plane. Afterwards, Hara and co-workers have investigated this zone in other districts, and concluded that the shear zone formed, being associated with the formation of Fossa Magna syntax under a non-uniform compression from the Pacific Ocean side (Hara *et al.* 1977, 1980a). At that time, Hayama, Yamada and co-workers (Ryoke Research Group) also investigated the geological structure and the time relationship between the mylonitization and the plutonism in Chubu, Kinki and Kyushu Province (Hayama & Yamada 1980, Hayama *et al.* 1982a & b). They recognized two phases of the mylonitization, which are the Kashio and Ryuhozan phase. Then, Takagi (1984) described the detailed deformation microstructures of various minerals in the Takato-Ichinose district, Nagano Prefecture. After that, Takagi and co-workers investigated the macro to microstructures in the Kayumi district (Takagi 1985), Kishiwada district (Takagi *et al.* 1988) and Hiki Hills (Takagi & Nagahama, 1987), and suggested that sinistral strike slip shearing with subordinate component of vertical slip took place under metamorphic condition of epidote-amphibolite facies during the mylonitization, followed by the activation of present MTL.

In 1987, important facts on the formation of RSMSZ which could overthrow the previous results were reported by Ohtomo (1987) in the Sakuma district, and by Yamamoto and Masuda (1987) in the Misakubo district, Chubu province. They suggested that the bulk shear plane of RSMSZ is initially subhorizontal and the asymmetric microstructures show top to the southward (westward to the this kinematic configuration is confirmed by Hayasaka *et al.*

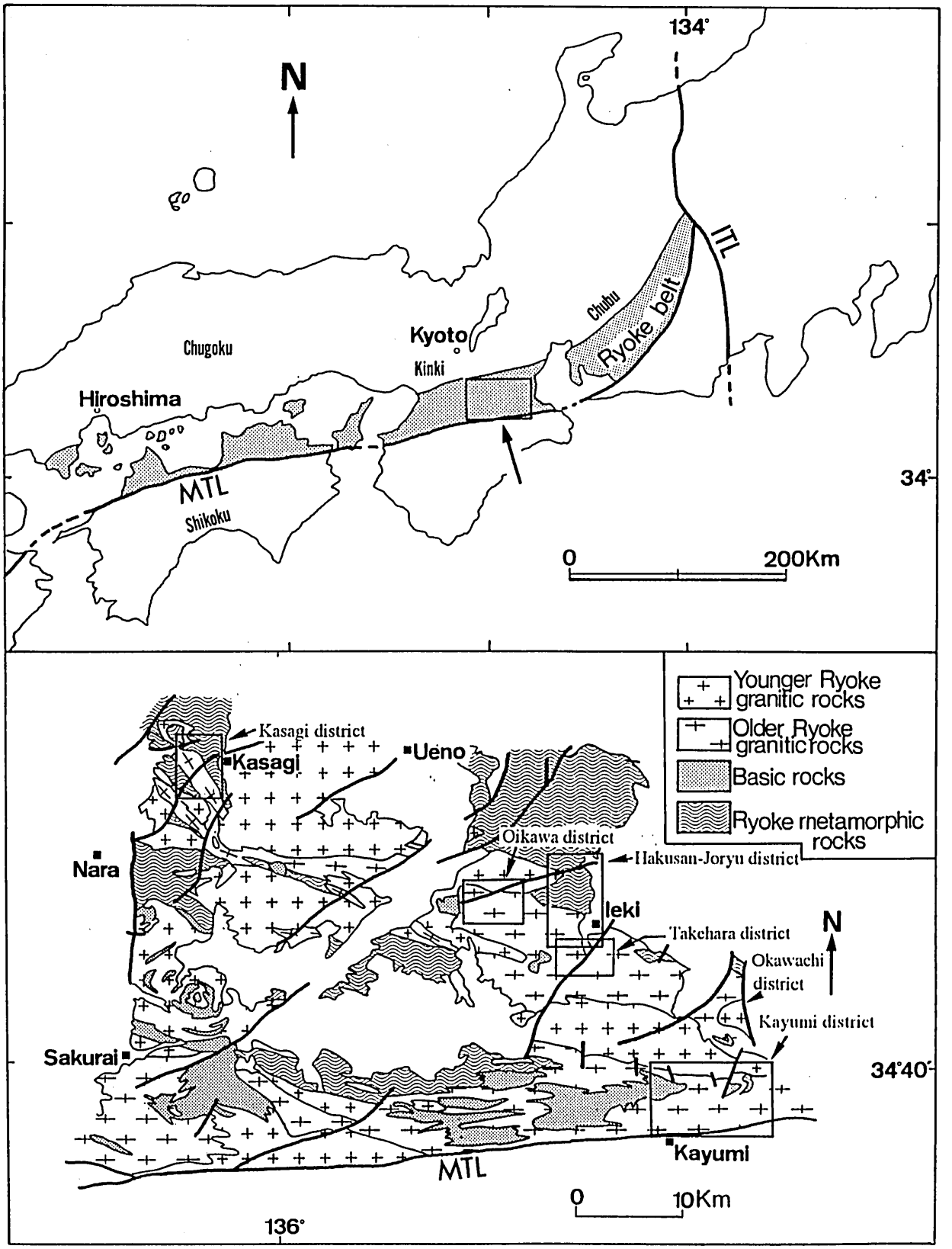

Fig. 1. Index map of the Ryoke belt in the Kinki district.

(1989) in the Asaji district of Oita Prefecture, Okamoto *et al.* (1989) and Sakakibara (unpublished data) in the Ryuhozan-Kosa district of Kumamoto prefecture, west of the Chubu province) directed sense of shear. This conclusion has been insinuated by Masaoka (1987). Then, Sakakibara *et al.* (1989) in the Kayumi district, Ohtomo (1988, 1989, 1990, 1991) in the Wada-Horaiji district, Yamamoto & Masuda (1990) and Yamamoto (1994) in the Misakubo district. However, the problem if the bulk shear plane in the present high angle dipping region of the of the RSMSZ was initially horizontal or not remains unsolved, for example in the Ichinose-Takato district (Takagi 1984, 1986), Kamimura district (Michibayashi & Masuda 1993), Mt. Takami district (Ohira 1982), Kishiwada district (Takagi *et al.* 1988) and Awaji Island (Takahashi 1992, Takahashi & Hattori 1992). It is possible that these zone was initially formed as lateral ramp with sinistral strike slip movement. In order to clarify this problem, the barometric distribution during mylonitization within the shear zone should be examined. If the shear zone was subhorizontal, pressure before and during mylonitization decreases toward the upper structural level in the shear zone.

B. Ryoke inner region

In the inner region of the Ryoke metamorphic terrane, until 1960's, some workers have analyzed the macro to mesoscopic structures (e.g. Nakajima 1960, Katada *et al.* 1961, Plutonism Research Group of the Hokkaido University 1964, Yoshizawa *et al.* 1966). They showed some deformation phases and division of syntectonic and post-tectonic granitic rocks. Disciples of Dr. J. Kojima of the Hiroshima University analyzed LPOs of quartz, biotite and muscovite for the Ryoke metamorphic rocks and granitic rocks in addition to macro to mesostructural analysis (Nureki 1960, Okamura 1960, Hara 1962). These LPO patterns include interesting information from the point of view of present knowledge for LPO development (e.g. Okudaira *et al.* submitted).

From 1970's to early 1980's, the macro to mesoscale geological structures (trajectory of the foliation of the Ryoke metamorphic rocks and granitic rocks) in addition to the mutual relations of the granitic rocks were investigated by Ryoke Research Group in the Chubu and Kinki province (Ryoke Research Group 1972, Yamada *et al.* 1979, Kustukake *et al.* 1979, Hayama *et al.* 1982, Ohira 1982). While, Hara and co-workers started investigating stress configuration, P-T-d path and emplacement mechanisms of the granitic rocks, in order to clarify tectonics of the Ryoke metamorphic terrane. Yokoyama (1979) and Hara & Yokoyama (1981) showed stress configuration (σ_{Hmax}) from analysis of the direction of dyke swarms in the Chugoku-Setouchi district, whose directions varied with time from EW via NS and to EW (the direction of σ_3 varied from NS via EW to NS). Seo & Hara (1980) and Seo (1985) divided the tectono-metamorphic processes into four phases and suggested that the deformation mechanism of biotite changed from intracrystalline slip during the III phase to pressure solution during the VI phase. Furthermore, Hara *et al.* (1980a) suggested that the Ryoke granitic rocks are divided into the pre-upright folding gneissose older granitic rocks, syn-upright folding older granitic rocks and post-upright folding younger granitic rocks, and that the pre-upright folding older granitic rocks deformed with maximum elongation in NNW-SSE direction (L_0 phase). Intrusion mechanism of the younger granitic rocks (Yagyu granite) also was studied by Sakurai & Hara (1979) and Hara *et al.* (1980b) based on the foliation pattern and spatial distribution of size of quartz pool and grain in the Yagyu district. They suggested that these plutons forcefully intrude and were emplaced into the wall rocks, accompanied by dynamic recrystallization of quartz.

Then, Toriumi and co-workers investigated the microstructures and strain patterns of metacherts in the Yanai and Tatsuno-Yabuhara district, and argued that the strain magnitude increases with increasing metamorphic temperature and pressure-solution dominates deformation (Toriumi & Masui 1986, Toriumi *et al.* 1986, Toriumi & Kuwahara 1988). Recently, Ohtomo (1991, 1993) analyzed the geological structures in the Hiraoka-Sakuma district and described large scale recumbent fold of the older Ryoke granitic rocks and metamorphic rocks, which is related to development of the RSMSZ. Okudaira *et al.* (1991, 1992, 1993) and Hara *et al.* (1991) investigated the tectono-metamorphic process in the Yanai district, and clarified the nappe structure based on thermal and barometric deference of the peak metamorphism between nappes and indicated that the sense of shear varied from the top to the NE-ward directed during D1 phase, to the SW-ward directed during D2 phase.

Tectonic environments during intrusion of the Ryoke granitic rocks were proposed by Kanaori (1990) and Kanaori *et al.* (1990). They concluded that the plutonic activity of the Ryoke granitic rocks occurred in triangle gaps formed by the block rotation of the crust which were induced by the transpressive sinistral strike slip movement of the two major bounding faults (MTL and Sikhote-Alin fault). Furthermore, Kanaori *et al.* (1991) described microstructures of quartz, biotite and feldspar in the Inagawa granite around Asuke town and estimated the deformation temperature.

Existence and features of shear zones in the inner region of the Ryoke metamorphic terrane have not been sufficiently recognized with the exception of the brief description by Inoue (1980 MS) and Hayama *et al.* (1982). Recently, Sakakibara & Hara (1992) and Sakakibara (1993) reported macro to microstructures of the mylonitized older Ryoke granitic rocks in the inner region of the Ryoke belt, Kinki Province. They suggested that (1) maximum elongation direction is oriented to the NW-SE, (2) development of each of different shear zones ceased at various temperature, (3) top to the SE-ward directed sense of shear significantly dominates during deformation, although the shear direction is non-uniform.

III. Structural evolution of the Ryoke southern marginal shear zone

A. Introduction

As mentioned above, the previous studies suggests that the Ryoke southern marginal shear zone (RSMSZ) was subhorizontaly developed with westward directed sense of shear as detachment zone of the crust. However, deformation environments (deformation temperature & pressure, three dimensional shape of the finite strain and strain magnitude) have not been fully investigated. In this

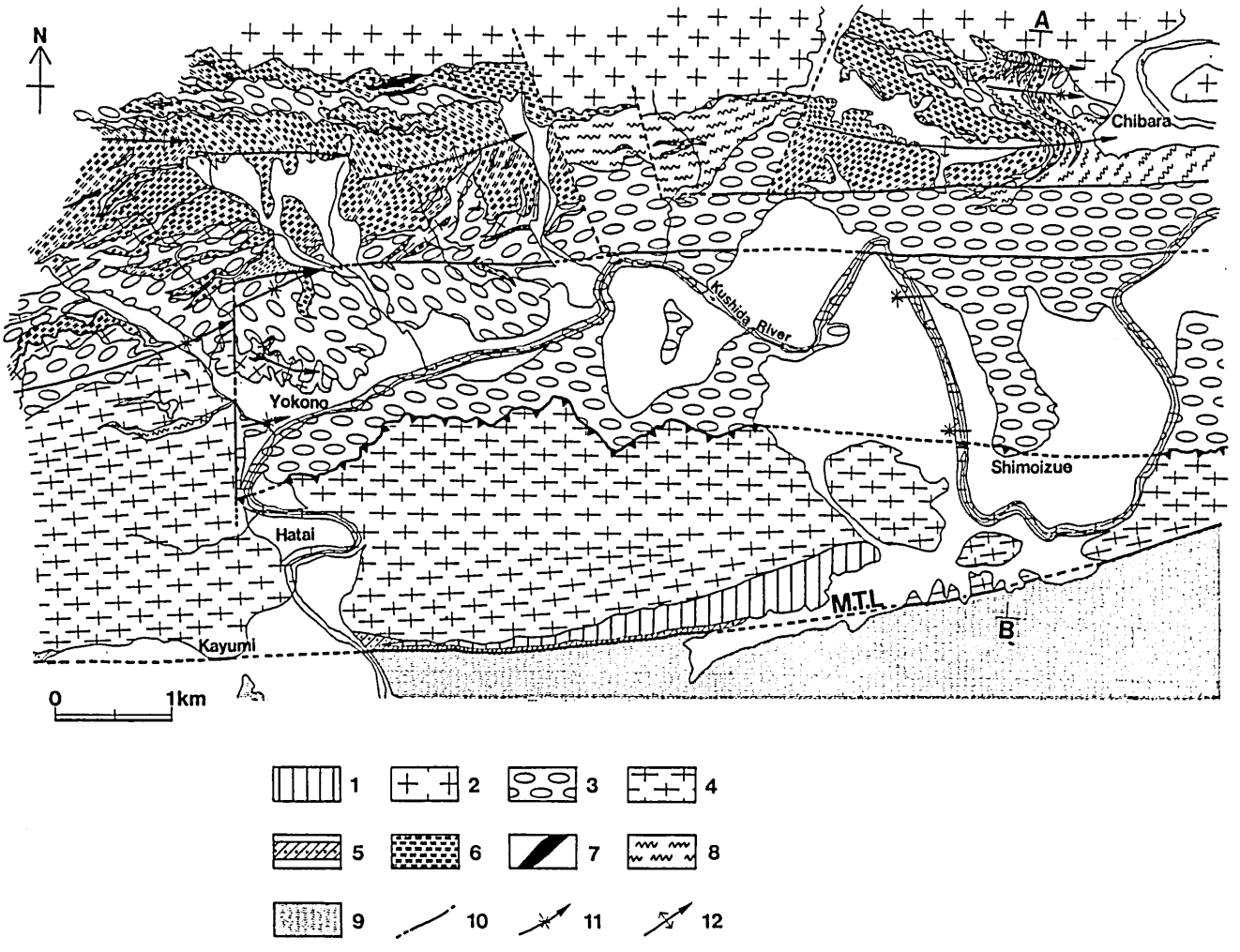

Fig. 2. Geological map of the Kayumi district. 1: Izumi Group, 2: Misugi tonalite, 3: Yokono granite, 4: Hatai tonalite, 5: Granitic mylonite, 6: Basic rocks, 7: Hornblende gabbro, 8: Ryoke metamorphic rocks, 9: Sambagawa metamorphic rocks, 10: Fault, 11: Synform, 12: Antiform.

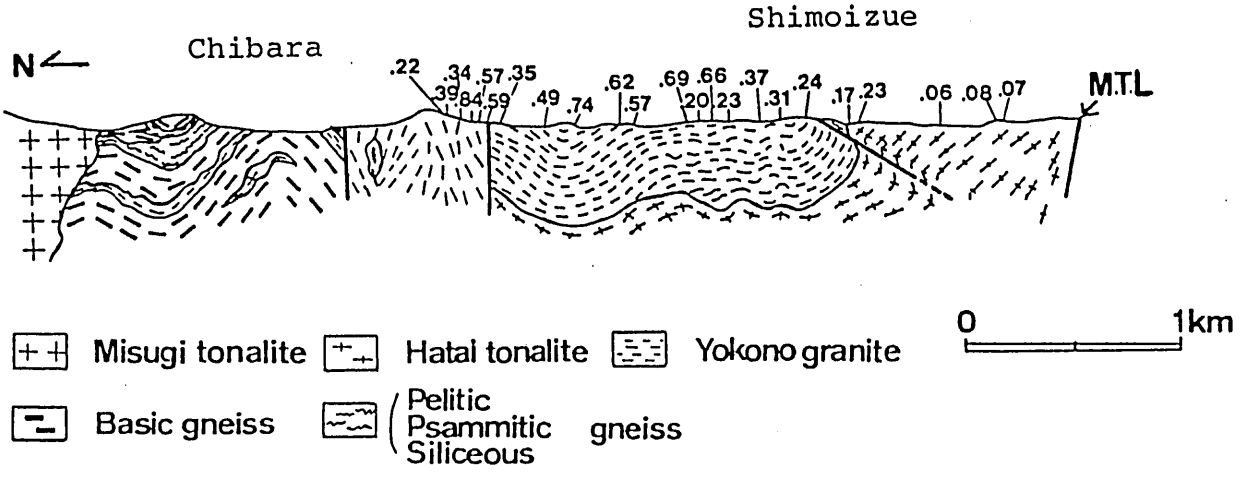

Fig. 3. Profile with k-values (numbers) in the Kayumi district. A-B is illustrated in Fig. 2.

chapter, present author will mainly report results of strain analysis, microstructures of quartz, lattice preferred orientation (LPO) of quartz, sense of shear and mineral chemistry with macro to mesoscopic structures in the Kayumi district of the RSMSZ. Kinematic model of the RSMSZ, which there is inverted thermal gradient within the shear zone and stretching direction was temporally changed, will be discussed in the later chapter, based on these data.

B. Geologic setting

1. Outline of geology

The Kayumi district is located in the eastern part of Kii Peninsula along MTL (Fig. 1). Geology of the Kayumi district of the Ryoke metamorphic belt has been previously reported by many authors (Sugiyama 1944, Yoshizawa *et al.* 1966, Araki & Kitamura 1968, Echigo & Kimura 1973, Ito 1978, Hayama & Yamada 1980, Hayama *et al.* 1982, Takagi 1985, Sakakibara *et al.* 1989, 1990, Shoji *et al.* 1992). Fig. 2 and 3 shows a geological map and profile of the district. Rocks of the Ryoke belt in the district consist of the Ryoke metamorphic rocks (pelitic, psammitic and siliceous gneiss), basic rocks (metadiabase, metagabbro younger basic dyke), granitic mylonite, Hatai tonalite, Yokono granodiorite, Misugi tonalite and Izumi group. The mutual relations of the granitic rocks were investigated by Ito (1978), Hayama (1982). They suggested that the Hatai tonalite and Yokono granodiorite which are correlated with the older Ryoke granitic rocks are intruded by the Misugi tonalite correlated with the younger Ryoke granitic rocks, and that the Hatai tonalite are intruded by the Yokono granodiorite.

Geochronological analysis by Takagi *et al.* (1988) shows that K-Ar ages of hornblende, biotite and K-feldspar from the Hatai tonalite and Yokono granodiorite range from 63 to 83 Ma with exception of K-Ar ages of the rocks near MTL. MTL as high angle dipping brittle fault strikes EW and cuts the foliation of the mylonitic rocks. Recently, Shoji *et al.* (1992) suggested that the "Izumi Group" in the district is reinterpreted as the Sennan group.

Rocks in the district are mylonitized as whole with exception of the Misugi tonalite and "Izumi Group", although the intensity of foliation development spatially varies. Near MTL, these mylonitized rocks and "Izumi Group are cataclastically deformed (Takagi 1985). The mylonitic foliation in the center of the district is modified by gentle upright folding which followed the mylonitization (Fig. 2 & 4). Recently, Shoji *et al.* (1992) reported that in the southern district near MTL, upright folds develops. The average trend of axes of the upright folds is oriented to EW and plunges at 30 °E. The lineation defined by alignment of biotite, amphibole and elongated quartz pools has EW trend (Fig. 4).

In the centre of district, the Hatai tonalite and Yokono granodiorite are bounded by the low angle dipping brittle thrust which drags the mylonitic foliation of both the granitic rocks. However, initial structural relationship between both the granitic masses during the intrusion of Yokono granodiorite into the Hatai tonalite is considered such that the Hatai tonalite is overlain by the Yokono granodiorite, shown in the western district (Fig. 5).

The Misugi tonalite shows distinct foliation and lineation defined by the alignment of amphibole and biotite flakes. The foliation throughout the entire area strikes to EW and dips at from 60 to 90° toward N. Similarly, the boundary between the Misugi tonalite and older granitic rocks strikes to EW, which is significantly bumpy (Hayama *et al.* 1982).

2. Description of rock type and microstructure

The Ryoke metamorphic rocks are mainly composed of pelitic, psammitic and siliceous gneiss (Hayama *et al.* 1982). These rocks are concordantly intruded by the older Ryoke granitic rocks and discordantly by the Misugi tonalite. The pelitic, psammitic and siliceous gneiss are exposed in the Chibara area and in the narrow zone around the Shimoizue (Echigo & Kimura 1973, Hayama *et al.* 1982). The mineral assemblage of the pelitic gneiss are:

1. quartz + muscovite + biotite + plagioclase
2. quartz + muscovite + biotite + plagioclase + garnet
3. quartz + muscovite + biotite + plagioclase + garnet + K-feldspar

Garnet, plagioclase and K-feldspar are porphyroclastic with asymmetric pressure shadow composed of quartz, biotite and muscovite. Si schistosity composed of quartz, plagioclase, muscovite and biotite are developed in the core of some garnet porphyroclasts (Fig. 6a). Most of alignment of Si in garnet porphyroclast is randomly oblique to the external mylonitic foliation. Some porphyroclastic mica grains whose long axis is parallel to S-plane of type II S-C mylonite after Lister and Snoke (1984) show the asymmetrical fish microstructure. The alignments of these fish tails composed of the recrystallized grains are mainly divided into that parallel to S-plane and C-plane of type II S-C mylonite after Lister and Snoke (1984). Some plagioclase porphyroclasts indicate deformation twining and microboudinage (extension crack), whose boudinaged space is filled by relatively large quartz grains.

Basic rocks in the district are mainly composed of metadiabase, metagabbro (Ito 1978, Hayama *et al.* 1982). The metadiabase is widely exposed at the axial area of antiform of the upright fold in the north of the district, showing alternate layering with the older Ryoke granitic rocks. The metadiabase is composed of quartz, plagioclase, amphibole, biotite and opaque mineral. In the lowermost structural level (Chibara area and southern margin area of the district), some grains of biotite and amphibole are replaced by chlorite and epidote. Mylonitic foliation of the metadiabase is parallel to that of the older granitic rocks. Biotite grains commonly show undulatory extinction and rarely kink band structure. Shear band foliation oblique to the mylonitic foliation at angle of ca. 30 ° is generally formed by the alignment of recrystallized biotite grains. Some of plagioclase grains indicate a microboudinage structure and bending of the twin plane. The formation of subgrain occur in the mantle of plagioclase porphyroclasts. Metagabbro is exposed as small masses in the core of the metadiabase in the northern part of district. It is composed of plagioclase, amphibole, biotite, ±pyroxene and opaque mineral. Development of the foliation is weaker than the other mylonitized rocks. Plagioclase and amphibole grains show slightly undulatory extinction.

Granitic mylonite is exposed in the western area of the district along the MTL. It has been referred as the Arataki granodiorite by Ito (1978). Hayama *et al.* (1982) and

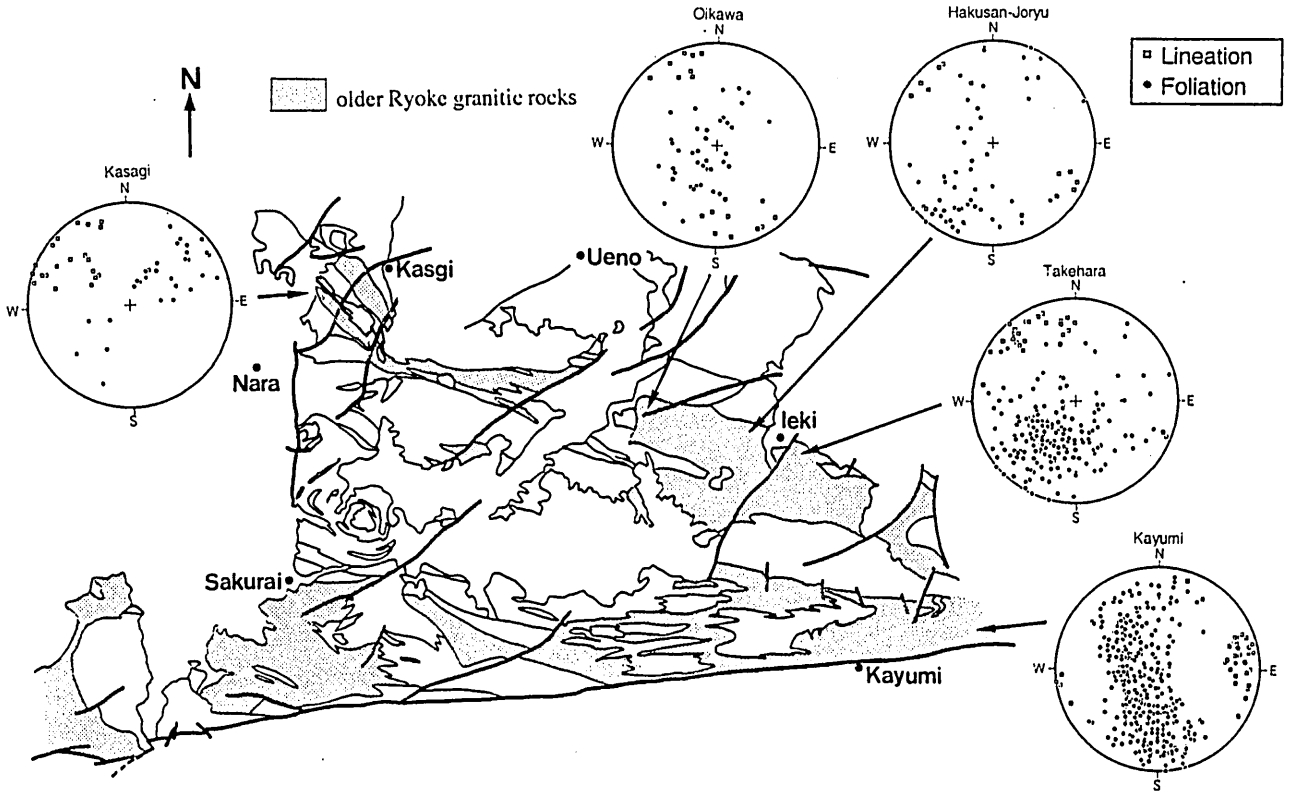

Fig. 4. Structural elements (foliation and lineation) in the investigated districts of the Kinki Province in the Ryoke belt. Schmidt net, lower hemisphere.

Takagi (1985) interpreted the mylonite as granodioritic facies of the Hatai tonalite. The granitic mylonite mainly consists of quartz, plagioclase, K-feldspar, biotite and ±amphibole with accessory titanite, zircon, allanite and magnetite. The mylonitic foliation of the granitic mylonite, which is defined by the preferred dimensional orientation of biotite, amphibole, elongate quartz pools and micro-aplite layers (fine grained band after Yamagishi 1992) which consists of the recrystallized fine grains of quartz, plagioclase and K-feldspar, strikes EW and dips at 50 to 90° toward N. The mylonitic lineation plunges horizontally trending EW. The Granitic mylonite suffered strong ductile deformation particularly in the southernmost part, and were transformed to fine-grained ultramylonite in which biotite is replaced by muscovite and chlorite. In the southernmost part, the cataclasitization (brittle deformation) characterized by microbrecciation and fracture filled with the veins composed of quartz, calcite, chlorite and prehnite oblique to the mylonitic foliation. Plagioclase porphyroclasts in the granitic mylonite show spindle shape elongated subparallel to the mylonitic foliation in XZ section with asymmetric pressure shadow composed of fine-grained quartz, muscovite plagioclase and K-feldspar grains. The porphyroclasts also show extensional fracture which is filled by equant-shaped strain-free quartz grains. Undulatory extinction with glide twinning on the plane of albite twin (010) is strongly developed in the porphyroclasts. Extensional and shear fracturing in K-feldspar porphyroclasts is common, accompanied by dynamic recrystallization (Sakurai & Hara 1990). Width of the fractures is shorter than that in the plagioclase porphyroclasts. Undulatory extinction is strong and irregular due to microfracturing. Myrmekite is ubiquitous in the porphyroclasts, most notably on the long sides of inequant grains which face on the shortening direction of the finite strain (Simpson 1985, Simpson & Wintsch 1989). Asymmetric pressure shadow of σ-type (Passchier & Simpson 1986) is well developed as well as in the plagioclase porphyroclasts. The tail of pressure shadow in the K-feldspar porphyroclasts is connected with the fine grained bands (Behrmann & Mainprice 1987, Yamagishi 1992) composed of quartz, K-feldspar and plagioclase. Muscovite porphyroclasts show asymmetrical mica fish microstructure (Simpson & Schmid 1983, Lister & Snoke 1984). The recrystallized tail of the fish is rarely developed.

The Hatai tonalite (Ito 1978, Hayama *et al.* 1982), is mainly exposed in the southern part of the Kayumi district and near axial part of the antiform in the northern part of the district, which corresponds to lower structural level. It intrudes into the Ryoke metamorphic rocks and basic rocks. The contact plane by the intrusion is parallel or subparallel to the mylonitic foliation of these rocks. Basic inclusions whose long axis is parallel to the mylonitic foliation are

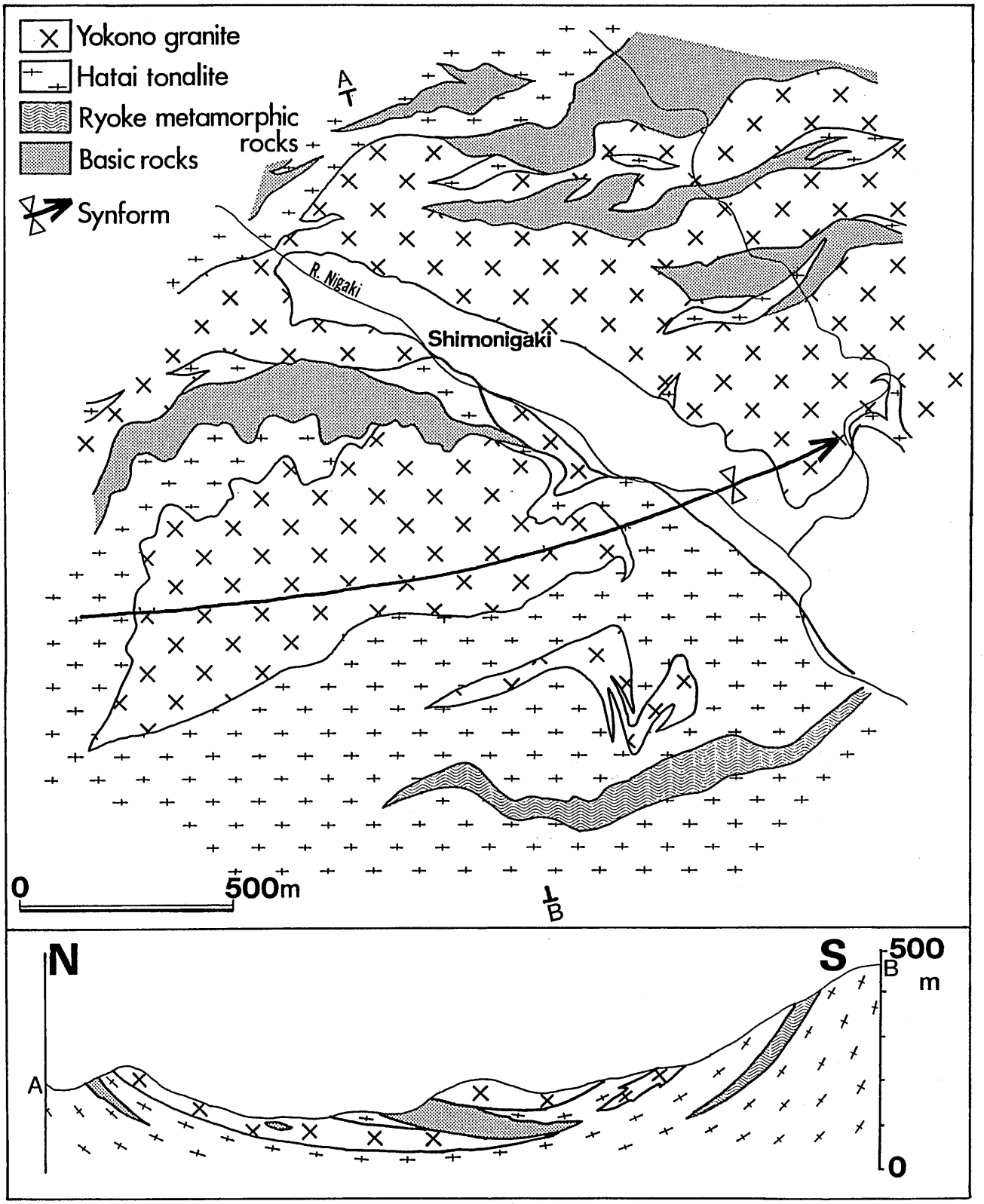

Fig. 5. Geolpgical map and profile of the Simonigaki area in the western part of the Kayumi district (left margin in Fig. 2).

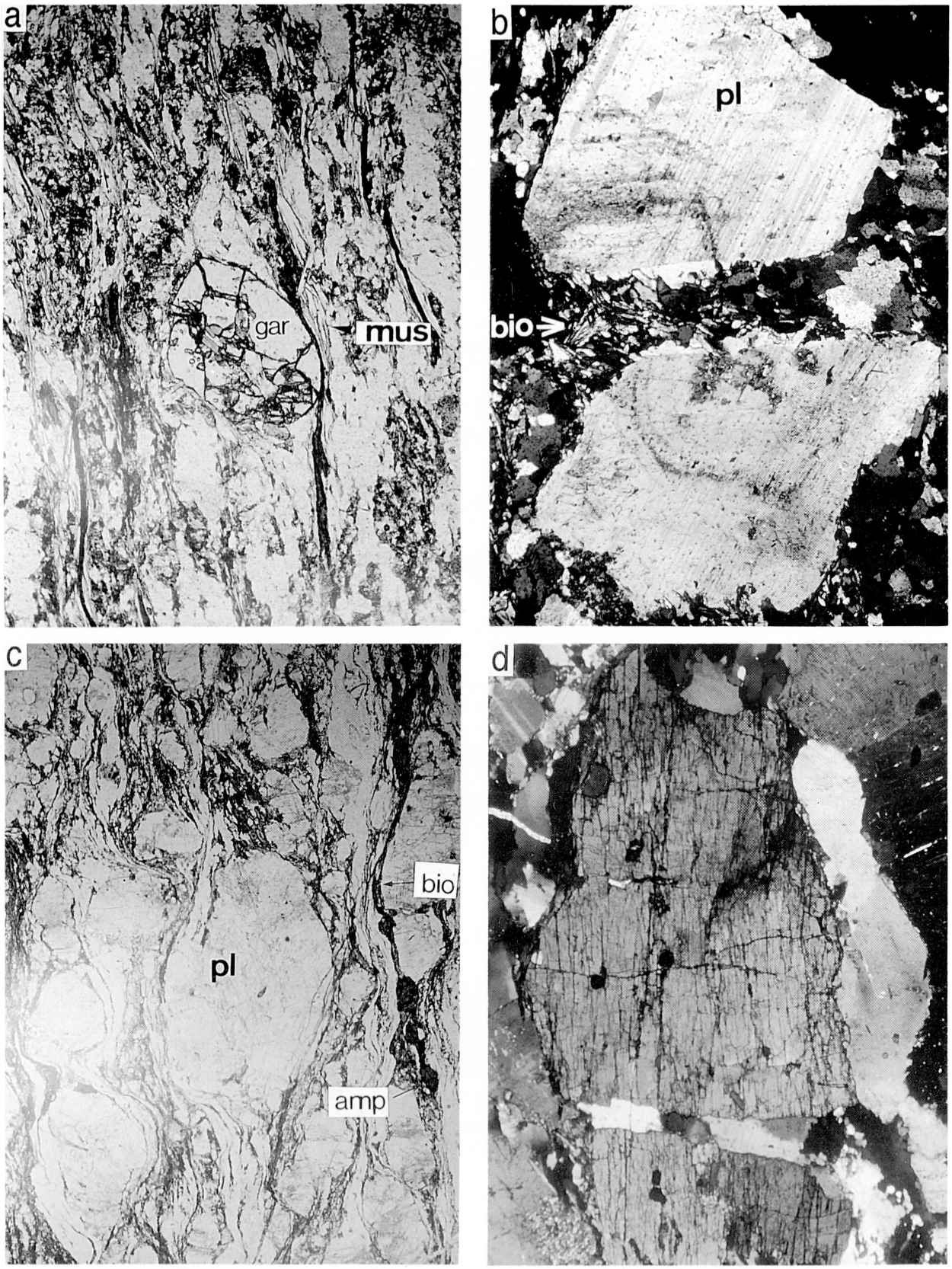

Fig. 6. a) Microphotograph of the Ryoke metamorphic rocks. Note the asymmetrical features in biotite aggregates around garnet porphyroclasts. b) Microphotograph showing extensional fracturing of plagioclase porphyroclasts in the Hatai tonalite. c) Microphotograph showing a strong preferred dimensional orientation biotite and amphibole grains in the Hatai tonalite. d) Microphotograph showing extensional fracturing of the amphibole porphyroclasts in the Hatai tonalite.

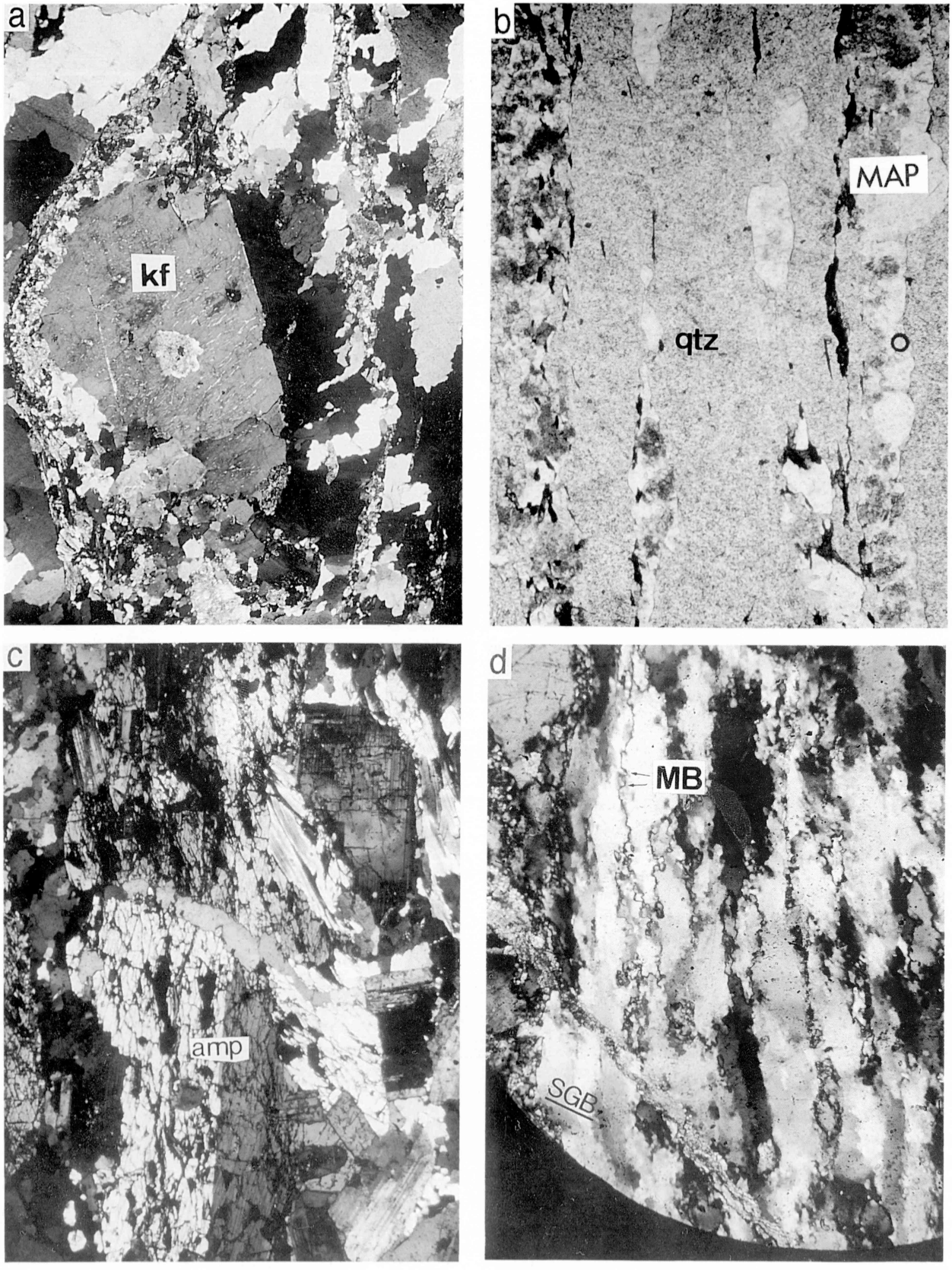

Fig. 7. a) Microphotograph showing strain-related myrmekite occurred along the grain boundary of the K-feldspar porphyroclasts. b) Microphotograph showing microaplite (MAP) layer in the Yokono granodiorite. The layer consists of small quartz, plagioclase and K-feldspar grains. c) Microphotograph of the extensional fracturing of amphibole in the Misugi tonalite. d) Microphotograph of the granitic mylonite. 'Mantle and core' texture and microbulging (MB) parallel to subgrain boundary (SGB), are remarkable.

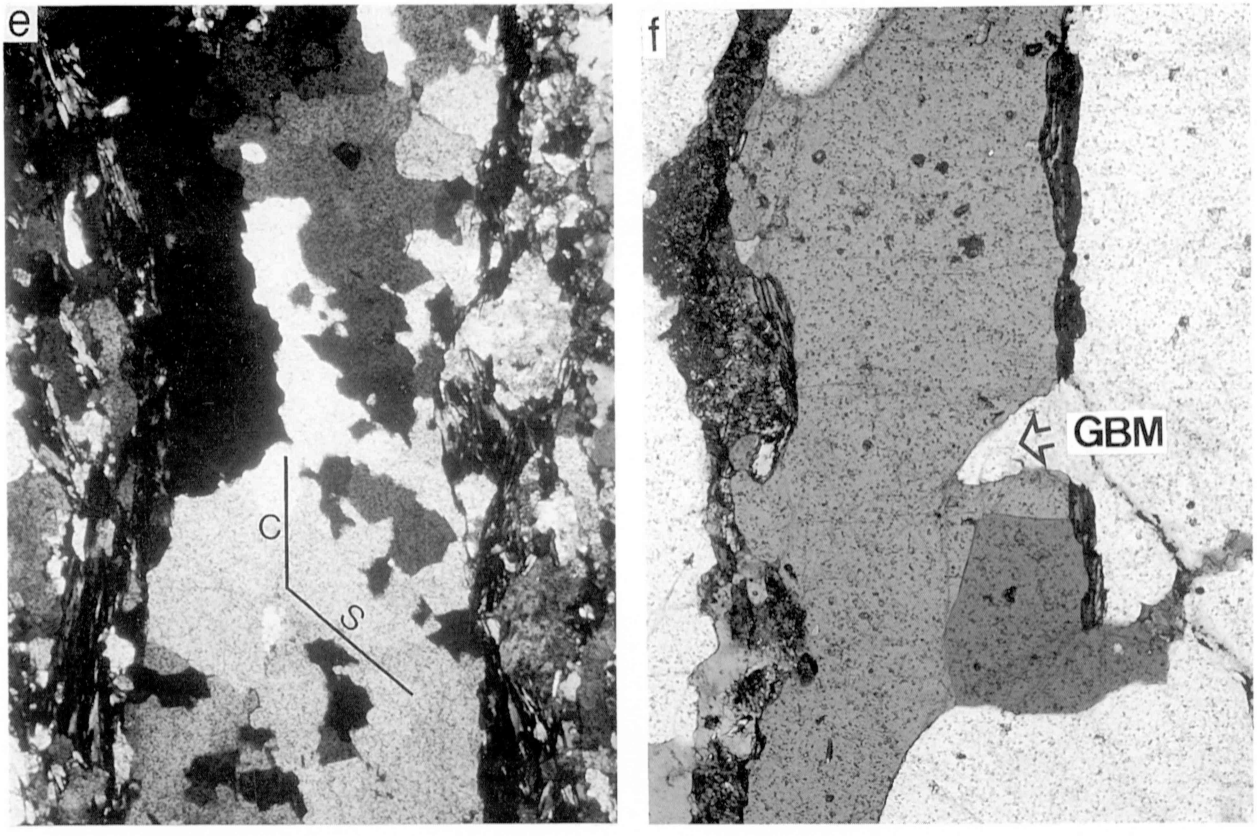

Fig. 7 e) Microphotograph showing type II S-C structure of quartz grains in the Yokono granodiorite. f) Grain boundary migration of quartz in the Yokono granodiorite.

observed in the Hatai tonalite. The tonalite mainly consists of quartz, plagioclase, biotite, amphibole and ±K-feldspar with accessory allanite, titanite, zircon and apatite. The mylonitic foliation in the southern part of the district strikes EW and dips at 30 to 70° toward N, although near the axial part of upright antiform in the northern part it gently dips (Fig. 2). Near a thrust in the central part of the district, the mylonitic foliation is locally dragged forward the thrust plane. The mylonitic lineation horizontally plunges toward the east. Plagioclase porphyroclasts are deformed dominantly in semi-brittle manner, which is indicated by extensional fracture and deformation twinning. Plane of extensional fractures is highly oblique or perpendicular to these of albite twins (Fig. 6b). Deformation twinning on (010) plane with bending of the porphyroclasts is common. In the mantle of some porphyroclasts, subgrains occur with misorientation to neighbor host grain at angle of 1 to 5°. Pressure shadows of σ-type (Passchier & Simpson 1986) are developed at the sides of plagioclase porphyroclasts (Takagi & Ito 1988). Asymmetry of the pressure shadows is weak. Recrystallization of biotite is extensive. Recrystallized biotite aggregates form the layerings parallel to the mylonitic foliation and anastomoses around the plagioclase porphyroclasts. Shape of biotite porphyroclasts is symmetrical to the mylonitic foliation. Amphibole grains are porphyroclastic and show a strong preferred dimensional orientation (Fig. 6c). Undulatory extinction with bending (deformation twinning on (101) planes) is ubiquitous. Some amphibole porphyroclasts show extensional fractures (Fig. 6d). In the fractured space biotite, chlorite and titanite (sphene) are grown (Fig. 6d). There are also fragments of amphibole separated from the host grains in the fractured space. Some allanite is deformed in brittle manner by extensional fracturing. The plane of fracturing cuts the initial compositional zoning.

The Yokono granodiorite (Ito 1978, Hayama *et al.* 1982), is exposed in the central part of the district and northern margin of the district near the contact of the Misugi tonalite, which corresponds to the upper structural level (USL). It intrudes the Hatai tonalite, basic rocks and Ryoke metamorphic rocks, and is regarded as sheet-like mass (Fig. 2 & 5). The Yokono granodiorite mainly consists of quartz, plagioclase, K-feldspar, biotite and amphibole with accessory titanite, zircon, apatite, allanite and opaque minerals. Most of plagioclase is replaced by serisite probably due to hydrothermal alteration. The mylonitic foliation strikes EW and dips at from 0 to 50 ° (Fig. 2). In the central part, the foliation forms gently upright folds. It is dragged toward the thrust in the central part of the district as well as that of the Hatai tonalite. The mylonitic (stretching) lineation horizontally plunges toward the EW. K-feldspar grains are divided into large elongate porphyroclast (up to 50 μm) and small, equant recrystallized

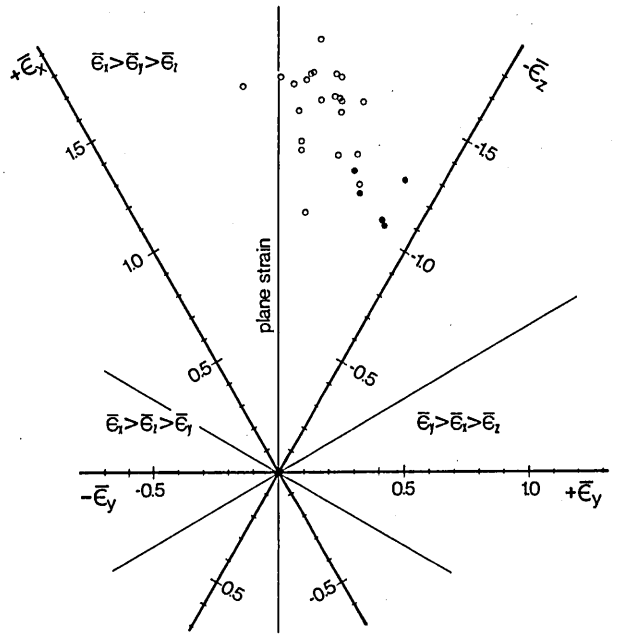

Fig. 8. Three axis diagram (Lisle 1984). open circles: data from the Yokono Granodiorite (USL), solid circles: data from the Hatai tonalite (LSL). Kinematic framework is roughly defined as x is parallel to EW, y parallel to NS and z orthogonal to the earth surface.

grain. K-feldspar porphyroclasts are aligned parallel or subparallel to the mylonitic foliation and locally control the quartz ribbon orientation. Some porphyroclasts show extensional fracturing which is filled with equant quartz and plagioclase grains. Myrmekite is common in the space created by extensional fracturing and long side of grain boundaries of K-feldspar porphyroclast that are parallel to the S (mylonitic) foliation (Fig. 7a). Plagioclase porphyroclasts show extensional fractures and deformation twins on (010) plane. Subgrains occur on the grain boundaries of the some porphyroclasts, which show misorientation of plane of albite twin to the host porphyroclasts at angles of 1 to 7 °. Recrystallized small grains consist of the microaplite layers (fine grain band) that alternate with pure quartz layers. These small grains show a equidimensional shape and strain-free feature (no or slightly undulatory extinction) (Fig. 7b). Biotite is recrystallized and its aggregate forms layer structure with or without small grains of quartz, K-feldspar, plagioclase. Asymmetry of the grain shape is obscure.

The Misugi tonalite is exposed in the northern part of the district and referred as the younger Ryoke granitic rocks (Hayama *et al.* 1982). It intrudes into the Hatai tonalite and includes the xenolith of the basic rocks and Hatai tonalite (Hayama *et al.* 1982). The Misugi tonalite mainly consists of quartz, plagioclase, biotite, amphibole and ±K-feldspar with accessory titanite, zircon, allanite and opaque mineral. It characteristically includes cummingtonite (Hayama *et al.* 1982). Development of the foliation and lineation in the southern part of the tonalite near the contact of the older rocks is stronger than in the central part of the tonalite. The foliation strikes EW to N 70° W and dips at 90 to 50° toward N. The contact plane with the older rocks is subparallel or oblique to the foliation. Development of lineation is weak, although the foliation is strongly developed. Quartz grains show no or less strain features such as equidimensional grain shape, random preferred dimensional orientation and no dynamic recrystallization. However, in the southern marginal part of the Misugi tonalite dynamic recrystallization accompanied by grain size reduction (down to 200 μm in av. size) occurs in mechanism of subgrain rotation, which result in P type (regime 3) microstructure. Grain boundaries are straight or slightly curved. Extensional fracturing of plagioclase and amphibole porphyroclasts occur in the southern marginal part of the tonalite (Fig. 7c). These porphyroclasts rarely show dynamic recrystallization near the grain boundaries. If these microstructures in the southern marginal part of the Misugi tonalite developed during the mylonitization of the older rocks or diapir (ascent-emplacement) process of the tonalite, is difficult due to few information about spatial distribution of deformation-induced microstructure in the other part of the tonalite.

D. Results

1. Strain analysis

a. Method

Strain analysis is performed in order to determine some kinematic factors which are the bulk strain magnitude and bulk cumulative strain mode (three dimensional shape of the finite strain). In order to measure the strain ellipsoid of the mylonitized rocks (the Hatai tonalite and Yokono granodiorite), the deformed shape of initially spherical quartz pool was used as strain marker. Quartz pools as individual domains is occupied only or almost only by recrystallized quartz grains and bounded mainly by the other minerals (Sakurai & Hara 1979, Hara *et al.* 1980b). The quartz pools are considered to be a microstructure caused by magmatic crystallization, initially being single quartz grains.

The ratios (x/z) of the long diameter (x) and the short diameter (z) were measured on the XZ plane of the rocks slabs, and the ratios (y/z) of the intermediate (y) and short diameter (z) were measured on the YZ plane of the slabs. Plagioclase and K-feldspar grains on the rocks slabs used for the measurement were dyed by the method of Bailey & Stevens (1960) in order to distinguish the quartz pools from the feldspar aggregates. The measurement was made for 10-70 pools on both plane in each of 25 localities along the Kushida river in the central part of the district (Fig. 3). Natural strain values defined by

$$\bar{\varepsilon} = \ln(1+\varepsilon)$$

about the each finite strain axis (ε_x, ε_y, ε_z) and k value (Flinn 1962) defined by

$$k = \frac{x/y - 1}{y/z - 1}$$

were calculated from the data of the average ratios, assuming no volume loss. The other factors with respect to strain

Table 1. Strain analysis from quartz pools

Sample No.	av.x/z (n)	av.y/z (n)	calc. x/y	*k*-value	ε_z (%)	ε_s-value	ν-value
(USL)							
88042602	12.66 (9)	5 .07 (18)	2.50	0.369	-75.0	1.82	0.279
88042603	11.66 (6)	5.11 (5)	2.28	0.312	-74.4	1.77	0.329
88042604	15.23 (15)	5.60 (16)	2.72	0.374	-77.3	1.95	0.265
88042606	8.59 (9)	4.68 (10)	1.84	0.228	-70.8	1.57	0.434
88042607	9.00 (13)	3.44 (10)	2.62	0.664	-68.2	1.56	0.124
88042608	7.10 (18)	4.31 (21)	1.65	0.196	-68.0	1.44	0.489
88042609	14.15 (14)	4.30 (14)	3.29	0.693	-74.6	1.88	0.101
88042611	6.97 (16)						
88042612	5.97 (32)	2.89 (22)	2.07	0.576	-61.3	1.27	0.186
88042613	9.62 (17)	3.64 (17)	2.64	0.619	-69.4	1.61	0.142
88042614	9.52 (22)						
88042615	12.49 (14)						
88042616	11.69 (19)	3.80 (14)	3.08	0.743	-71.8	1.74	0.085
88042618	12.51 (24)	4.55 (27)	2.75	0.493	-74.0	1.80	0.199
88042619	14.39 (23)						
88042620	21.39 (13)						
88042622	14.72 (21)	5.63 (16)	2.61	0.348	-77.1	1.93	0.287
88042701	14.94 (10)	4.68 (17)	3.19	0.595	-75.7	1.92	0.142
88042703	18.76 (31)	5.36 (38)	3.50	0.573	-78.5	2.08	0.145
88042704	13.83 (20)	3.96 (13)	3.49	0.841	-73.7	1.86	0.048
88042706	13.68 (26)						
88042707	8.65 (15)	4.15 (33)	2.08	0.343	-69.7	1.55	0.320
88042709	13.10 (21)	5.06 (37)	2.58	0.390	-75.3	1.84	0.263
88042712	12.63 (10)	6.05 (20)	2.09	0.216	-76.4	1.85	0.418
88042718	12.70 (57)	4.91 (26)	2.58	0.323	-74.8		
88042722	9.28 (23)						
88042732	14.94 (23)	4.60 (26)	3.25	0.625	-75.6	1.92	0.133
88042733	14.88 (25)	3.98 (29)	3.74	0.919	-74.3	1.91	0.023
88042737	13.54 (27)	2.93 (46)	4.56	1.810	-70.7	1.85	-0.163
(LSL)							
87042713	5.33	4.30	1.24	0.073	-64.8	1.16	0.744
87042711	5.51	4.33	1.27	0.081	-65.3	1.31	0.720
87042301	7.20	5.63	1.28	0.061	-70.9	1.52	0.750
87042310	7.69	4.36	1.76	0.23	-69.0	1.48	0.449
87042311	6.77	4.30	1.57	0.17	-67.5	1.41	0.528

Note: (n) = number of measured pools for each specimens

magnitude (ε_s) and three dimensional shape (ν) (Nadai 1963) are also calculated. These factors are defined by

$$\varepsilon_s = \frac{1}{\sqrt{3}} [(\varepsilon_x-\varepsilon_y)^2 + (\varepsilon_y-\varepsilon_z)^2 + (\varepsilon_x-\varepsilon_z)^2]^{1/2}$$

$$\nu = (2\varepsilon_y - \varepsilon_x - \varepsilon_z) / (\varepsilon_x - \varepsilon_z)$$

These kinematic factors are summarized in Table 1 with source data.

b. Result

On the three-axis diagram (Fig. 8) (Lisle 1984, partially modified by Ratschbacher 1986), the average bulk three dimensional shape and its orientation on the fixed kinematic coordinates are displayed. Most of the three dimensional shapes are of flattening types with wide range of *k* value (1.5-0.06).

Because the mylonitic foliation of the Yokono granite is gently folded with macroscopic scale, the spatial variation of *k* value shown in Fig. 3 has to be interpreted with reference to structural level, which is defined by the trajectory of the mylonitic foliation inferred from the geologic investigation. It can be said that the bulk *k* value for quartz pools in the Yokono granodiorite is nearly constant within the same structural level and its spatial variation tend to be controlled by structural level. Namely, the quartz pools have bulk *k* value of 1.0-0.5 in the upper structural level of the Yokono granodiorite and of 0.5-0.2 in the lower structural level of the granodiorite. While, they in the Hatai tonalite, which underlies the Yokono granodiorite, have bulk k value of 0.2-0.05. These values in the Hatai tonalite have good correspondence to the development of S (dimensional) fabric (Takagi 1985); development of the mylonitic lineation is weak. If the bulk *k* value from quartz pools for the Hatai tonalite is also nearly constant within the same structural level, then it could concluded that the three dimensional shape of quartz pools caused by the deformation related to the formation of the mylonitic foliation approximately gradually varies from plane strain in the upper structural level to nearly axial flattening in the lower structural level.

The bulk strain magnitude of quartz pools defined by ε_s

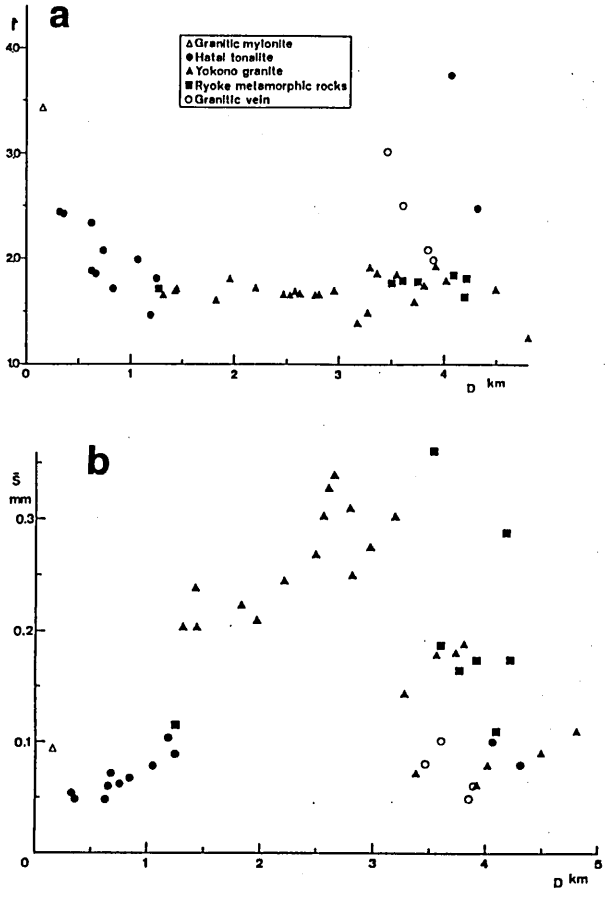

Fig. 9. a) Average aspect ratio of the dynamically recrystallized quartz grains vs distance from MTL diagram in the Kayumi district. D: distance from MTL. b) Average size of dynamically recrystallized quartz grains vs distance from MTL diagram.

value (Nadai 1963) is between 1.3 and 2.1 within the Yokono granodiorite and between 1.2 and 1.5 within the Hatai tonalite (Table 1). The strain magnitude appear to be smaller in the Hatai tonalite than in the most part of the Yokono granodiorite. The bulk strain magnitude tends to be higher for the quartz pools with higher k value.

2. Microstructures of quartz

As slightly mentioned above, the microstructures of quartz, which are represented by average grain size, average aspect ratio, feature of the grain boundary, are different between the lower and upper structural levels (LSL & USL). The LSL mainly consists of the Hatai tonalite, Granitic mylonite and basic rocks, and the USL mainly consists of the Yokono granodiorite and Ryoke metamorphic rocks. The optical observation of the microstructures have been made on the thin sections parallel to the stretching lineation and perpendicular to the mylonitic foliation (XZ sections).

Average sizes of the dynamically recrystallized quartz grains (average of √long diameter * short diameter) range between 40 and 100μm in the LSL (Fig. 9a). These values gradually decrease toward lowest level. Aspect ratios of the recrystallized grains (av. long diameter/short diameter) increase gradually from 1.5 to 3.8 toward the lowest level (Fig. 9b). The quartz grains which show higher (>2.5) average aspect ratios correspond to S type (Masuda & Fujimura 1981) and/or regime 2 microstructure (Hirth & Tullis 1992). The grains showing lower aspect ratios (<2.5) correspond to P type (Masuda & Fujimura 1981) and/or regime 3 microstructure (Hirth & Tullis 1992). The grain boundaries of S type microstructure are serrated and complicated with microbulging to the adjacent grains (Fig. 7d). Some of these grains show asymmetrical microbulging (Drury & Humphreys 1988) due to 'local' grain boundary migration (Hirth & Tullis 1992) and asymmetrical alignment of the subgrain boundaries which are high dislocation density regions and enhance grain boundary migration. Some recrystallized new small grains occur remarkably near the grain boundaries, forming a core and mantle texture (White 1976) (Fig. 7d). These features indicate that there is a shear strain gradient within the individual grains and shear strain increases heterogeneously toward the grain boundary (Lloyd *et al.* 1992).

In the USL, the average size of dynamically recrystallized quartz grains ranges from 100 to 400 μm (Fig. 9a). It tends to decrease toward lower structural level. The aspect ratios in the USL are lower than these in the LSL and constant at 1.5-1.8 (Fig. 9b). Thus, the recrystallized quartz grains in the USL correspond to P type and/or regime 3 microstructure. The grain boundaries are straight or slightly curved with microbulging to the adjacent grains. They show a preferred dimensional orientation as type II S-C structure (Lister & Snoke 1984) oblique to the mylonitic foliation at angle of 30 to 60° (Fig. 7f). This values are significantly higher than that in the LSL. Subgrain boundaries are prismatic and oblique to the mylonitic foliation at high angle (70-60°) as well as in the LSL. Some grains indicate the characteristic microstructures such as 'window' microstructure (Jessell 1986) and 'left over' grains (Urai *et al.* 1986) produced by grain boundary migration (Fig. 7e).

3. Lattice preferred orientation of quartz

a. Method

Quartz c-axis fabrics have been measured on a universal stage and a $\{11\bar{2}0\}$-, m $\{10\bar{1}0\}$- and r & z $\{10\bar{1}1\}$-poles have been measured with x-ray texture goniometer of the University of Tokyo. The each crystallographic planes were measured in combined reflection and transmission method (Decker's method), with a measuring time of about 6 hour per crystallographic plane (step angle of 5° for both a and b, and fixed time per one step angle of 10 second). For samples showing low purity of quartz grains, feldspar and layer silicate minerals have been removed by Kerrich & Starkey (1979) method, because the presence of feldspar and layer silicate minerals makes the isolation of specific quartz reflections and transmissions difficult.

b. Result

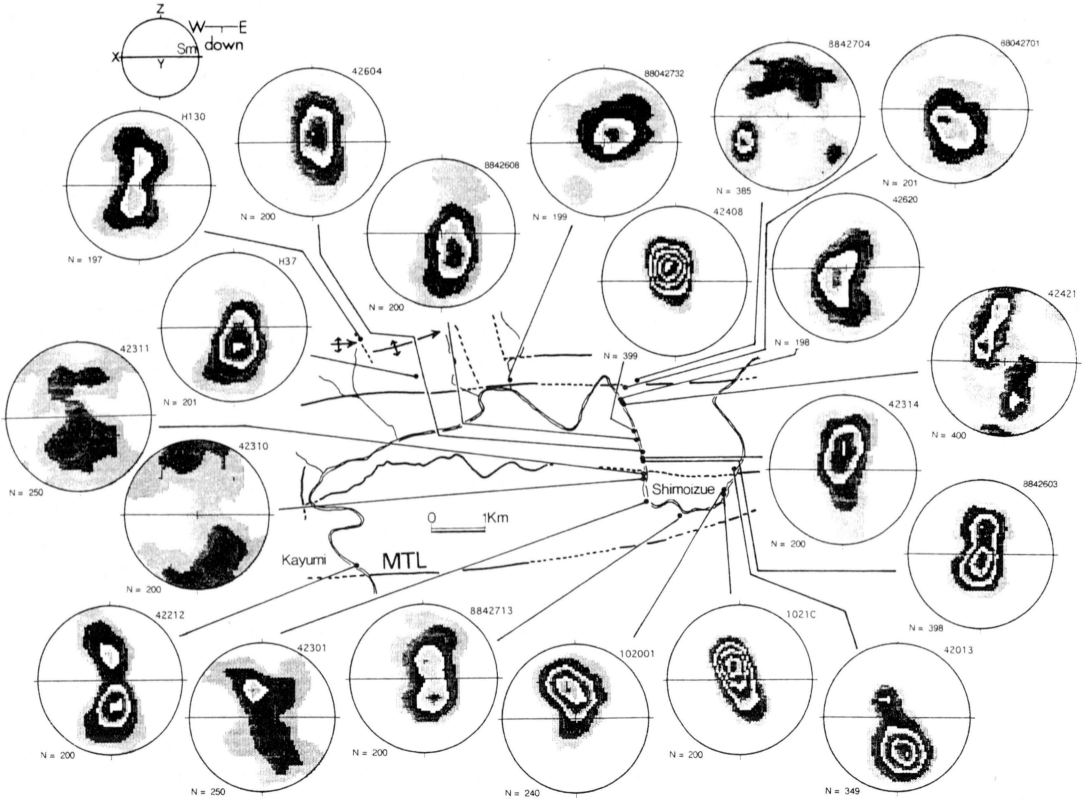

Fig. 10. Quartz c-axis fabrics in the southern part of the Kayumi district. Contour interval: 2σ (Kamb method). X, Y and Z are maximum, intermediate and minimum principle axes of the finite strain respectively.

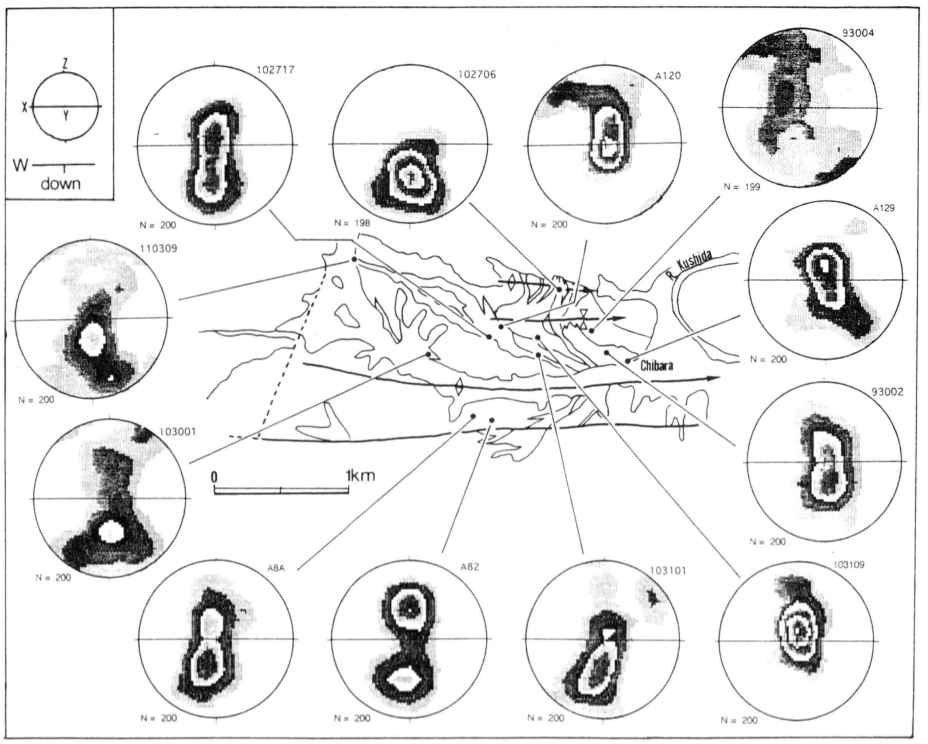

Fig. 11. Quartz c-axis fabrics in the northern part of the Kayumi district.

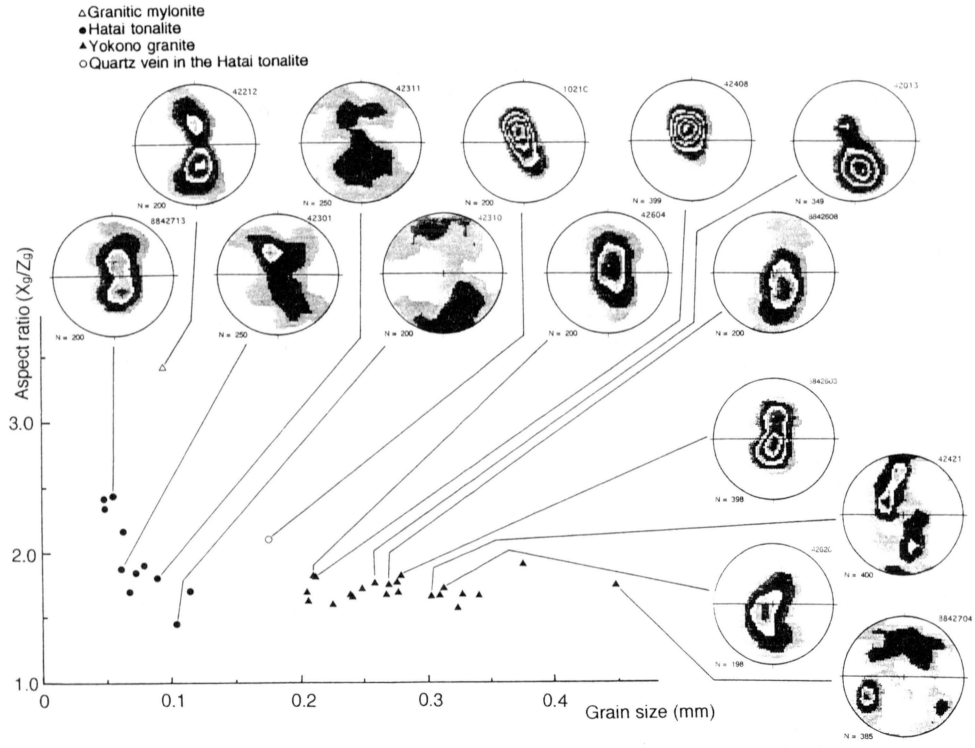

Fig. 12. Quartz c-axis fabrics on the grain size vs aspect ratio diagram from the southern part of the Kayumi district.

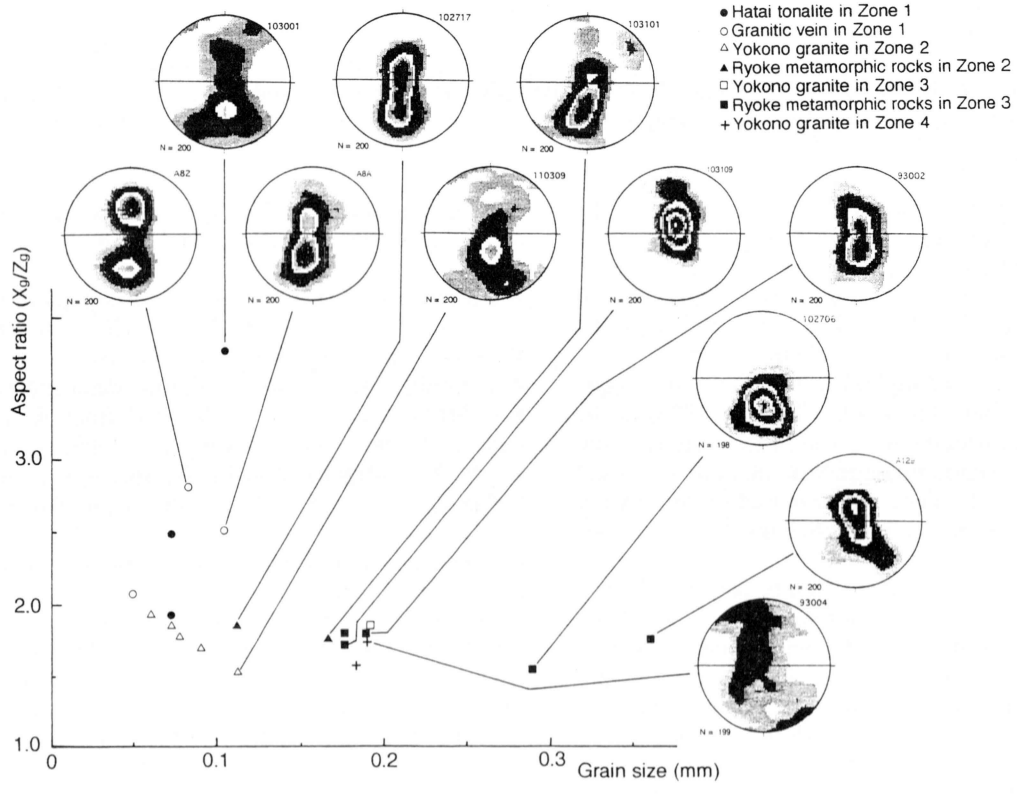

Fig. 13. Quartz c-axis fabrics on the grain size vs aspect ratio diagram from the northern part of the Kayumi district.

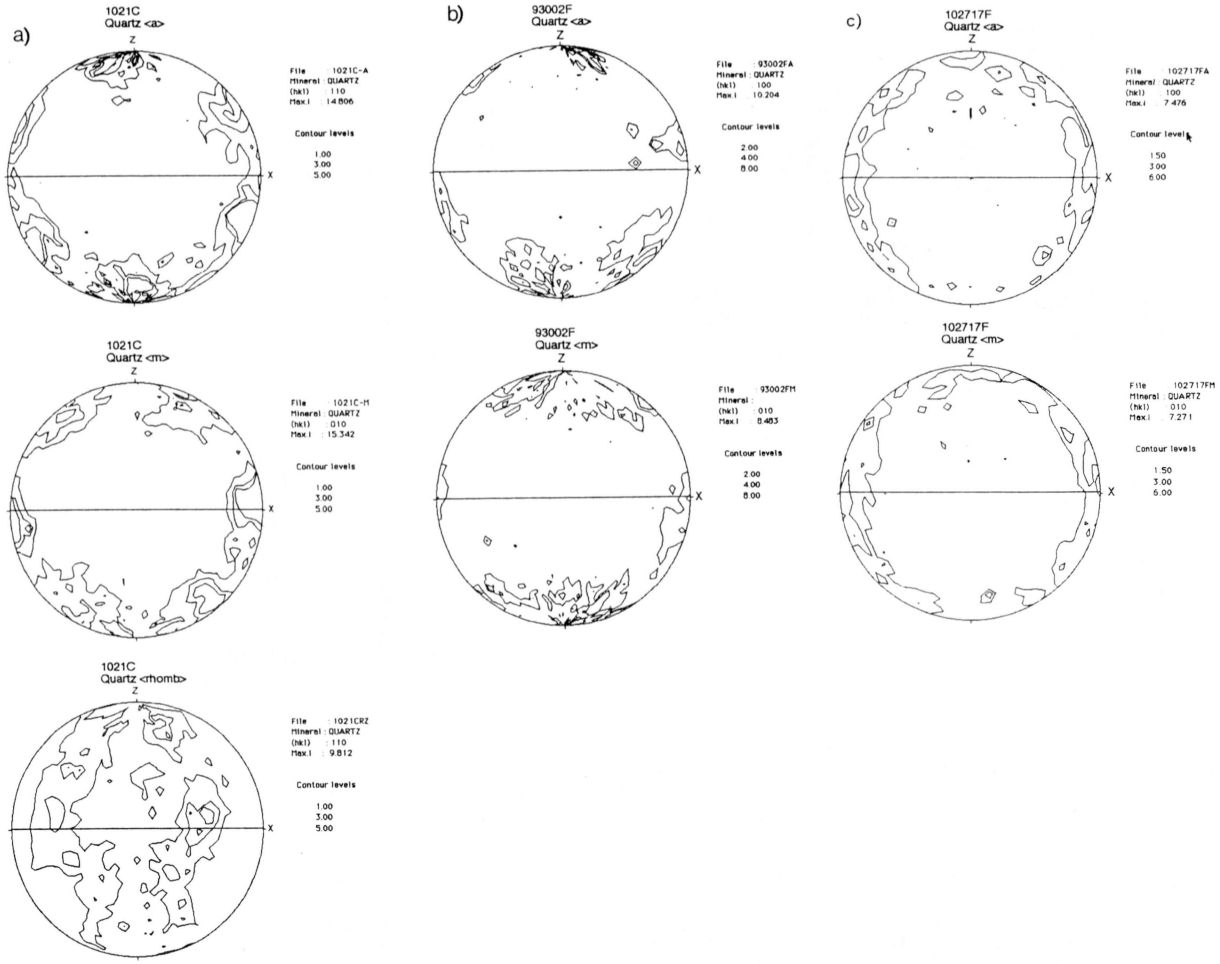

Fig. 14. Pole figures of the second order prisms $(11\bar{2}0)$, -first order prisms $(10\bar{1}0)$ and r & z $\{10\bar{1}1\}$. The contours are given in multiples of a uniform distribution. a: sample 1021C (LSL), b: sample 102717 (USL), c:93002 (USL).

Quartz c-axis fabrics in the Kayumi district of the Ryoke southern marginal shear zone are shown Fig. 10, 11, 12 & 13. In the USL, patterns of the c-axis fabrics show type-II crossed girdle and incomplete single girdle with a strong concentration close to Y (Burg & Laurent 1978) of the finite strain ellipsoid and/or with maxima on the YZ plane at angle of 30-50 ° from mylonitic foliation. Analogous patterns has been already reported by Ohtomo (1993) in the Hoji pass area. The patterns of a- and m-axis fabrics show an asymmetrical concentration near X of the finite strain and XZ girdle with the asymmetrically disposed triple maxima at interval angle of 60° respectively (Schmid & Casey 1986) (Fig. 14).

Whereas, in the LSL the c-axis fabric patterns show a type-I crossed girdle (Lister 1977) or single girdle at 30-50° from mylonitic foliation. The skeletal outlines of c-axis for specimens showing a type-I crossed girdle are asymmetrically distributed with leading edge and another legs (Simpson & Schmid 1983). Analogous patterns have been reported by Hara *et al.* (1977), (1980b) and Hayashi & Takagi (1987) in the LSL of the RSMSZ of the other district. However, a c-axis pattern from quartz vein in the Hatai tonalite is correlated with Y-point maximum. For this specimen, the a- and m-axis show the XZ girdle with triple maxima at interval angle of 60° and r & z-axis fabrics show a small circle pattern around Y (Fig. 14).

4. Chemical analysis of feldspars and amphibole

In this section, results from chemical analysis of feldspars and amphiboles are shown, using electron microprobe. Deformation conditions (temperature, pressure and differential stress) are calculated from these chemical data in the later section, using two feldspar thermometer (myrmekitic plagioclase and K-feldspar in pressure shadow) and geobarometer of total Al content in amphibole.

a. Chemical composition of myrmekitic plagioclases and K-feldspars in pressure shadows

The results of electron microprobe analysis are show in Fig. 15 and Table 2. Mole fraction of albite of myrmekitic plagioclase in the USL ranges form 0.72 to 0.82, that in the LSL widely ranges from 0.61 to 0.83 (Fig. 15). The mean mole fraction of albite of the plagioclase per sample in the USL and LSL ranges from 0.73 to 0.79 and from 0.64 to 0.80 respectively. The mole fraction of orthoclase of the K-feldspar in pressure shadow region in the USL is constant around 0.90, although in the LSL it ranges from 0.90 to 0.96. The mean mole fraction of orthoclase content

Table 2. Calculated temperature from chemical composition of myrmekitic plagioclase and K-feldspar in the pressure shadow.

Sample no.	Myrmekite			K-feldspar			calc. T (°C)	
	An	Ab	Or	An	Ab	Or	S	H
88042732 (USL)	0.203	0.785	0.012	0.002	0.124	0.874	464	473
F31 (USL)	0.255	0.735	0.010	0.002	0.096	0.902	466	453
88042701 (USL)	0.258	0.732	0.010	0.001	0.097	0.901	468	453
G124 (LSL)	0.194	0.800	0.006	0.000	0.059	0.941	388	349
H130 (LSL)	0.275	0.714	0.010	0.003	0.074	0.923	435	403
H102 (LSL)	0.354	0.637	0.010	0.001	0.071	0.928	448	425
TA9D (RISZ)	0.364	0.624	0.012	0.001	0.095	0.904	497	490

Note: (S) = Stormer (1975); (H) = Haselton et al. (1983). Temperatures calculated at pressure = 4 kbar. Samples 88042732, F31, 88042701 G124, H130 and H102 are collected from the Kayumi district. Sample TA9D is collected from the Takehara district.

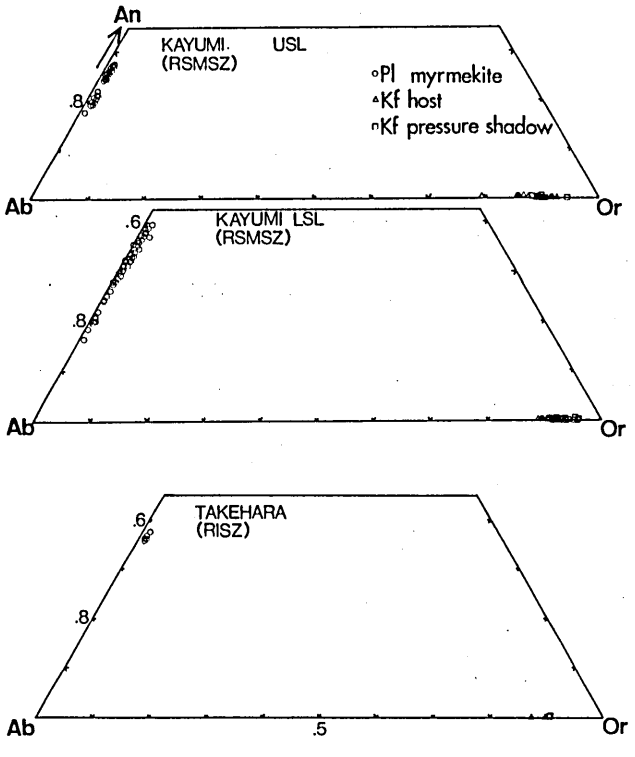

Fig. 15. Compositional variations of the myrmekitic plagioclase and K-feldspar porphyroclasts on the phase diagram for An-Ab-Or system.

per sample in the LSL ranges from 0.92 to 0.94, which is significantly higher than that in the USL (0.87-0.90).

b. Total Al and Ti content of amphibole core and rim

In the Hatai tonalite from the northern part of district, there are differences in composition between the core and rim of the matrix amphiboles. Some of these amphiboles show extensional fracturing. The rim compositions near extensional fracturing and pressure shadow region in sample H104 and H130 have been measured, as shown in Fig. 16 and Table 3. Al^T contents of the core range from 1.38 to 1.78, while the Al^T contents of the rim range from 1.43 to 1.99. The averaged values of amphibole core in the sample H104 and H130 are 1.48 and 1.68 respectively. The averaged values of amphibole rim are 1.56 and 1.74 respectively. Ti contents of the cores of matrix amphiboles, which range from 0.12 to 0.29, significantly higher than those of the rim ranging from 0.05 to 0.23 (Fig. 16).

The Al^T content of the amphibole in the Misugi tonalite which is referred to as one of younger Ryoke granitic rocks has been also measured (Table 3). The averaged Al^T content of core and rim per sample ranges from 1.04 to 1.40.

5. Sense of shear

The mylonitized rocks in the RSMSZ of the Kayumi district exhibit an asymmetric pattern of structures on all scales which indicates that bulk non-coaxial flow has occurred (Choukroune *et al.* 1987) with the sense of shear of dominantly top to the westward. On the mesoscopic scale the S-shaped drag folds with horizontal axes indicate the top to the westward directed sense of shear (Fig. 17).

The following microstructural features indicate a top to the westward directed sense of shear (Fig. 17), according to Simpson & Schmid (1983) and Lister & Snoke (1984).

(1) The mylonitic foliation is intersected by shear planes (C or C'-plane) defined by the tail of mica fish (type II S-C mylonite) or discrete high shear strain zone with elongation and grain size reduction of ductile minerals (type I S-C mylonite).

(2) Brittle porphyroclast systems are reliable indicators of the sense of shear in the USL. Non-rotated type (σ-porphyroclasts after Passchier & Simpson 1986) only occurs (Fig. 7a).

(3) Elongate quartz subgrains and recrystallized grains are frequently oriented obliquely to the foliation plane. Such grains are interpreted by Brunel (1980) to be a consequence of dynamic recrystallization, and, as Burg (1986) demonstrated, this feature is a very reliable indicator of the sense of shear.

(4) In the quartz c-axis fabrics of the mylonites, the asymmetrical distribution of the girdles is uniformly and consistently developed and can thus be considered as a further indicator of the sense of shear.

Table 3 Representative chemical composition of amphobole in the Kayumi district.

Sample No.	H104-a01 core Htn	H104-a18 rim Htn	H104-b02 core Htn	H104-b05 rim Htn	H104-c05 core Htn	H104-c23 core Htn	H130-g01 Htn core	H130-e02 Htn rim
SiO_2 (wt%)	44.59	43.54	44.13	43.00	44.33	41.50	41.58	42.46
TiO_2	1.62	0.93	1.48	1.52	1.27	1.29	1.41	0.76
Al_2O_3	9.22	10.20	8.97	9.55	10.42	10.42	10.81	11.69
FeO	21.08	21.68	21.70	21.20	21.01	21.34	23.53	23.26
MnO	0.61	0.51	0.64	0.64	0.57	0.63	0.83	0.83
MgO	7.75	7.29	7.78	7.68	7.43	7.46	5.44	5.43
CaO	11.05	11.82	11.28	11.27	11.44	11.62	11.65	11.75
Na_2O	1.43	1.04	1.39	1.10	1.08	1.29	1.41	1.21
K_2O	0.71	0.81	0.74	0.72	0.75	0.88	1.46	1.43
Total	98.05	97.82	98.04	98.68	98.31	96.43	98.10	98.83
Si	6.872	6.732	6.803	6.831	6.817	6.528	6.466	6.539
Ti^C	0.250	0.144	0.228	0.238	0.195	0.203	0.219	0.118
Ti^T	0.000	0.000	0.000	0.000	0.000	0.000	0.000	0.000
Al^{IV}	1.128	1.268	1.197	1.169	1.183	1.472	1.534	1.461
Al^{VI}	0.292	0.310	0.186	0.287	0.419	0.168	0.148	0.339
Fe^{2+}	2.801	2.649	2.700	2.774	2.805	2.456	2.779	2.730
Fe^{3C}	0.448	0.704	0.645	0.504	0.426	0.902	0.880	0.852
Fe^{3T}	0.000	0.000	0.000	0.000	0.000	0.000	0.000	0.000
Mn	0.094	0.079	0.099	0.092	0.088	0.099	0.128	0.128
Mg	1.194	1.127	1.199	1.171	1.143	1.173	0.846	0.836
Ca	1.702	1.828	1.738	1.721	1.758	1.828	1.811	1.810
Na^B	0.220	0.160	0.205	0.214	0.167	0.172	0.189	0.186
Na^A	0.000	0.000	0.000	0.000	0.000	0.031	0.030	0.000
K	0.109	0.126	0.114	0.115	0.115	0.139	0.227	0.220
Total	15.109	15.126	15.114	15.115	15.115	15.17	15.257	15.220

Sample No.	H156-a3 core Mtn	H156-a4 rim Mtn	H93-c02 core Mtn	H93-a03 rim Mtn	J23-d01 core	J23-b01 rim Mtn
SiO_2 (wt%)	44.138	46.270	44.964	46.122	47.852	45.693
TiO_2	1.929	0.921	1.931	0.936	0.615	0.857
Al_2O_3	9.312	7.900	8.466	7.636	5.891	7.814
FeO	19.052	19.026	17.206	17.739	19.125	20.168
MnO	0.449	0.476	0.418	0.601	0.832	0.874
MgO	9.100	9.575	10.835	10.407	10.157	9.077
CaO	11.411	11.801	11.533	11.914	11.550	11.626
Na_2O	1.351	1.002	1.297	1.010	0.868	1.153
K_2O	0.963	0.846	0.927	0.810	0.515	0.819
Total	97.707	97.817	97.576	97.175	97.406	98.081
Si	6.844	7.157	6.977	7.274	7.407	7.047
Ti^C	0.299	0.142	0.300	0.075	0.096	0.133
Ti^T	0.000	0.000	0.000	0.000	0.000	0.000
Al^{IV}	1.156	0.843	1.023	0.726	0.593	0.953
Al^{VI}	0.288	0.379	0.292	0.456	0.319	0.251
Fe^{2+}	2.623	2.740	2.482	2.644	2.825	2.623
Fe^{3C}	0.331	0.203	0.189	0.094	0.136	0.488
Fe^{3T}	0.000	0.000	0.000	0.000	0.000	0.000
Mn	0.070	0.074	0.065	0.078	0.128	0.134
Mg	1.411	1.481	1.682	1.654	1.537	1.400
Ca	1.769	1.769	1.789	1.898	1.788	1.794
Na^B	0.209	0.209	0.201	0.102	0.135	0.177
Na^A	0.000	0.000	0.000	1.898	0.000	0.000
K	0.149	0.149	0.144	0.102	0.080	0.126
Total	15.149	15.131	15.144	15.129	15.081	15.127

As the top to the westward directed sense of shear is developed in all samples with exception of 2 locations (Fig. 17), one can assume that this is not a local effect but rather shows that bulk non-coaxial flow with the sense of top to the westward under plain strain occurred in the RSMSZ of the Kayumi district.

D. Discussion

1. Deformation condition

Table 3. continued.

Sample No.	AV. Al^T	Pressure (kb)
H104 core (Hatai tonalite)	1.48	4.0
H104 rim	1.56	4.4
H130 core (Hatai tonalite)	1.68	5.0
H130 rim	1.74	5.2
H156 core (Misugi tonalite)	1.40	3.7
H156 rim	1.30	3.2
H156 inclusion in Pl	1.42	3.7
H93 core (Misugi tonalite)	1.34	3.4
H93 rim	1.21	2.7
J23 core (Misugi tonalite)	1.04	1.9
J23 rim	1.22	2.8

Pressures are calculated by Schmidt (1992)'s equation.

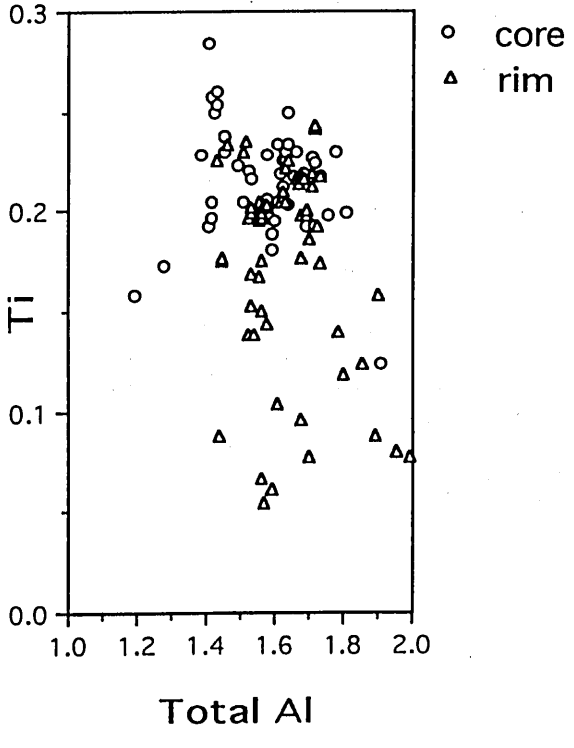

Fig. 16. Compositional variation in Al^T and Ti of amphibole in the Hatai tonalite.

Mechanical behavior of rocks during deformation is generally controlled by temperature, differential stress, strain rate, (OH) content, hydrostatic pressure and pore pressure (see Hobbs & Ord 1989, Shimamoto 1989). Microstructure and LPO of various minerals are varied with these factors. Therefore, these factors are roughly estimated from the microstructure and LPO. Usual geo-thermometer and barometer should be used only for minerals related to the deformation microstructures, in order to recognize P-T condition during deformation. In this section, deformation conditions (temperature, pressure and differential stress) from both microstructures & LPO and geothermo-barometry are examined.

a. Estimation of the deformation condition from microstructures and LPOs

As described above, microstructures of various minerals (particularly quartz and feldspar) and LPOs of quartz are varied with the structural levels (USL and LSL). In the USL, microstructural type of quartz corresponds with P type and/or regime 3 microstructure. On the other hand, in the LSL that corresponds with S & P type and/or regime 2 microstructure. Masuda & Fujimura (1981) suggested that P type microstructure is produced at higher temperature or slower strain rate than S type microstructure. Subsequently, Hirth & Tullis (1991) suggested that regime 3 microstructure is produced at higher temperature or slower strain rate than regime 2 microstructure. Because the line of microstructure defined by Masuda & Fujimura (1981)'s transition in temperature vs strain rate diagram is parallel or subparallel to a line of dislocation creep of the constant stress (e.g. Kocks et al 1989), P type microstructure is concluded to be produced at lower differential stress than S type microstructure (Fig. 18). Therefore, in the USL the ductile deformation occurred at higher temperature or slower strain rate (lower differential stress) than that in the LSL.

Dynamically recrystallized grain size of quartz has been used as 'paleopiezometer' to estimate the paleo-stress in the crustal shear zone (e.g. Kholstedt & Weathers 1980, Christie & Ord 1980, Ord & Christie 1984, Hacker *et al.* 1992). Since the grain size in the USL is smaller than that in the LSL, magnitude of differential stress in the USL is lower than that in the LSL. This interpretation is not concerned with the rate of stress drop and grain growth on the grain size during and after ductile deformation. Knipe (1989) discussed that the rate of stress drop at the end of deformation event and the temperature history after deformation. Hacker *et al.* (1992) also recalculated the magnitude of the differential stress, taking account into post-deformational grain growth during annealing. Drury *et al.* (1985) suggested that different type of dynamic recrystallization mechanism as function of temperature and magnitude of the driving force results in different relationship between the grain size and differential stress. Likewise, Shimizu (1991) pointed out that the grain size and its distribution depend on the rate of dynamic grain growth as function of temperature. Therefore, there are two possibilities for reason why the difference of grain size between the USL and LSL occurred: (1) magnitude of differential stress in the USL is lower than that in the LSL, (2) deformation temperature in the USL is higher than that in the LSL.

As mentioned above, dominant mechanism of dynamic recrystallization in the USL and LSL is subgrain rotation & grain boundary migration and subgrain rotation respectively. Therefore, deformation temperature in the USL is higher than that in the LSL (e.g. Guilopè & Poirier 1979, Tungatt & Humphreys 1981).

LPO pattern is one of useful indicator of temperature during deformation. Critical resolved shear stress ratio between each slip systems, which control the LPO pattern, varies with temperature, strain rate and water content etc.

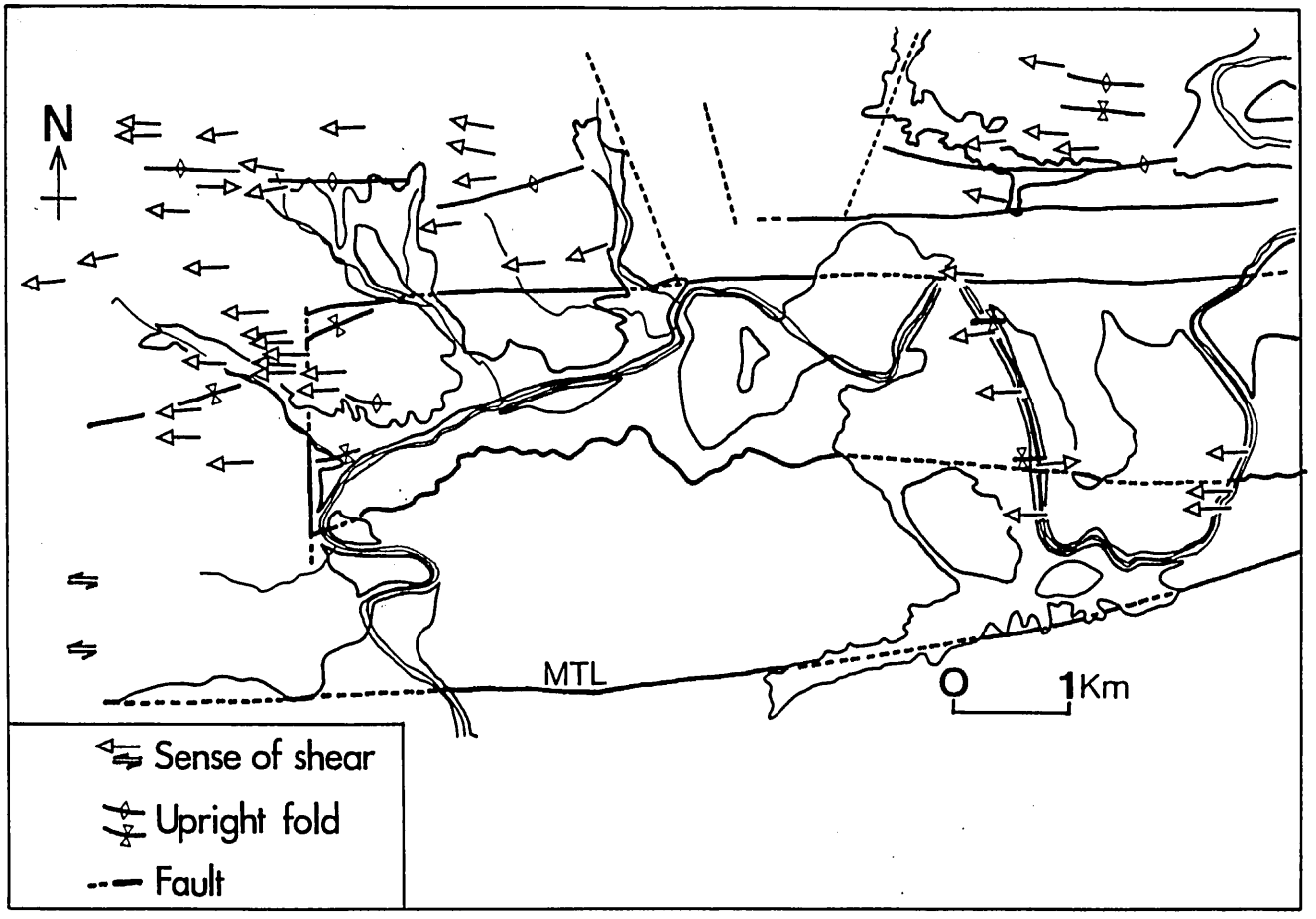

Fig. 17. Orientations of stretching lineations showing sense of shearing in the Kayumi district.

Schmid & Casey (1986) suggested that Y-point maximum pattern of quartz c-axis is produced in plane strain and non-coaxial regime when $\{10\bar{1}0\}<11\bar{2}0>$ slip systems dominate deformation. Wenk *et al.* (1989) produced the c-axis patterns similar to Y-point maximum pattern on the condition that the critical resolved shear stress value of $\{10\bar{1}0\}<11\bar{2}0>$ systems is lower than the other slip systems. Therefore, in the USL $\{10\bar{1}0\}<11\bar{2}0>$ systems dominate mylonitization.

The LPO patterns (type I crossed girdle) from the LSL except from quartz vein imply that ductile deformation (mylonitization) in the LSL occurs under plane strain (k = 1) and lower rotational component of the finite strain than in the USL (Hara 1971, Law *et al.* 1984, Schmid & Casey 1986) and on the condition that $(0001)<11\bar{2}0>$ slip systems are dominant according to Lister & co-worker's and Wenk & co-worker's numerical studies (Lister 1977, Lister *et al.* 1978, Lister & Hobbs 1980, Takeshita & Wenk 1988, Wenk *et al.* 1989).

Previous experimental results suggested that prismatic slip dominate at higher temperature than basal slip (Blacic 1975). Natural analyses also suggested that Y-point maximum pattern is developed at higher temperature than type-I crossed girdle (or single girdle with maxima in Z of the finite strain) (Schmid & Casey 1986, Mainprice & Bouchez 1987, Mainprice & Nicolas 1989). Therefore, the LPOs of quartz in the USL (Y-point maximum) were produced at higher temperature than in the LSL (type-I crossed girdle). However, transition of LPO pattern and dominant slip system depends on strain rate and water content too (Tullis *et al.* 1973, Blacic 1975, Jaoul *et al.* 1984). Effects of these factors on the LPO development in the district is obscure.

From these facts it is concluded that during the mylonitization temperature (and/or magnitude of differential stress) in USL is higher (and/or lower) than that in the LSL. This conclusion is apparently comparable with the result of Michibayashi & Masuda (1993)'s analysis.

b. Estimation of the deformation condition from geothermobarometry

In this section, P-T condition during mylonitization by electron microprobe analysis is discussed. A pair of myrmekitic plagioclase intergrown with quartz grains on the long side of inequant K-feldspar porphyroclast facing the finite shortening direction, and K-feldspar recrystallized in the pressure shadow is used as feldspar-feldspar geothermometer according to Yamagishi (pers. commun.). Simpson & Wintsch (1989) suggested that such growth of myrmekite and recrystallization of K-feldspar are related to deformation and that replacement of K-feldspar by myrmekite can be written in the form of

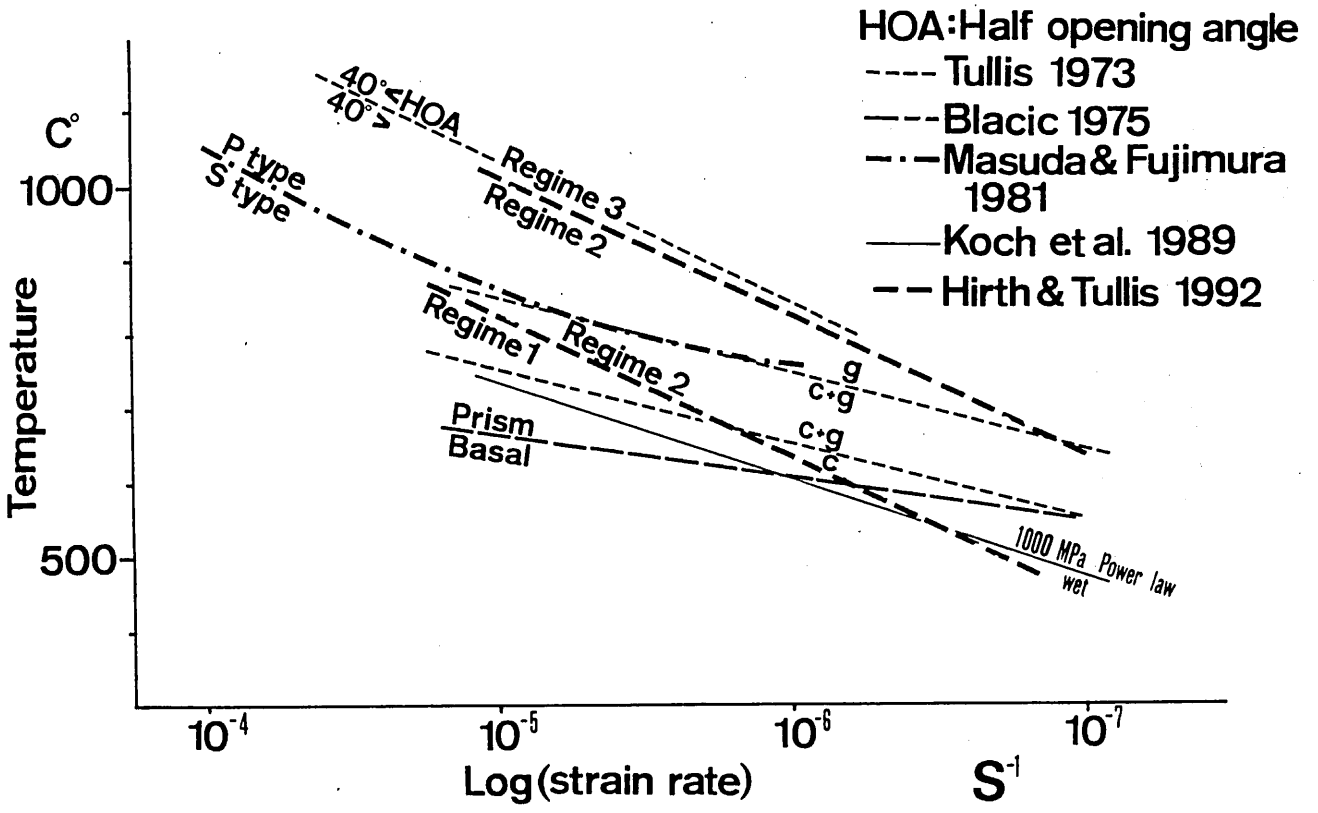

Fig. 18. Temperature vs strain rate diagram showing microstructural and LPO's transitional line from Tullis et al. (1973), Blacic (1975), Masuda & Fujimura (1981) and Hirth & Tullis (1992). Note that the line of microstructural transition crosses the line of dominant slip system transition.

$$\text{Orthoclase} + Na^{+} + Ca^{2+} = \text{Oligoclase} + K^{+} + \text{quartz}$$

K^{+} rich fluid in the right side of the formula can be considered to be precipitated and recrystallized in the lower normal stress region (pressure shadow). Therefore, temperature estimated from the geo-thermometer using these feldspar pair may indicate that during deformation (mylonitization). The results of electron microprobe analysis and temperature calculated from usual geo-thermometers are shown in Table 2. The calculated temperature from the thermometer by Stormer (1975) and Haselton *et al.* (1983) range 450-470 °C and 350-450 °C in the USL and LSL respectively.

Quartz c-axis fabric patterns from the samples analyzed by electron microprobe are shown in Fig. 19. Variation of these patterns between the USL and LSL corresponds to deformation temperature mentioned in the previous section. The value of deformation temperature estimated for the boundary between the USL and LSL could correlated with transition of the quartz LPO patterns between type-I crossed girdle (or single girdle with double maxima at angle of 30-40° from mylonitic foliation) and Y point maximum The variation in deformation temperature between the USL and LSL can not only explain the variations in the LPO patterns, but also those in dynamically recrystallized grain size and aspect ratio of quartz. Many authors suggested that strain-related myrmekite occurs at or above epidote-amphibolite facies (ca. >400 °C) (Simpson 1985, Pryer 1992, Fits Gerald & Stünitz 1993), though the myrmekite in the LSL occur at upper green schist facies (<400 °C). The number of myrmekite per area and total area of myrmekitic bulge per thin section is larger in the USL than that in the LSL. Simpson & Wintsch (1989) suggested that strain energy arisen from elastic strain, or strain associated with tangled dislocations acts important roll in driving the replacement reaction. Sakurai & Hara (1990) also pointed out that the modal ratio of myrmekite at given modal ratio of K-feldspar from strongly deformed granitoids is higher than that from massive, less deformed granitoids. Therefore, the occurrence of myrmekite is concluded to be a function of strain energy as well as a function of temperature, pressure, chemical activities Thus, in locally higher stress region the limit of occurrence of myrmekite may be changed toward at lower temperature.

The pressure during the solidification and mylonitization of the Hatai tonalite has been determined using the total Al content (Al^{T}) of amphibole (Hamarstrom & Zen 1983, Hollister *et al.* 1987, Rutter *et al.* 1989, Schmidt 1992). According to Schmidt (1992), pressure of 4.0-5.0 and 4.4-5.2 kb are estimated from the averaged values of the cores and rims (near extensional fractures and pressure shadows) respectively (Table 3). Rasse (1974) suggested that Ti content of the amphibole increases with increasing

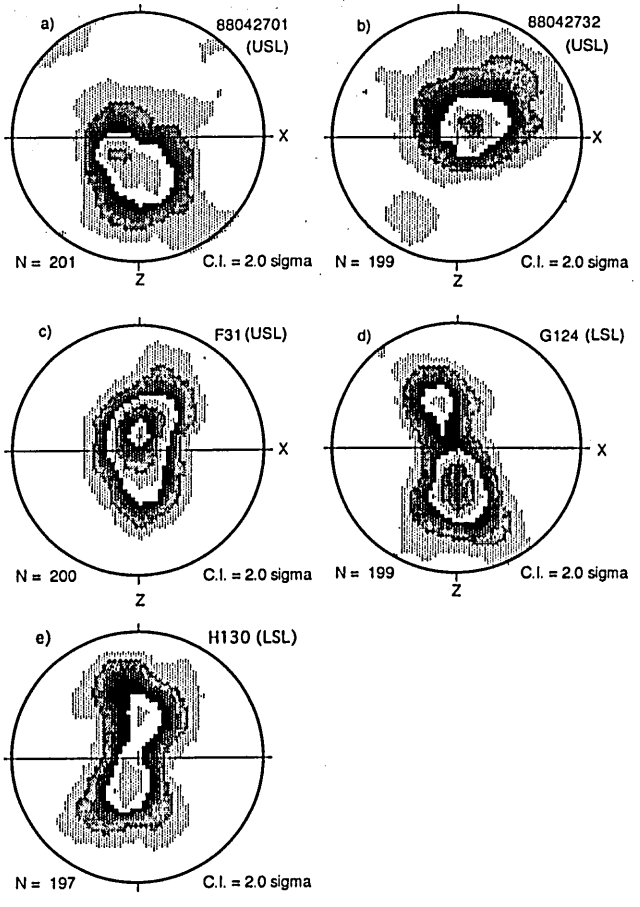

Fig. 19. Quartz c-axis fabrics from the samples used for feldspars thermometer. a:88042701, b: 88042732, c: F31, d: G124, e: H130. Contour interval = 2σ. Compare with Table 2.

metamorphic grade. According to Rasse, the compositions of the core and rim namely indicate the granulite facies and higher grade amphibolite facies metamorphic temperature respectively (Fig. 16). The lower content of Ti in the rim of fractured area implies that the composition of amphibole rim was exchanged during retrogressive phase of cooling of the Hatai tonalite (L-T mylonitization below 450 °C).

Assuming that the composition of the core and rim of amphibole is frozen during the stage of the crystallization and mylonitization of the Hatai tonalite respectively, the above results imply that the tonalite was descended with decreasing temperature. It is suggested that the formation of the Ryoke southern marginal shear zone resulted in the crustal thickening.

The igneous pressure estimated from Al^T content from the Misugi tonalite ranges from 1.9 to 3.7 kb, which is significantly lower than that from the Hatai tonalite. This result implies that the intrusion of the Misugi tonalite into the Hatai tonalite occurred after the L-T and M-T mylonitization and exhumation of the whole RSMSZ from ca. 4.8 kb (ca. 18 km in depth) to ca. 3.0 kb (ca. 11 km in depth).

2. Kinematic model

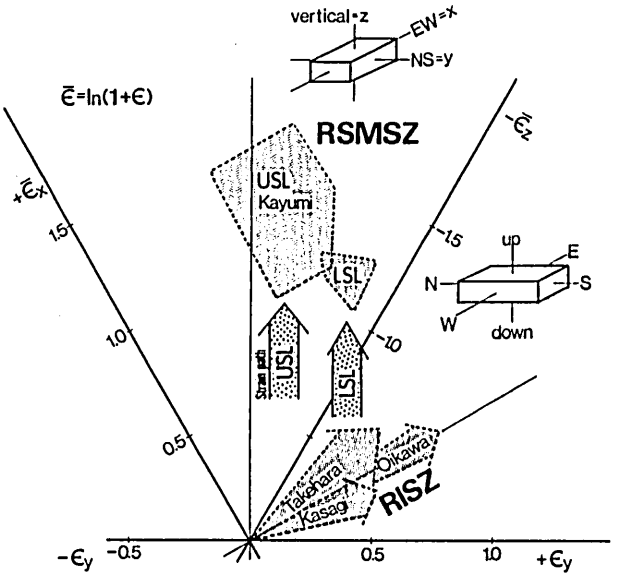

Fig. 20. Three axis diagram showing strain path partitioning between the USL and LSL, inferred from strain analysis for quartz pools and LPO analysis.

As mentioned above, total strain magnitude and three dimensional shape of the finite strain from the strain analysis of quartz pools are different between the USL and LSL. The k value in the USL mainly ranges from 1.0 to 0.5 (plane strain to general flattening), and in the LSL from 0.2 to 0.05 (uniaxial flattening). However, the k value from quartz LPO analysis in the LSL is around 1.0 (plane strain) (Fig. 8). The k value from quartz LPO analysis indicate the three dimensional shape of the finite strain during latest stage of strain increments (Lister & Price 1978, Brunel 1980, Lacassin & Van den Drissche 1984).

Development of distinctive LPO pattern from random LPO needs 30% shortening strain based on numerical analyses (Lister & Hobbs 1980, Jessell 1988) or 20-30% shortening strain based on experimental analyses (Tullis *et al.* 1973, Dell'Angelo & Tullis 1986) at least. Therefore, if the strain path is not only constant during the latest stage of mylonitization, but also during the bulk stage of the mylonitization, the principle extension axis of finite strain before the mylonitization related to the EW stretching in the LSL must be in NS direction (Fig. 20). The NS stretching before the mylonitization of RSMSZ will be discussed in later section. On the other hand, in the USL the three dimensional shape of finite strain from the strain analysis of quartz pools is similar to that obtained from the quartz LPOs. Therefore, a very large magnitude of plane strain is necessary to change the principle direction of the finite strain in the USL. If the principle direction is temporally changed in the USL, the principle directions of finite strain in the USL before the mylonitization is different with those in the LSL. The strain magnitude in each principle strain axes (X, Y, Z) before the mylonitization with EW stretching in the USL may be very small, if there is no rotational component of finite strain. However, if the mylonitization was associated with some rotational component, the stretching direction before the

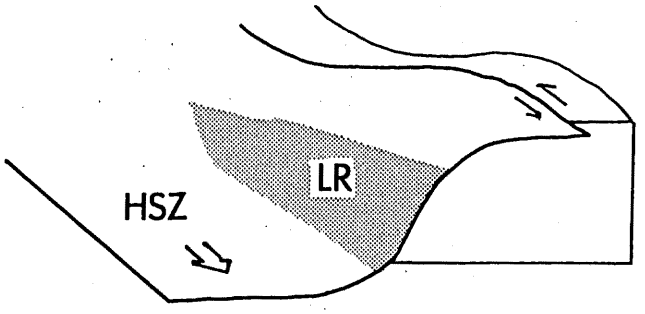

Fig. 21. Diagram showing "lateral ramp" (LR) region with sinistral strike slip and horizontal shear zone (HSZ) with westward directed sense of shear within the whole of RSMSZ.

mylonitization could be variously oriented (e.g. vertical direction) (Fossen & Tikoff 1993). In either case, the stretching direction before the mylonitization at medium to low temperature was changed to EW direction. Since the rotational component in the LSL is low based on the quartz LPO patterns, it could be concludes that EW stretching related to MT and LT mylonitization occurred after NS stretching related to the deformation event at higher temperature.

Ohtomo (1993) has already reported that in the RSMSZ of the Hoji Pass area the final (bulk) three dimensional shapes of finite strain derived from quartz pools are dominantly from general extension to uniaxial flattening in the lower strain zone and general flattening in the higher strain region, though quartz c-axis fabrics indicate that the plane strain during the last stage of mylonitization dominates strain path. Her result is entirely identical with present conclusion. Therefore, it is possible to be concluded that the principle extension direction of finite strain temporally changed from N-S to E-W all over the RSMSZ.

3. Tectonic implication

Horizontal E-W stretching during the mylonitization of the RSMSZ occurs at 350-450 °C in the LSL and 450-470 °C in the USL with some rotational component. Takagi *et al.* (1989) reported that K-Ar age of biotite in the Hatai tonalite is 60-70 Ma, and that the K-Ar age of hornblende ranges from 73 to 83 Ma. The closure temperature of biotite and hornblende is ca. 340 and 550 °C respectively (Dodson 1973, Harrison et al. 1985), assuming that the cooling rate of the Hatai tonalite is 40 °C/Ma and pressure is 4 kb. Therefore, the mylonitization occurs at 83-60 Ma, which agrees with Ohtomo (1993)'s suggestion that the western portion of the Ryoke belt (Kyushu province) was uplifted at about 90 Ma and was followed by the uplift of the eastern portion at 60 Ma. The L-T mylonitization in the LSL was ceased during 60-70 Ma, because the closure temperature of biotite correspond with lower limit of deformation temperature mentioned above.

Until 1985, it has been considered that in the Ryoke southern marginal shear zone developed as the sinistral strike slip fault (Hara *et al.* 1977, 1980, Takagi 1984, 1985, 1986). Then, Ohtomo (1987) and Yamamoto & Masuda (1987) have reinterpreted the RSMSZ as horizontal ductile shear zone with a top to the westward directed sense of shear, although Masaoka (1987) already indirectly pointed out the fact. Recently, analogous results have been reported by Hayasaka *et al.* (1989) in the Asaji district, Okamoto *et al.* (1989) and in the Kosa district, Takahashi (1992) in the Awaji island. However, the RSMSZ in the Takato-Ichinose district (Takagi 1984, 1986), Kishiwada district (Takagi *et al.* 1987) and Kamimura district (Michibayashi & Masuda 1993) appears to develop as the sinistral strike slip ductile shear zone with high angle dipping bulk shear plane. The ductile shear zone in these district may develop as a 'lateral ramp' region continually connected with horizontal shear zone (Coward 1984) (Fig. 21).

The difference in deformation temperature between the USL and LSL implies that (1) there is a thermal gradient during the mylonitization which synchronously closed in the USL and LSL or (2) the ductile deformation in the USL ceased earlier than that in the LSL as suggested by Michibayashi & Masuda (1993). K-Ar age of hornblende in the Hatai tonalite significantly increases from 73-74 Ma to 83 Ma tower the lowermost structural level (Takagi *et al.* 1989). It suggests that there is a inverse thermal gradient within the shear zone before the L-T and M-T mylonitization, since closure temperature of hornblende is 550 °C (Harrison et al. 1985). Therefore, the assumption (1) that there is a thermal gradient during the mylonitization which synchronously closed in the USL and LSL is reasonable rather than the assumption (2) that the ductile deformation in the USL ceased earlier than that in the LSL. Hollister & Crawford (1986) , Shi & Wang (1989) and Ruppeal & Hodges (1994) suggested that inverse thermal gradient within the movement zone result from overthrusting processes with fast displacement rate. Therefore, the displacement rate in the RSMSZ is fully fast to develop the inverse thermal gradient.

E. Conclusions

The Ryoke southern marginal shear zone in the Kayumi district is a subhorizontal ductile shear zone accompanied with westward directed sense of shear during 83-60 Ma. Accommodation of initial shear zone structures occurred after the mylonitization. There was a thermal difference within the Ryoke southern marginal shear zone during the mylonitization. The mylonitization occurred at 470-450 °C in the upper structural level and at 450-350 °C in the lower structural level. Microstructures and lattice preferred orientation are also varied with structural level, which is good indicator of deformation temperature. Before the EW stretching related to the formation of the Ryoke southern marginal shear zone (MT and LT mylonitization), the NS stretching occurred at higher temperature condition. The development of the Ryoke southern marginal shear zone occurred at pressure of 4-5 kb. Afterward, intrusion of the younger Ryoke granitic rocks into the older granitic rocks occurred at pressure of 4-2 kb, so that the shear zone wholly exhumed from 18 to 11 km in depth after MT and LT mylonitization.

IV. Structural evolution of the Ryoke inner shear zone

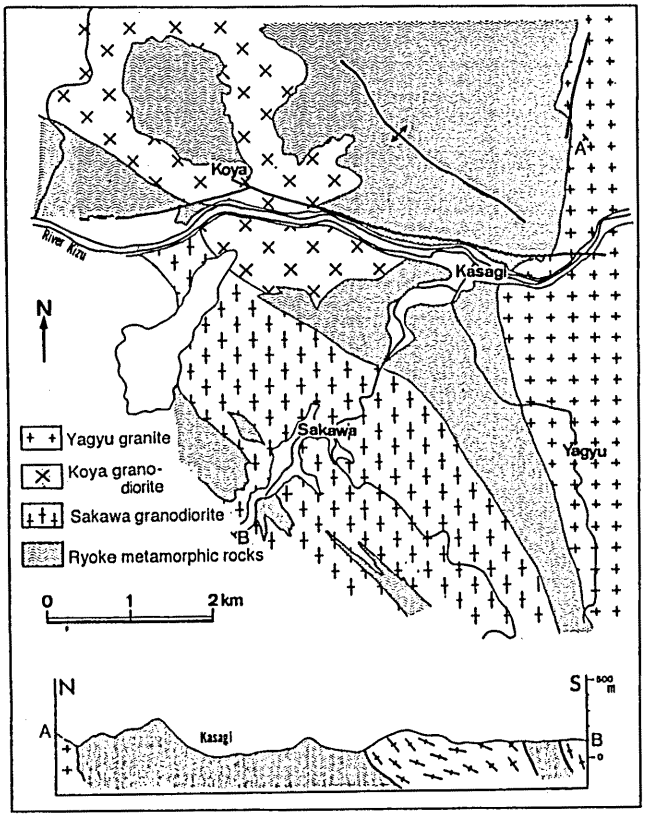

Fig. 22. Geological map and profile of the Kasagi district.

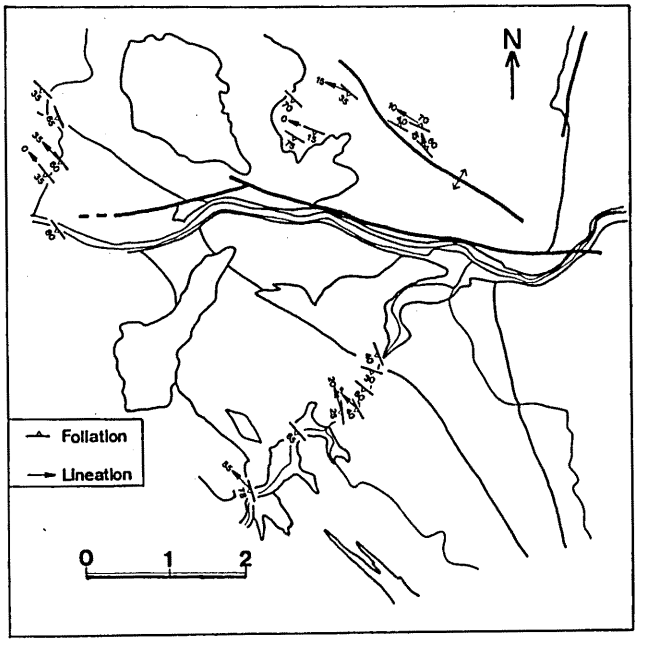

Fig. 23. Foliation and lineation map of the Kasagi district.

A. Introduction

The Ryoke inner shear zone (RISZ) is developed in the north of the RSMSZ at distance ca. 20-30 km from the Median Tectonic Line, which is intermittently continued from Kasagi district to Takehara district. In the RISZ, the older Ryoke granitic rocks and Ryoke metamorphic rocks are strongly mylonitized. Existence and features of shear zones in the inner region of the Ryoke metamorphic terrane have not been sufficiently recognized with the exception of the brief description by Inoue (1980 MS) and Hayama *et al.* (1982). Therefore, structural informations from present study in the RISZ give new perspectives for understanding the tectonics of the Ryoke metamorphic terrane. In this chapter, present author will mainly report results of microstructures of quartz, lattice preferred orientation (LPO) of quartz, sense of shear and mineral chemistry with macro to mesoscopic structures in the Kasagi, Oikawa, Hakusan-Joryu and Takehara district of the RISZ, as well as in the former chapter. The deformation condition, kinematic model and tectonic implication will be discussed, based on these data.

B. Geological setting

1. Kasagi district

a. Outline of Geology

The Kasagi district is located in the southern part of the Kyoto Prefecture (Fig. 1). The structural analysis of the Kasagi district on macro to micro scale has been performed by Hara (1962), and afterwards, Yoshizawa *et al.* (1966) investigated the geology. Fig. 22 shows a geological map and profile of the district compiled from Hara (1962) and Yoshizawa *et al.* (1966). Rocks in the district consist of the Ryoke metamorphic rocks (pelitic, psammitic and siliceous gneiss), Sakawa granodiorite, Yagyu granite, Koya granodiorite.

Detailed internal structures (variation of the foliation) of the Yagyu granite have been investigated by Sakurai & Hara (1979) and Hara *et al.* (1980b). Hara (1962) suggested that the Sakawa granodiorite is referred to as the older Ryoke granitic rocks, and that the Yagyu granite and Koya granodiorite belong to the younger Ryoke granitic rocks. The boundaries between the older rocks (the Ryoke metamorphic rocks and Sakawa granodiorite) are parallel to the NW-SE trend. Migmatization of the Ryoke metamorphic rocks by the Sakawa granodiorite is observed in the southernmost part of the district.

The Ryoke metamorphic rocks and Sakawa granodiorite in the Kasagi district is mylonitized with various deformation-induced microstructures. In the central to southern part of the district, the foliation strikes NW and dips at 30-60° toward SW. The stretching lineation of the Ryoke metamorphic rocks and Sakawa granodiorite has NW-SE trend (Fig. 3). The orientation of mylonitic foliation of the Sakawa granodiorite is slightly bent from NW-SE to N-S toward the Yagyu granite. The gneissosity (mylonitic foliation) of the Ryoke metamorphic rocks is folded with the upright axial plane and horizontal axis in northern part of the Kasagi district (Fig. 22).

The Yagyu granite and Koya granodiorite discordantly intrude into the Ryoke metamorphic rocks and Sakawa granodiorite (Hara 1962, Sakurai & Hara 1979), and the surface of the intrusions by the formers cut the foliation of the laters. The foliation of the Yagyu granite is parallel to its external spherical shape with bending the foliation of the older rocks. These features indicate that the Yagyu granite forcefully intrude and emplace into the older rocks during diapiric uprise. While, the Sakawa granodiorite concordantly intrudes into the Ryoke metamorphic rocks.

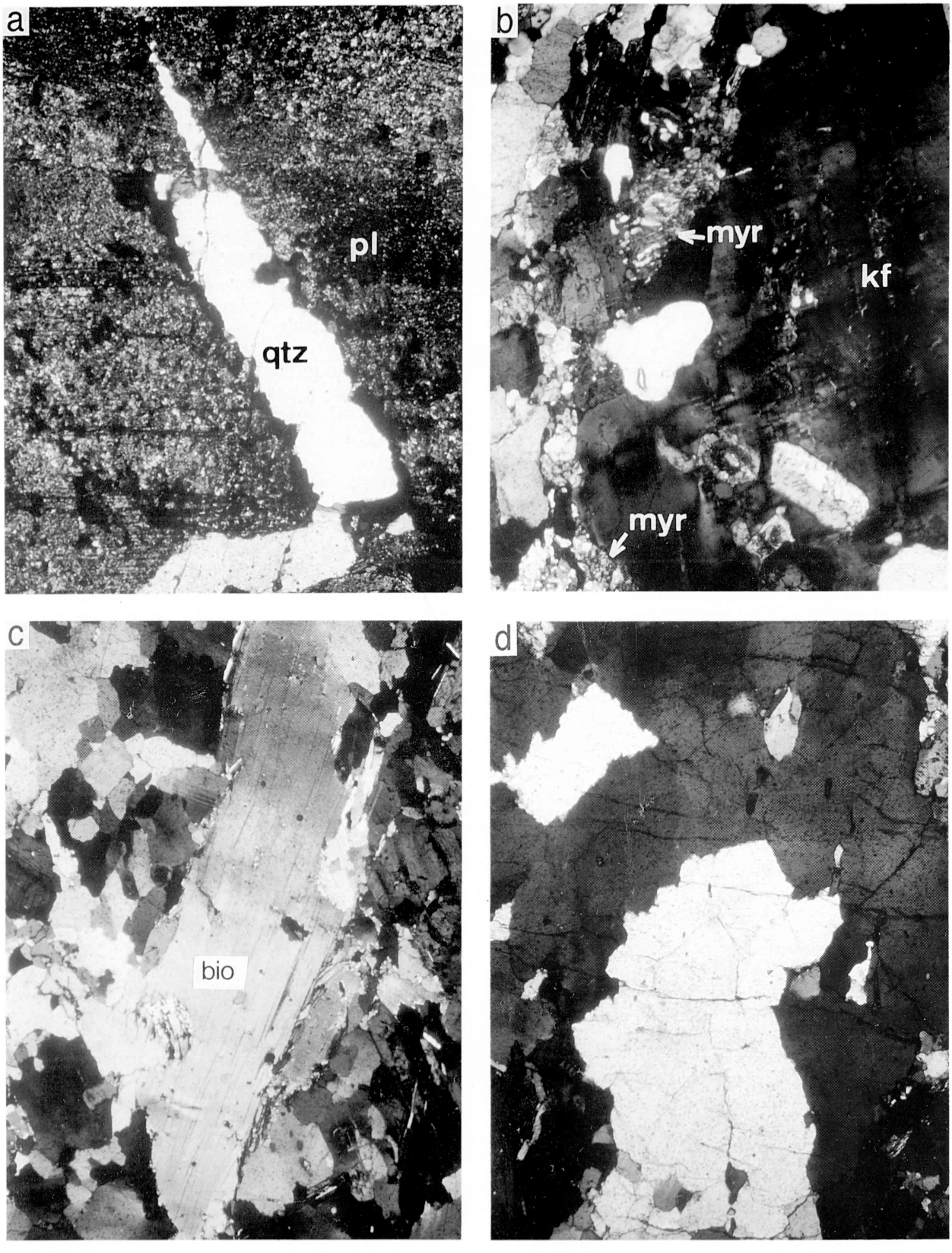

Fig. 24. a) Extensional fracturing of plagioclase porphyroclast in the Sakawa granodiorite. b) Myrmekite (MYR) on the grain boundary of K-feldspar porphyroclast. c) Microphotograph showing asymmetrical mica fish microstructure of biotite in the Sakawa granodiorite. d) Microstructures of quartz in the Sakawa granodiorite.

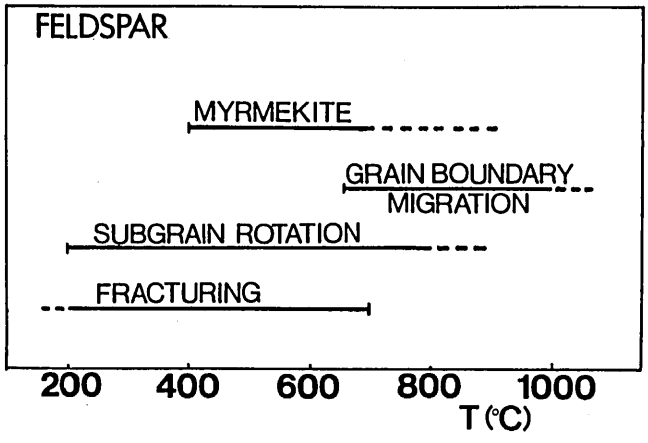

Fig. 25. Deformation style and recovery mechanism of feldspar compiled from Table 1 of Fitz Gerald & Stünitz (1993).

The boundary between them is parallel to the mylonitic foliation, implying that the intrusion of the Sakawa granodiorite into the Ryoke metamorphic rocks is syntectonic (e.g. Paterson 1989).

Brittle faults along river Kizu striking EW slightly modify the distribution of the geological mass.

b. Description of rock types and microstructures

The Ryoke metamorphic rocks are widely exposed in the Kasagi district and mainly composed of pelitic rocks with layers of subordinate psammitic and siliceous rocks (Fig. 22). Metamorphic grade increase toward south with the mineral assemblage of

1. quartz + plagioclase + muscovite + biotite
2. quartz + plagioclase + K-feldspar + muscovite + biotite + cordierite + andalusite
3. quartz + plagioclase + muscovite + biotite + cordierite + sillimanite + garnet

Sillimanite or fibrolite occurs in the south of the river Kizu. Cordierite porphyroblasts occur as pseudomorph in the wide area of the district. The foliation (gneissosity) of the metamorphic rocks strikes N10 to 50° W and dips at from 30 to 60° toward SW in the southern part of the district. In the north of antiform (upright fold), it dips at from 40 to 70° toward S. Lineation defined by the strong preferred dimensional orientation of micas and cordierite plunges horizontally trending N30 ° W.

Most of quartz grains show P type (Masuda & Fujimura 1981) and/or regime 3 microstructure (Hirth & Tullis 1992). The grain boundaries is straight or slightly curved, and undulatory extinction sometimes occurs within the grains. Subgrain boundaries are basal and prismatic, and oblique to the foliation at high angle. Biotite and muscovite porphyroclasts occur as mica fish and are recrystallized to the finer grains in the tail of these porphyroclasts. Some of the recrystallized grains form the shear band foliation slightly oblique to the foliation. Asymmetry of the mica fish is remarkable, although the uniformity related to the sense of shear is not constant. LPOs of micas ([001] fabrics) indicate YZ girdle with maxima near Z (Hara 1962). Cordierite porphyroblasts show inequant grain shape whose elongation axis is parallel to the foliation. In the pressure shadow developed at extension side of the porphyroclasts, quartz, biotite and muscovite are recrystallized and grown. The shadows are relatively symmetric, implying that non-coaxiality is low during development of the foliation.

The Sakawa granodiorite is coarse to fine-grained and exposed in the southern part of the district with elongated external shape of the body. The granodiorite mainly consists of quartz, plagioclase, K-feldspar and biotite, with accessory titanite, zircon, allanite, apatite and opaque minerals. Hara (1962) described that the Sakawa granodiorite is divided into the fine-grained and coarse-grained facies.

The mylonitic foliation defined by a preferred dimensional orientation of biotite and elongated quartz pools strikes NW and dips at from 30 to 60° toward SW (Fig 23). Foliation is more conspicuous in the XZ plane than in the YZ plane. These feature implies that L-fabric (constrictive strain) dominate deformation. The mylonitic lineation plunges toward NW at angles of 0 to 30°.

Plagioclase grains occur as coarse-grained porphyroclasts and fine-grained aggregates. The plagioclase porphyroclasts show extensional micro-fracturing and the fractured spaces are filled by large quartz grains (Fig. 24a). However, deformation twinning on (010) plane with bending or undulatory extinction of the porphyroclasts dominate the mylonitization rather than extensional micro-fracturing (Fig. 25). In the mantles of a few plagioclase porphyroclasts dynamic recrystallization occurs by subgrain rotation. The misorientation angle between the porphyroclasts and recrystallized new grains by subgrain rotation ranges from 1 to 3°. The pressure shadows at extensional side of the porphyroclasts are relatively symmetric. In the region of the shadow, biotite and quartz grains are recrystallized and grown. K-feldspar occurs as large symmetrically spindle-shaped porphyroclasts. Myrmekite is found along grain boundaries of the K-feldspar porphyroclasts that are parallel to the S-mylonitic foliation (Simpson 1985, Simpson & Wintsch 1989) (Fig. 24b). In the pressure shadows of the porphyroclasts, new K-feldspar grains are precipitated and recrystallized. Fine grained plagioclase aggregates are also recrystallized in the marginal tail region of the shadows and the layerings of grains continuous from the shadow develops parallel to the mylonitic foliation. Some of biotite porphyroclasts show asymmetric mica fish microstructure (Simpson & Schmid 1983) related to C-plane or shear band foliation (Fig. 24c). New recrystallized fine grains intermittently develop in the tail region of the fish.

2. Oikawa district

a. Outline of geology

The Oikawa district is located in central part of Kinki Province near the Iga-ueno and Nabari city (Fig. 1). Geology and meso to macroscopic structure have been investigated by Yoshizawa *et al.* (1966), Inoue (1977MS & 1979MS) and Hayama *et al.* (1982). Inoue (1977MS) and Hayama *et al.* (1982) briefly described the microstructures of various minerals. Geological map with some structural elements and profile of the district compiled from Inoue

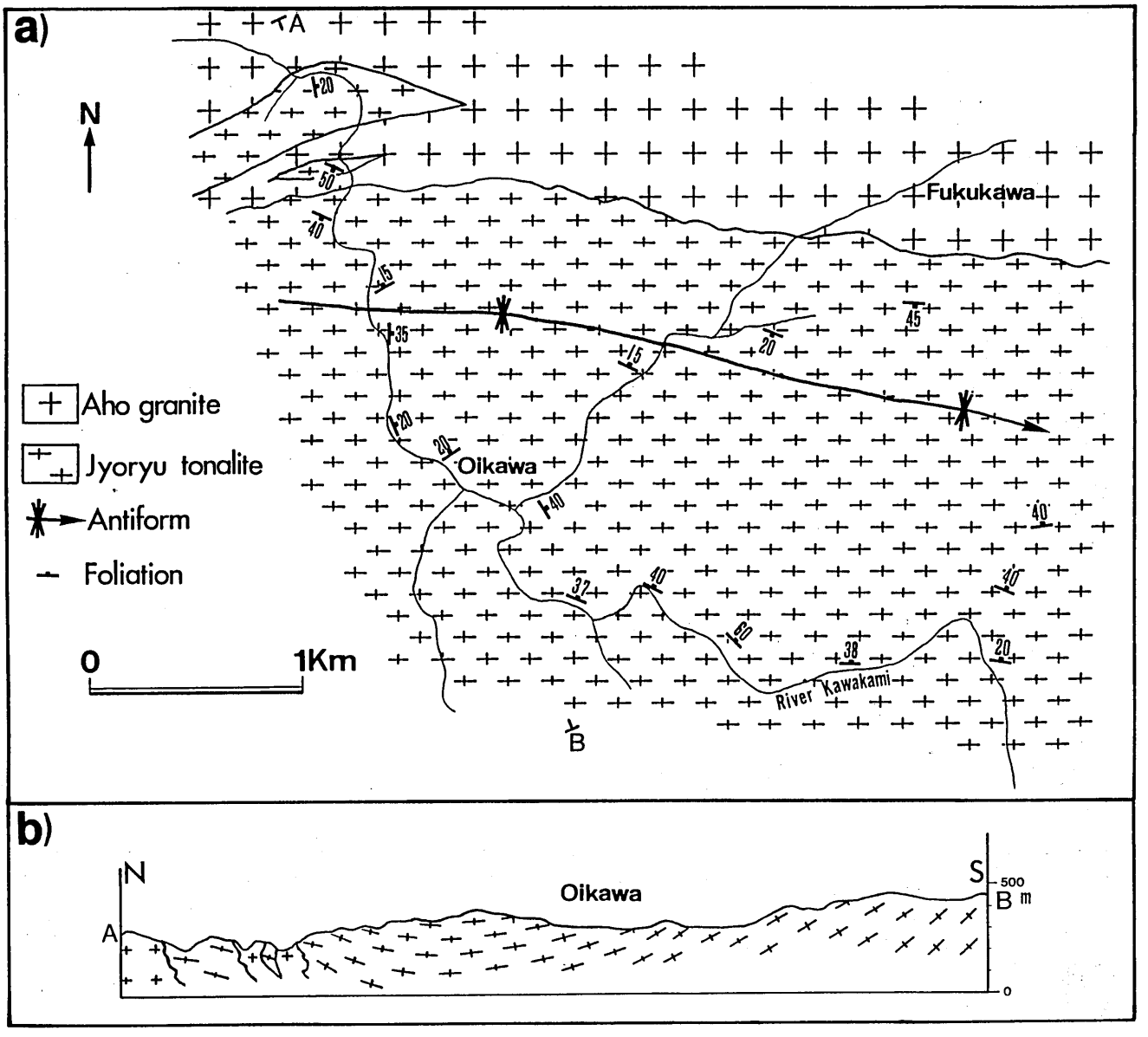

Fig. 26. Geological map and profile of the Oikawa district.

(1979MS) is shown in Fig. 26. The Oikawa district mainly consists of the Joryu tonalite and Aho granite (Hayama *et al.* 1982). The mutual relationship between both the granitic rocks has been investigated by Hayama *et al.* (1982). The Aho granite which is massive or weakly foliated intrudes into the Joryu tonalite strongly foliated in discordant manner (Fig. 26) and includes the xenoliths of the Joryu tonalite. The Joryu tonalite has inequant-shaped basic inclusions. The Joryu tonalite and Aho granite are interpreted as the older and younger Ryoke granitic rocks respectively by Hayama *et al.* (1982).

The Joryu tonalite shows a strong foliation and lineation produced by the mylonitization. The mylonitic foliation is folded in the central part of the district (Fig. 26), forming a synform. The fold axis plunges toward SW at low angle, and the axial plane dips at high angle toward SW. Therefore, it is suggested that the upright fold was developed after mylonitization of the Joryu tonalite. The mylonitic foliation defined by the preferred dimensional orientation of biotite, amphibole and quartz pools strike NW and dips at from 0 to 60° SW or NE. The mylonitic lineation horizontally plunges toward SE. It is oblique to the axis of the upright fold at angle of ca. 20° (Fig. 4).

b. Description of rock types and microstructures of the Joryu tonalite

The Joryu tonalite (Hayama et al. 1982), is widely exposed in the Oikawa district. It consists of quartz, plagioclase, biotite, amphibole, ±K-feldspar and ±pyroxene, with accessory apatite, zircon, titanite, allanite and opaque minerals. The Joryu tonalite is classified into tonalite to granodiorite in narrow sense in terms of Qtz-Pl-Kf modal ratio (Inoue 1979MS, Hayama *et al.* 1982). The development of mylonitic foliation and lineation is strong

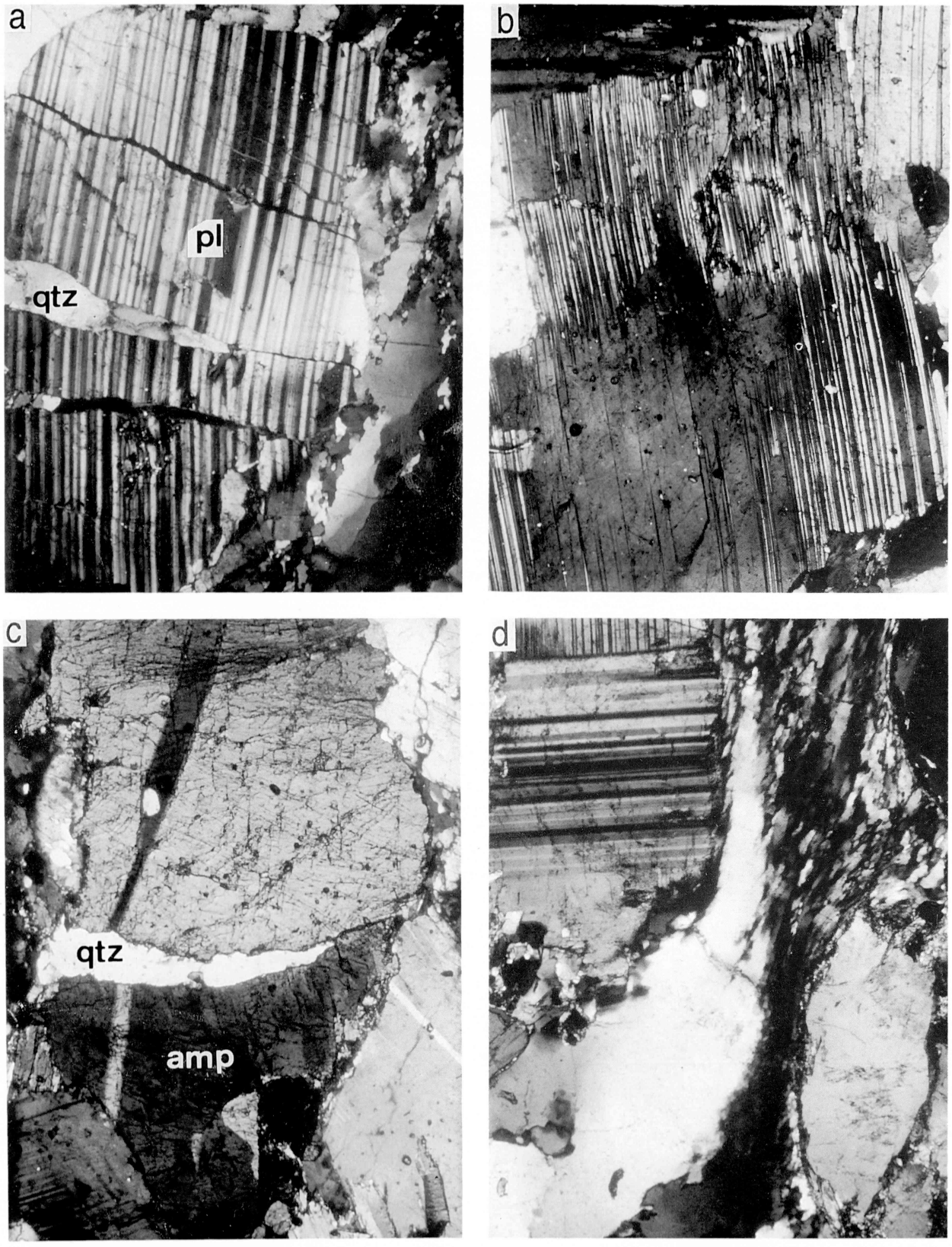

Fig. 27. a) Extensional fracturing of plagioclase porphyroclast in the Joryu tonalite in the Oikawa district. b) Deformation twinning with bending of plagioclase porphyroclast in the Joryu tonalite in the Oikawa district. c) Extensional fracturing of amphibole porphyroclast in the Oikawa district. d) Development of heterogeneous micro shear zone in quartz aggregate of the Joryu tonalite in the Oikawa district.

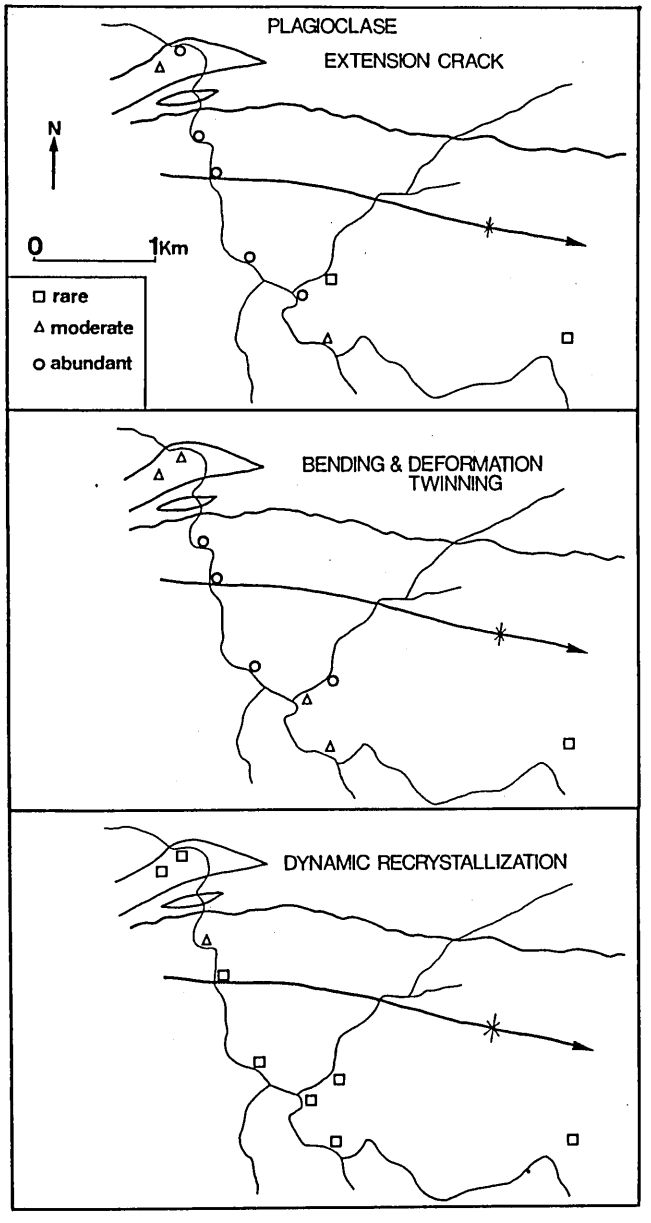

Fig. 28. Variations in plagioclase microtextures (extensional fracturing, deformation twinning, dynamic recrystallization) of the Joryu tonalite in the Oikawa district.

particularly near the central part of district. The mesoscopic structures (intensity of development of the mylonitic foliation and lineation) on the XZ, YZ and XY plane of the tonalite show L-S fabric (Ramsay & Huber 1987).

The average size of dynamically recrystallized quartz grains remarkably decreases down to 200 μm at the axial part of synform which corresponds with highest structural level in the district. Aspect ratio of the grains (long diameter/short diameter on the XZ plane) ranges from 1.7 to 2.5 throughout the district. The higher value of the ratios is observed near the axis of synform. Detailed microstructures of quartz are described in the later section.

Extensional fracturing of plagioclase porphyroclasts is ubiquitous in the district (Fig 27a & 28), which is perpendicular to the mylonitic foliation. The fractured space is filled by biotite, chlorite and large quartz grains (Fig. 27a). The extensional fracturings show asymmetrical 'V'-shaped gaps between the separated fragments (Hippertt 1993). Deformation twinning on (010) plane) with bending and kinking are developed in the porphyroclasts (Fig. 27b). Dynamic recrystallization by subgrain rotation rarely occurs in the rim of the porphyroclasts, which produces the misorientation at angle of 1-5° between the host plagioclase porphyroclast and recrystallized grain. σ-type pressure shadow (Passchier & Simpson 1986) asymmetrically developed at extension side of the porphyroclasts, mainly consists of quartz and biotite. Biotite porphyroclasts show asymmetrical 'mica fish' microstructure (Simpson & Schmid 1983, Lister & Snoke 1984). In the tail region of fish, recrystallized fine-grained biotite grains occur, related to C-plane of type II S-C structure (Lister & Snoke 1984). Bending and undulatory extinction of the biotite porphyroclasts are ubiquitous around the plagioclase porphyroclasts. Most of amphibole grains are porphyroclastic and elongated parallel or subparallel to the mylonitic foliation. Axial colors vary from brown to brownish green toward the rim of the porphyroclast. In some amphibole porphyroclasts, extensional fracturing occurs (Fig. 27c), which is filled by quartz, biotite and sphene. Fibrous growth of brownish green amphibole occurs in the fractured parts of host amphiboles.

3. Hakusan-Joryu district

a. Outline of Geology

The Hakusan-Joryu district is located in the west of the Ieki of the Mie Prefecture (Fig. 1). Yoshizawa *et al.* (1966) investigated a geology and spatial distribution of the Ryoke granitic rocks. Inoue (1977MS, 1979MS) investigated the geology and structure on macro to micro scale. Afterward, Hayama *et al.* (1982) reported the geology, macro to mesoscopic structure and mutual relationship of the granitic rocks.

Geological map of the district are shown in Fig. 29, compiled from the present investigation, Inoue (1979MS) and Hayama *et al.* (1982). Rocks exposed in the district consist of the Ryoke metamorphic rocks derived from sedimentary rocks (pelitic, psammitic and siliceous gneiss), Joryu tonalite (the older Ryoke granitic rocks), Aho granite (the younger Ryoke granitic rocks) and Tertiary sediments. As mentioned above, Inoue (1979MS) and Hayama *et al.* (1982) clarified that the Joryu tonalite is intruded by the Aho granite. The Ryoke metamorphic rocks is intruded by the Joryu tonalite and Aho granite (Inoue 1979MS, Hayama *et al.* 1982).

The foliation developed in the Ryoke metamorphic rocks and Joryu tonalite is folded in the central part of the district (Fig. 30). These folds (synform and antiform) correspond to the upright fold referred by Hara (1977), whose axial plane vertically dips and axes plunge toward the east at angle of ca. 10°. The synform may be connected with that in the Oikawa district.

Brittle faults strike NE and dip sub-vertically (Tsuneishi 1970). The offsets of the geological body by faults show left lateral strike slip displacement.

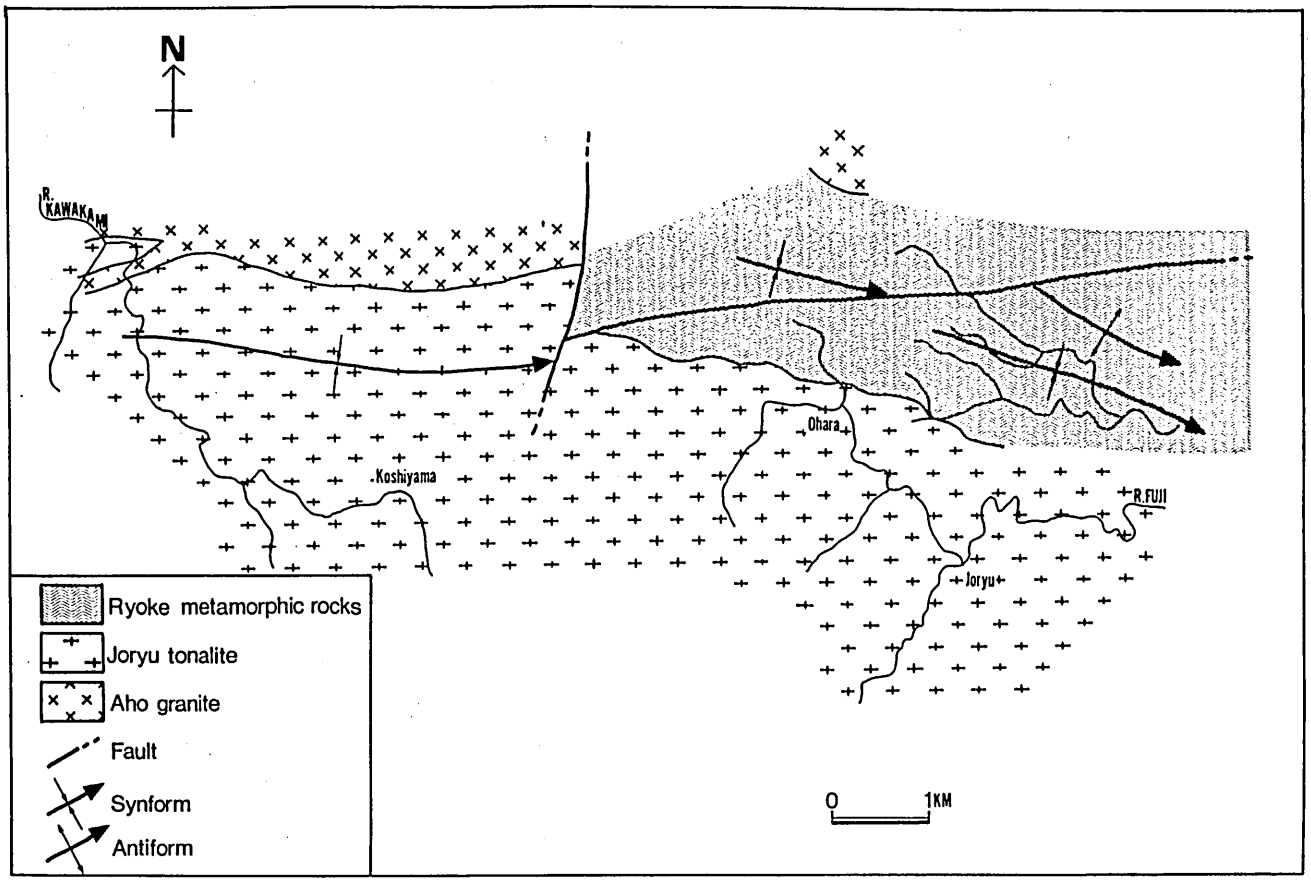

Fig. 29. Geological map of the Oikawa district and Hakusan- Joryu district.

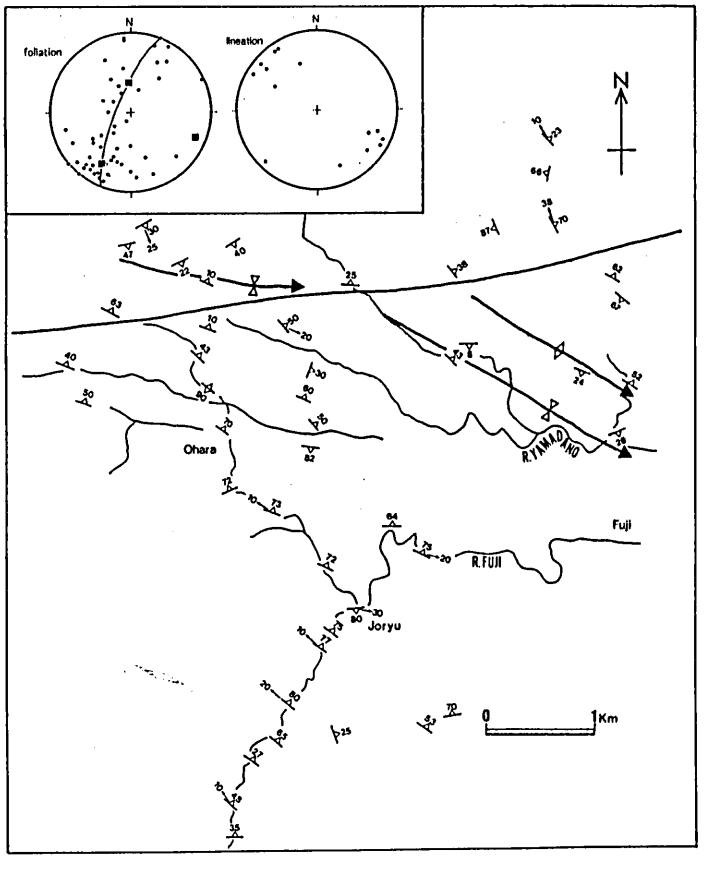

Fig. 30. Foliation and lineation map of the Hakusan-Joryu district. Note that trend of the upright fold is similar to that in the Oikawa district. Development of retrograde shear zone occurs in the proximity of the synform.

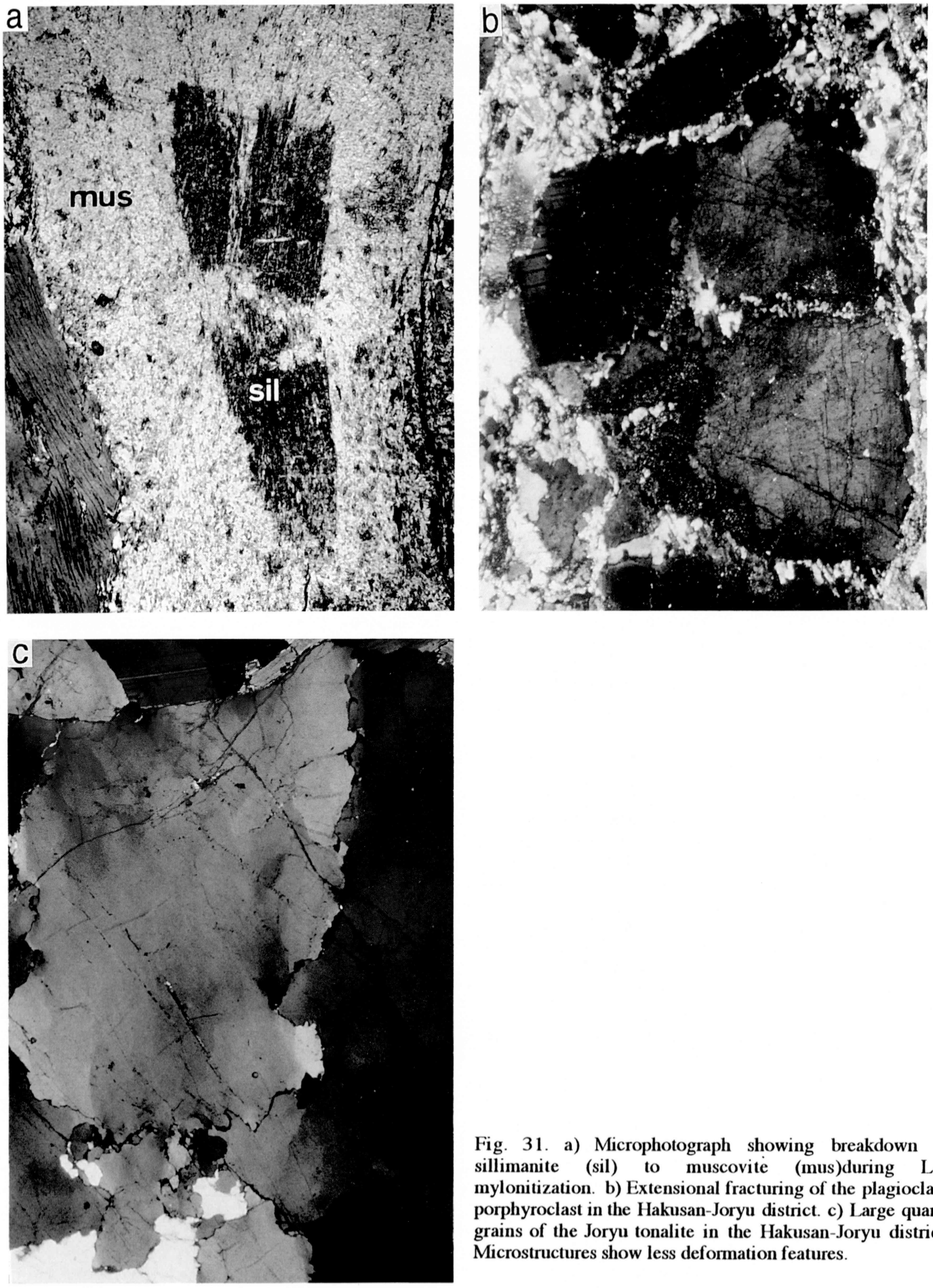

Fig. 31. a) Microphotograph showing breakdown of sillimanite (sil) to muscovite (mus)during L-T mylonitization. b) Extensional fracturing of the plagioclase porphyroclast in the Hakusan-Joryu district. c) Large quartz grains of the Joryu tonalite in the Hakusan-Joryu district. Microstructures show less deformation features.

b. Description of rock types and microstructures

The Ryoke metamorphic rocks is widely exposed in the northern half of the Hakusan-Joryu district. They mainly consist of pelitic gneiss and subordinate psammitic and siliceous gneiss. These rocks is banded with the alternation of mica rich layers and quartz-feldspar rich layers. The spacing and width of these layers are varied in the district. The mineral assemblages of pelitic gneiss are:

1. quartz + plagioclase + K-feldspar + biotite + muscovite + cordierite + garnet

2. quartz + plagioclase + K-feldspar + biotite + muscovite + sillimanite (fibrolite) + cordierite + garnet

Some of sillimanite aggregates show strongly elongate shape parallel to the foliation, which are continuous from matrix to the core of feldspar porphyroblast. Garnet porphyroblasts include biotite, muscovite and quartz grain. The internal foliation (Si) defined by the preferred dimensional orientation of these minerals in the garnet porphyroblasts is weak or do not develop.

Quartz grains in the siliceous gneiss commonly show large grain size (>1000 μm) and low aspect ratio (<2.0) to be comparable with the duplex type of Masuda *et al.* (1990). The grain boundaries are micro-bulged. Both basal and prismatic subgrain boundaries are developed. The grain size locally decrease down to ca. 200 μm in the vicinity of EW striking fault in the central part of district. Aggregates of sillimanite in the rocks which show the remarkable decrease of the grain size of quartz, is broken down to the muscovite (Fig. 31a). This reaction can be written as

Sillimanite + K-feldspar + water $\rightarrow$ muscovite + quartz

This reaction has been reported by Passchier (1985) in the mylonite zone of the Pyrenees. The retrogressive reaction is not observed in the weakly deformed metamorphic rocks. This fact suggests that the metamorphic reaction and/or its kinetics is related to the magnitude of strain energy. The deformation-enhanced metamorphic reaction clarified by Wintsch & Dunning (1985) in experimental study and by Simpson & Wintsch (1989), Sakurai & Hara (1990) in natural study act a important role in the retrogressive metamorphism. Biotite and muscovite grains show a strong dimensional preferred orientation, whose long axes of the aggregates are parallel to the foliation. Some of plagioclase porphyroblasts in the northern part of the district show extensional microfracturing (Fig. 31b). Undulatory extinction of porphyroblasts is ubiquitous in the strongly deformed rocks. K-feldspar porphyroblasts also show the undulatory extinction, although they did not show any brittle microstructure.

The Joryu tonalite is widely exposed in the southern half of the Hakusan-Joryu district. The petrological features of the tonalite is similar to that in the Oikawa district. However, the development of the foliation and lineation is weaker than that in the shear zone of the Oikawa district. The foliation strikes N 20° W to EW and dips at angles from 30 to 90° toward NE. The representative average size of quartz grains is more than 1000 μm (Fig. 31c). Average aspect ratio of quartz grains is relatively low (up to 2.0). Undulatory extinction weakly develops. The grain boundaries show no preferred orientation. Misorientation by subgrain rotation in terms of c-axis between adjacent grains bounded by subgrain boundaries is small at angle of 1-2° Plagioclase porphyroclasts are slightly inequant. Deformation-induced microstructures (e.g. extensional fracturing and mechanical twinning) are rarely observed in the porphyroclasts. Biotite porphyroclasts show a preferred dimensional orientation which is weaker than that of the tonalite in the Oikawa district. Some of biotite grains are bent around plagioclase porphyroclasts. Amphibole grains show no or slightly intracrystalline plastic deformational feature. There is a preferred dimensional orientation of amphibole grains which define the mylonitic foliation. It may develops by rigid body rotation in viscous matrix.

4. Takehara district

a. Outline of Geology

The Takehara district is located in the south of the Hakusan-Joryu district (Fig. 1). Yoshizawa *et al.* (1966) have investigated regional geology and petrology of the granitic rocks and metamorphic rocks. Inoue (1977MS, 1979MS) showed the division of the granitic masses and briefly described the structures on micro to mesoscopic scale. Afterward, Hayama *et al.* (1982) reported the mesoscopic structure and mutual relationship between the granitic rocks.

Rocks in the district mainly consist of the Ryoke metamorphic rocks, Kimigano granodiorite, Fukudayama granodiorite (Hayama *et al.* 1982) (Fig 32). These granitic rocks are referred to as the older Ryoke granitic rocks (Hayama *et al.* 1982), and show a distinct strong foliation (so-called gneissosity) and lineation. The Fukudayama granodiorite shows the sheet-like external shape. Inoue (1979MS) suggested that it concordantly intrudes into the Kimigano granodiorite. The Kimigano granodiorite includes xenoliths of the Ryoke metamorphic rocks. Ishizaka (1969) reported the U-Pb age for zircon from the Kimigano granodiorite of the Takehara district is 90 Ma. The Ryoke metamorphic rocks in the district, which mainly consists of biotite gneiss, is strongly migmatized by the Kimigano granodiorite (Hayama *et al.* 1982), showing alternation of the mica-rich layers and quartz feldspar-rich layers.

The macroscopic structures (foliation) in the district show gently upright folding with NE-oriented axis (Fig. 32 & 33). The boundaries between each rocks are parallel or subparallel to the foliation. This feature and sheet-like shape of the Fukudayama granodiorite imply that the Fukudayama granodiorite syntectonically and passively intruded into the Kimigano granodiorite along the crustal failure (e.g. Hutton 1988a). The lineation defined by the preferred dimensional orientation of quartz pools, biotite and amphibole is well developed in the granitic rocks throughout the district. It plunges toward from north to NW at angle of 0-30°, which is parallel to general trend of the lineation in the other district of the inner zone. Inoue (1977MS) described the cataclastic deformation in the Fukudayama granodiorite along the river Kumozu. The cataclastic deformation is developed in the narrow zone.

b. Description of rock types and microstructures

The Kimigano granodiorite (Hayama *et al.* 1982) is

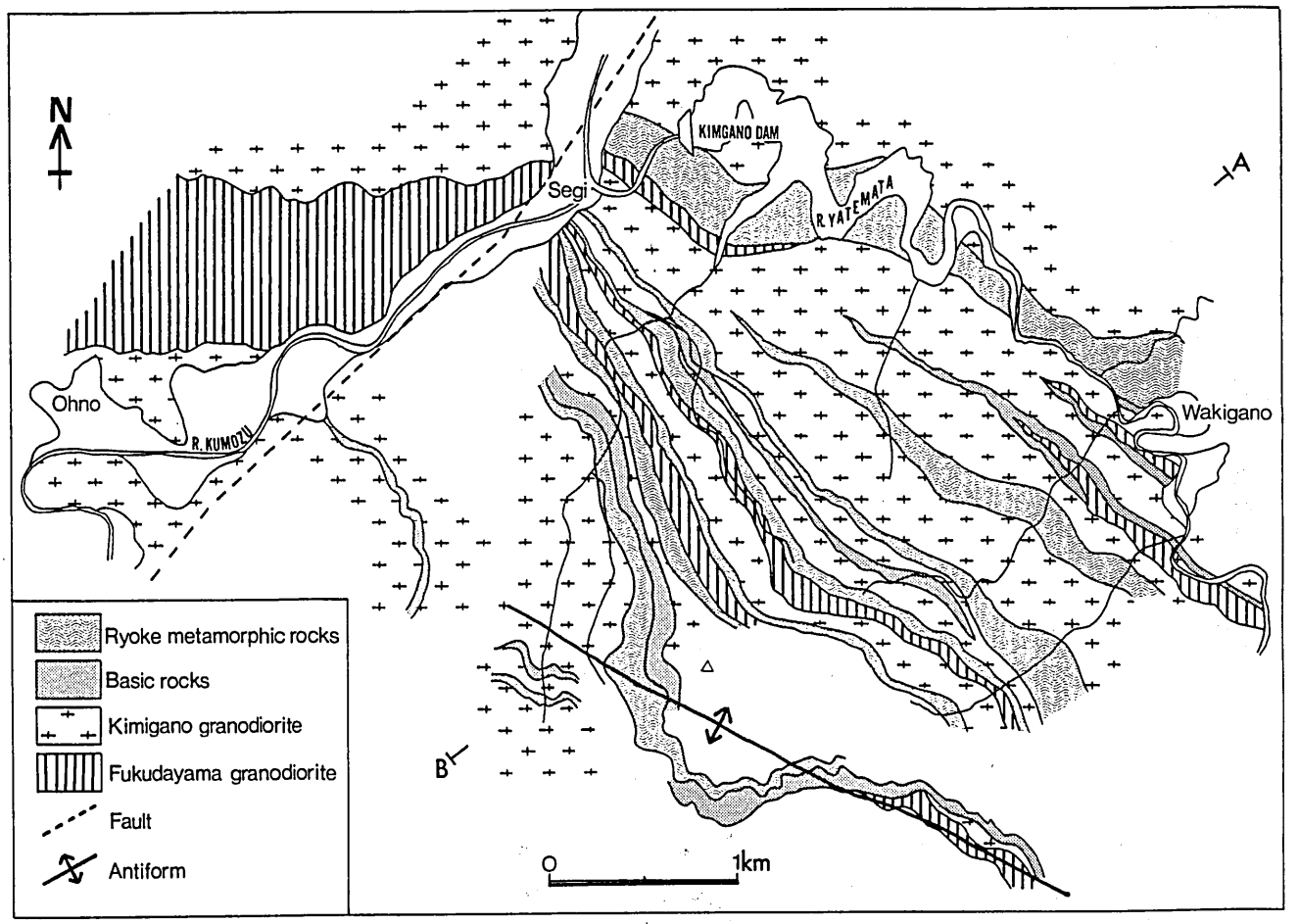

Fig. 32. Geological map of the Takehara district.

Fig. 33. Geological profile of the Takehara district on A-B line in Fig. 46.

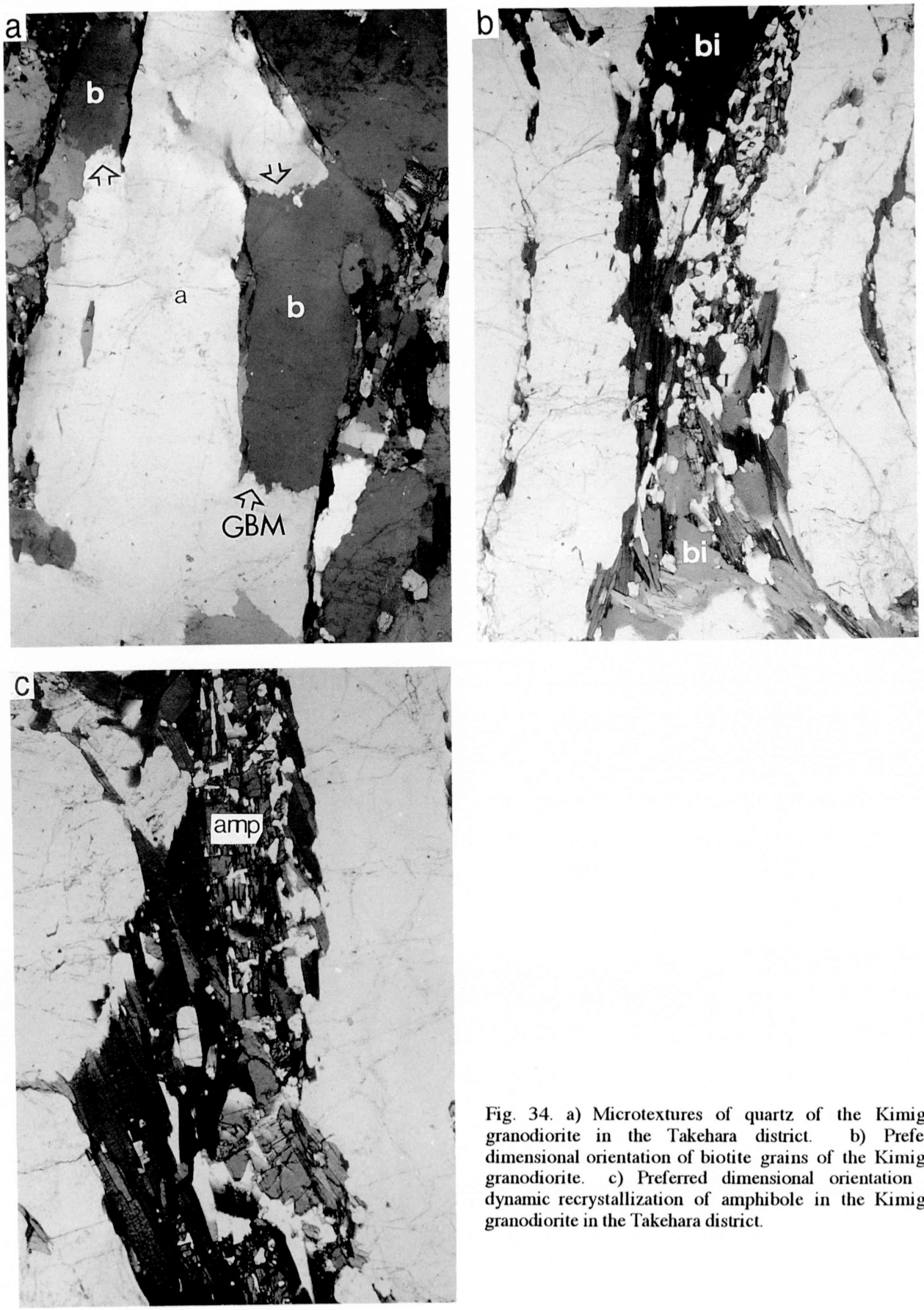

Fig. 34. a) Microtextures of quartz of the Kimigano granodiorite in the Takehara district. b) Preferred dimensional orientation of biotite grains of the Kimigano granodiorite. c) Preferred dimensional orientation and dynamic recrystallization of amphibole in the Kimigano granodiorite in the Takehara district.

exposed in the wide area of Takehara district. According to Hayama *et al.* (1982), it mainly consists of quartz, plagioclase, K-feldspar, biotite, amphibole (hornblende), ±clinopyroxene with accessory apatite, zircon, titanite and allanite. The intensity of the development of the foliation is varied within the district. Just below the Kimigano dam (near a intersection of the River Yatemata and River Kumozu) and in the south of the Lake Kimigano, the Kimigano granodiorite is strongly mylonitized.

The dynamically recrystallized grain size of quartz is relatively large (>500 μm) (Fig. 34a). The aspect ratio is randomly varied. The microstructure of quartz corresponds to irregular type of Masuda *et al.* (1989). The grain boundaries are complicated with the microbulging near the region in which the subgrain boundaries are well developed. Some of large quartz grains include the impure minerals (small biotite or amphibole). Plagioclase porphyroclasts show inequant external grain shapes. Some of the porphyroclasts show the microstructure from intracrystalline plastic deformation as undulatory extinction, formation of subgrains and deformation twining on (010) plane. Extensional fracturing of the porphyroclasts is moderately developed, which is mainly filled by large quartz grains and biotite. Myrmekite which is produced at compressional side of the K-feldspar porphyroclasts (Simpson & Wintsch 1989) is ubiquitous. K-feldspar porphyroclasts show undulatory extinction with the bending of grains, and no brittle microstructure. Biotite aggregates is continuously linked each other, which bound the quartz pools (Fig. 34b). New small biotite grains interstitially occur in the quartz-quartz grain boundaries or within the large quartz grains. Around the plagioclase and K-feldspar porphyroclasts, the biotite grains is bent with undulatory extinction. Amphibole in the granodiorite mainly occurs as aggregates of the small grains (Fig. 34c). Some of these small grains show synchronous extinction. These small grains may be produced by dynamic recrystallization (subgrain rotation) (Cumbest *et al.* 1989) without microfracturing .

The Fukudayama granodiorite (Hayama *et al.* 1982) is exposed in the central part of the Takehara district, which is a medium-coarse grained foliated biotite granodiorite, characterized by K-feldspar augen. It mainly consists of quartz, plagioclase, K-feldspar, biotite and ±amphibole with accessory apatite, allanite, opaque minerals and titanite (Hayama *et al.* 1982, present study). The mylonitic foliation is well developed in the granodiorite, which is defined by a preferred dimensional orientation of biotite, elongate quartz and layer of microaplite which consists of the fine-grained aggregates of quartz, plagioclase and K-feldspar. Also, the mylonitic lineation is well developed. Thus, L-S fabric is developed in the Fukudayama granodiorite, implying that plane strain provably dominate the mylonitization.

The size of quartz grains is relatively large and the aspect ratio is low. The microstructure of quartz in the Fukudayama granodiorite corresponds to the irregular type (Masuda *et al.* 1989) as well as in the Kimigano granodiorite. Plagioclase porphyroclasts show slightly inequant shape. Deformation twining with bending of the porphyroclasts is abundant. Dynamic recrystallization (subgrain rotation) of the plagioclase rarely occurs. Some of the porphyroclasts show extensional fracturing which is filled by large quartz grains. Myrmekite is ubiquitous in the Fukudayama granodiorite, which is found along K-feldspar grain boundaries that are parallel to the mylonitic foliation (S-foliation) direction (Simpson 1985, Simpson & Wintsch 1989). Some of the porphyroclasts show undulatory extinction. There is no brittle feature in the granodiorite. Biotite grains are divided into large porphyroclasts and recrystallized fine grains. Some of biotite porphyroclasts show asymmetrical 'mica fish' microstructure (Simpson & Schmid 1983). Undulatory extinction with bending of biotite grains occurs around plagioclase porphyroclasts.

C. Results

1. Microstructure of quartz

a. Microstructure of quartz in the Kasagi district

In the Sakawa granodiorite of the Kasagi district, dynamically recrystallized quartz grains show P type and/or regime 3 microstructure (Fig. 24d), which have low aspect ratios (<1.9). Average grain size of dynamically recrystallized grains is relatively large (>660 μm) in many samples (Fig. 35). A sample in the west of the Koya district show the lower grain size (278 μm).

Subgrain size is relatively large (few hundred μm) and its boundaries are dominantly prismatic with the misorientation angle of ca. 1-10° when expressed in term of the misorientation of the c-axis. Undulatory extinction is weakly developed. Direction of the elongation axis of the dynamically recrystallized grains is randomly oriented. Subbasal deformation lamellae occur in some quartz grains. Quartz pools are strongly elongated parallel to the mylonitic lineation, cut by the shear band foliation in the some samples.

b. Microstructure of quartz in the Oikawa district

All of microstructures for quartz in the Joryu tonalite of the Oikawa district are induced by plastic deformation (no brittle deformation). Spatial variation in average size of dynamically recrystallized quartz grains is shown in Fig. 36. It decreases down to 300 mm around the synform. Average

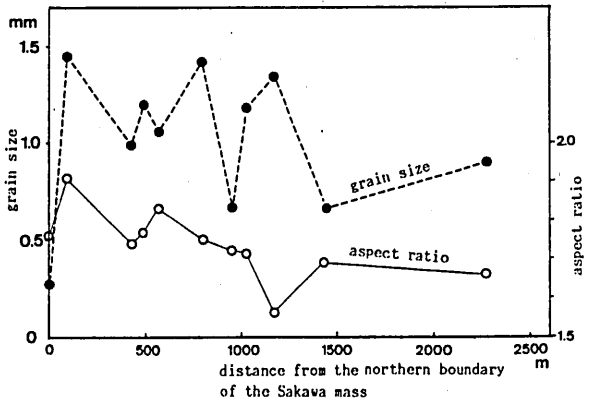

Fig. 35. Relationships between the average grain size and/or aspect ratio of dynamically recrystallized quartz and the distance from the northern boundary of the Sakawa granodiorite.

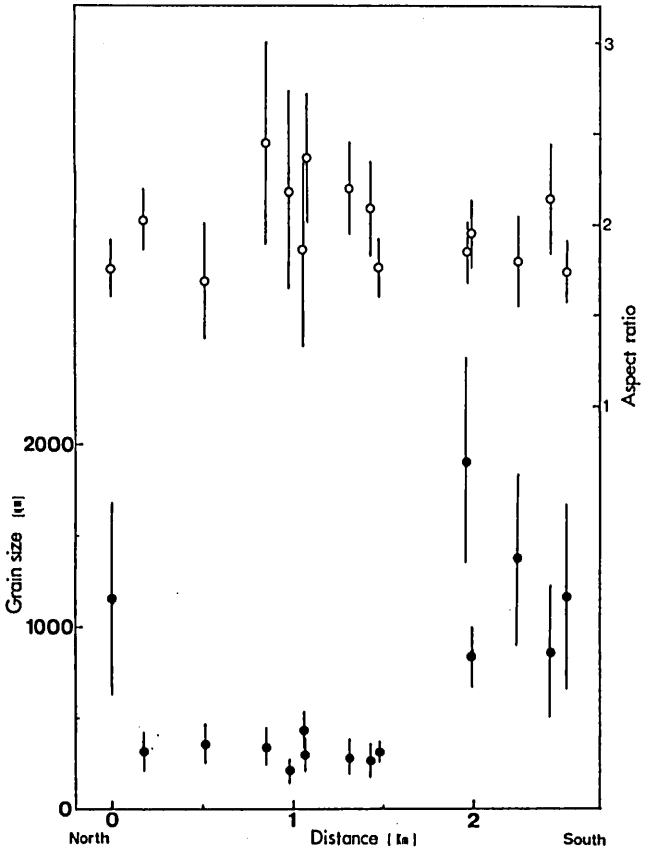

Fig. 36. Relationships between the average grain size and/or aspect ratio of dynamically recrystallized quartz and the distance from the northern boundary of the Joryu tonalite in the Oikawa district. Open circles: aspect ratio, solid circles: grain size, error bar: 95% confidence interval.

aspect ratio of the grains varies form 1.7 to 2.5. The recrystallized grains showing the higher values of aspect ratio are observed around the synform. Therefore, the average grain size and aspect ratio vary with the structural level. The average grain size is constant around the synform, since structural level is scarcely varied around that.

Microstructure of most of quartz grains is correlated to P type (Masuda & Fujimura 1981) and/or regime 3 microstructure (Hirth & Tullis 1992). However, a transitional type between P type (regime 3 microstructure) and S type (regime 2 microstructure) is observed in a sample showing highest aspect ratio (2.5). The grain boundaries within the quartz aggregates are slightly curved in weakly deformed samples. In strongly deformed samples, the grain boundaries are relatively serrate with microbulging particularly to the subgrain boundaries of the adjacent grains, which indicate high dislocation density. Most of subgrain boundaries are prismatic, implying that $<11\bar{2}0>$ slip direction dominate deformation. Subgrain rotation remarkably occurs near the grain boundaries, forming 'core and mantle' structure (White 1976).

Deformation lamellae oblique to the mylonitic foliation at angle of 30-40° are observed in the quartz grains showing high aspect ratio. In this sample (AH4), micro-heterogeneous shear zone illustrated by the trace of the grain shape and boundaries is developed (Fig. 27d). Thus, deformation within the sample is heterogeneous on microscopic scale. The heterogeneity is appeared to depend on spatial distribution of more rigid porphyroclasts of amphibole and plagioclase.

c. Microstructure of quartz in the Hakusan-Joryu district

The microstructures described in the above section suggest that the Joryu tonalite in the Hakusan-Joryu district is weakly deformed, and that the Ryoke metamorphic rocks are strongly mylonitized in the central part of district. The microstructure of quartz aggregates in siliceous gneiss without the retrogressive reaction, which shows large grain size and low aspect ratio, corresponds to duplex or irregular type of Masuda *et al.* (1989). The grain boundaries are complicated with microbulging due to grain boundary migration (Jessell 1986, Urai *et al.* 1986, Drury & Urai 1990). Subgrain boundaries in these grains are mainly basal, which imply that [0001] slip direction dominate intracrystalline plastic deformation.

On the other hand, the microstructure of quartz grains in the strongly deformed metamorphic rocks with retrogressive reaction of the sillimanite breakdown to muscovite indicates P and S type microstructure of Masuda & Fujimura (1981). These grains show small dynamically recrystallized grain size (<200 μm) and various aspect ratio. The dominantly grain boundary grains is relatively straight or slightly curved in P type aggregates and is serrate with microbulging in S type aggregates. Dynamic recrystallization mechanism is subgrain rotation, which resulted in the misorientation between adjacent grains bounded by prismatic subgrain boundaries. Undulatory extinction strongly develops. Some samples of the Ryoke metamorphic rocks show transitional microstructures between P type and duplex type.

d. Microstructure of quartz in the Takehara district

In the Takehara district, the microstructure of quartz in the Kimigano granodiorite and Fukudayama granodiorite is characterized by large grain size (>500 μm), low aspect ratio (1.6-1.8), corresponding to irregular type. The microbulging toward high dislocation density region as subgrain boundaries occurs in the quartz aggregates. The large quartz grains include isolate impure minerals as biotite, amphibole and plagioclase. The smaller quartz grains isolated around the very large quartz grains, which appear to indicate same color under gypsum plate show synchronous extinction, corresponding to 'left over' grains (Urai *et al.* 1986) (Fig. 34a). Subgrain boundaries are basal and prismatic. The large quartz grains are divided into rectangular domains of the subgrains surrounded by the two type of the subgrain boundaries (kink band boundaries ?).

2. Lattice preferred orientation of quartz

a. Lattice preferred orientation of quartz in the Kasagi district

Quartz c-axis fabrics of the Sakawa granodiorite are shown in Fig. 37. The types of the c-axis fabrics can be divided into three patterns as followings;

(1) Cleft girdle pattern (samples KA12, KA16 and KA24)

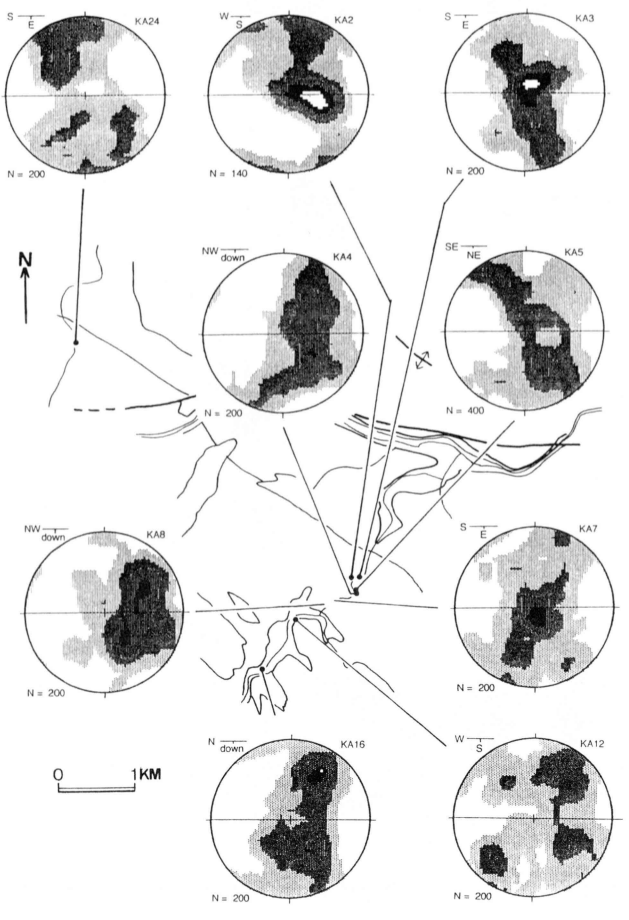

Fig. 37. Quartz c-axis fabrics from the Sakawa granodiorite in the Kasagi district. Contour interval = 2σ (Kamb method), n = number of c-axes.

(Price 1985). The developed maxima or skeletal outlines are asymmetrically distributed (samples KA5 and KA24). Degree of the c-axes dispersion is stronger than that for the other patterns.

(2) Type-II crossed girdle pattern (samples KA3, KA5 and KA7) (Lister 1977). The maximum of c-axes is developed near Y of the finite strain in both samples. The pattern for sample KA3 shows asymmetrical distribution of the skeletal outline to the mylonitic foliation (Lister & Hobbs 1980). There is a complete transition between this pattern and cleft pattern.

(3) Single girdle pattern (samples KA2, KA4, KA8 and KA16) (Burg & Laurent 1978). These patterns have a sigmoidal trend with two inclined maxima (samples KA4 and 8) or a single centered maximum (KA2). Pole of the girdle for two samples (KA4 and KA8) is oblique to the mylonitic lineation on the mylonitic foliation at angle of ca. 20° as well as Simpson (1980).

b. Lattice preferred orientation of quartz in the Oikawa district

Quartz c-axis fabric patterns in the Oikawa district measured by universal stage are shown Figs. 38 & 39. The patterns can be divided as follows.

(1) Random or dispersed maximum pattern (samples AH1, AH10, AH12 and AH21). The maximum in these samples display low concentration of c-axes less than 10s, although it is significantly located near X of the finite strain.

(2) Type-I crossed girdle pattern (samples AH2, AH7, AH8, AH9, AH14, AH16 and AH23) (Lister 1977, Lister & Williams 1979). In many samples (AH7, AH8, AH9 and AH16), this pattern is accompanied by the double maxima on YZ plane at angles of 20-50° from the mylonitic foliation. Some samples (AH8, AH16 and AH23) show transitional feature between type-I crossed girdle and cleft girdle pattern.

(3) Type-II crossed girdle (sample AH13) Lister 1977). It shows maximum near Y and between X and Z of the finite strain. Both girdles are crossed at angle of 10-20° from the mylonitic foliation (not just in Y). Therefore, it may be a transitional pattern between type-II crossed girdle and type I crossed girdle.

(4) Single girdle pattern (samples AH4 and AH6). These show maximum in Y and submaxima near Z. There is a indistinct transition between this pattern and type-II crossed girdle pattern (sample AH6).

d. Lattice preferred orientation of quartz in the Hakusan-Joryu district

The quartz c-axis fabric pattern in the siliceous gneiss showing this microstructure indicates a XY girdle with asymmetrical concentration near X (sample HK7 in Fig. 40). On the other hand, In the region with the retrogressive metamorphism and grain size reduction of quartz, the quartz c-axis fabric patterns correspond to asymmetrically arranged type-I crossed girdle (HA 32), type-II crossed girdle (Lister 1977) with asymmetrically distributed submaxima near Y and Z (sample HK3) and incomplete single girdle with maximum in Y of finite strain (HA38).

The quartz c-axis LPO pattern from the sample which indicates transitional features of microstructures of quartz between P type and duplex type (sample HK12) shows a slightly asymmetrical type-II crossed girdle with maximum at Y of the finite strain. This LPO pattern show slightly transitional feature to cleft girdle.

d. Lattice preferred orientation of quartz in the Takehara district

The quartz c-axis fabric patterns are shown in Fig. 41. These patterns can be divided into as follows;

(1) incomplete single girdle with maximum between Y and Z (sample KM3).

(2) X-point maximum (Schmid *et al.* 1983, Blumenfeld *et al.* 1986) (sample TA9A, TA9B, TA9D, KM2 and KM302). These patterns show asymmetrical distribution of c-axes with respect to the mylonitic foliation. There are sub-maxima around Y and Z of the finite strain. Some samples show transitional feature between X-point maximum and type-II crossed girdle (sample TA9B and TA9D).

(3) Incomplete type-II crossed girdle with maximum in Y (sample TA5, TA6, TA8 and KM137). There are submaxima between X and Z.

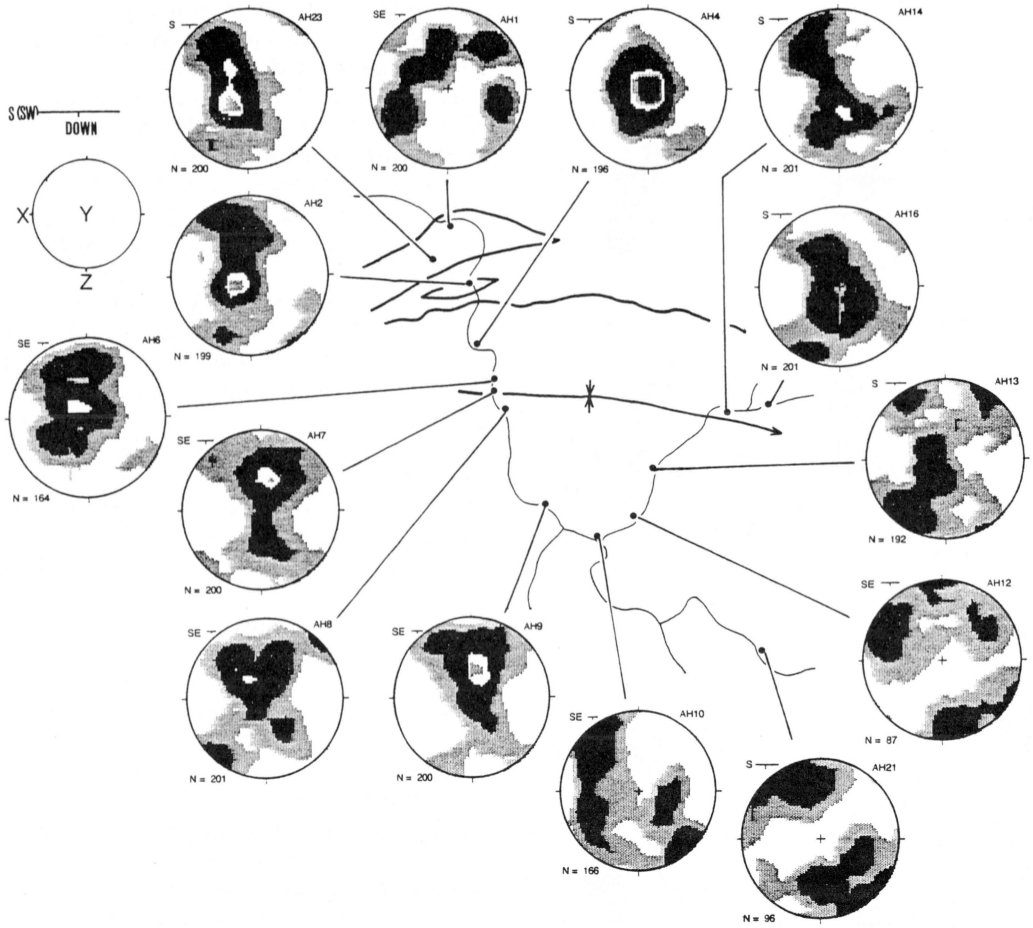

Fig. 38. Quartz c-axis fabrics from the Joryu tonalite in the Oikawa district. Contour interval = 2σ (Kamb method), n = number of c-axes.

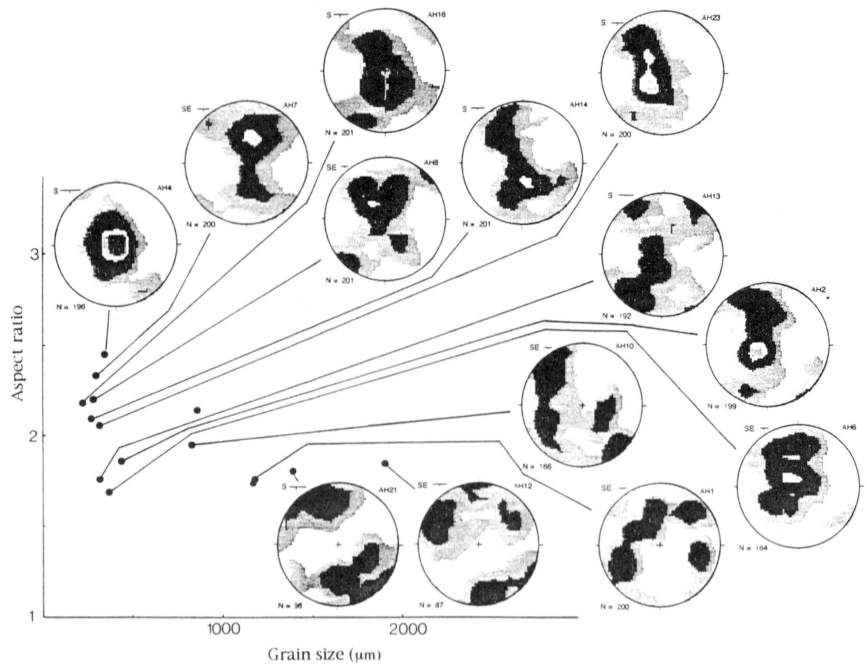

Fig. 39. Quartz c-axis fabric from the Joryu tonalite in the Oikawa district on the average size of dynamically recrystallized quartz grain vs average aspect ratio diagram.

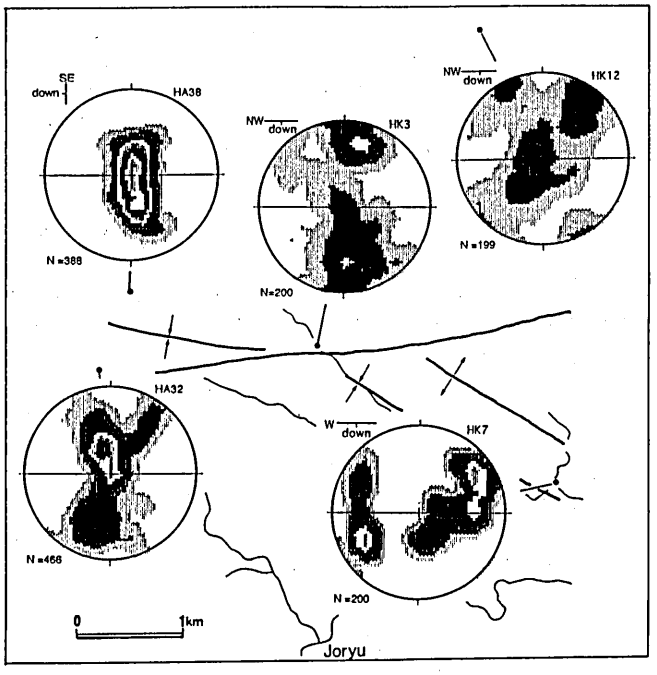

Fig. 40. Quartz c-axis fabrics from the Ryoke metamorphic rocks in the Hakusan-Joryu district. Contour interval = 2σ (Kamb method), n = number of c-axes.

(4) Double maxima in the XZ plane (sample TA1, TA2 and TA3). These maxima are symmetrically distributed at angle of 40-50° from the mylonitic foliation.

(5) XY girdle with maxima in Y (KM5). There is a asymmetrical sub-maximum between X and Z (Hippertt 1993), whose direction is subparallel to the shear band foliation (C').

Fig. 42 shows <11$\bar{2}$0>, <10$\bar{1}$0> and <10$\bar{1}$4> LPO patterns of sample TA9D, which are measured by X-ray texture goniometer (see section III-F-1 about measurement method). The <11$\bar{2}$0> maximum is located at angle of 30° from X, which is subparallel to the c-axis maximum. There is a sub-maximum near Z at angle of the 90° from the maximum. On the other hand, <10$\bar{1}$0> pattern shows a Z-point maximum.

3. Chemical analysis of feldspars and amphiboles

a. Chemical composition of myrmekitic plagioclase and K-feldspar in the pressure shadow from the Kimigano granodiorite in the Takehara district

Chemical composition of myrmekitic plagioclase along the grain boundary of K-feldspar porphyroclasts and K-feldspar precipitated in the pressure shadow domain of the K-feldspar porphyroclasts in the Kimigano granodiorite in the Takehara district is measured using EPMA, in order to estimate the deformation temperature. These results are shown in Fig. 15 and Table 2. The myrmekitic

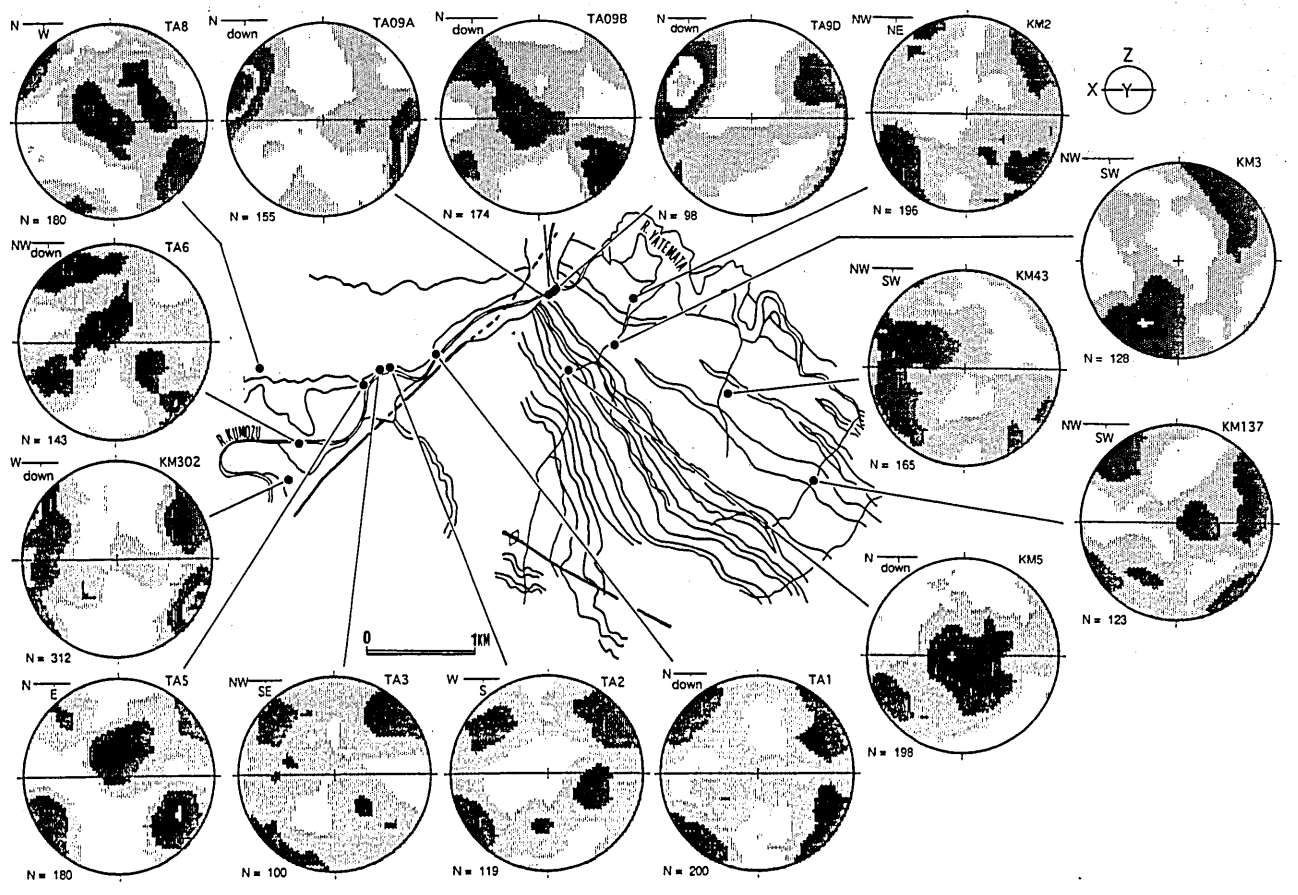

Fig. 41. Quartz c-axis fabrics from the Takehara district. Contour interval: 2σ (Kamb's method), n = number of quartz c-axes.

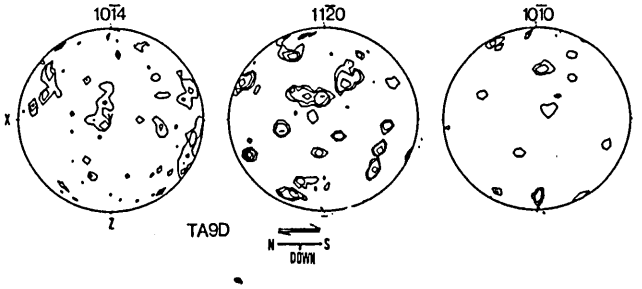

Fig. 42 Pole figures of the second order prisms (11$\bar{2}$0), first order prisms (10$\bar{1}$0) and π (10$\bar{1}$4) for sample TA9D. The contours are given in multiples of a uniform distribution. Asymmetry of (10$\bar{1}$4) pole shows southward directed sense of shear. Note significant concentration of pole to (11$\bar{2}$0) and (10$\bar{1}$0) near the maximum compression direction (Z), suggesting that the (11$\bar{2}$0) and (10$\bar{1}$0) plane dominate slip plane.

plagioclases range in composition from Ab_{61} to Ab_{63} which are significantly lower than that in the Ryoke southern marginal shear zone. The K-feldspars in the pressure shadows show Or_{90} in composition as well as in the USL of he Kayumi district. Its mole fraction is slightly higher than that of the porphyroclastic host K-feldspar grains (Or_{86-89}).

b. Total Al and Ti content of amphibole

Pressure during crystallization of the tonalite and the mylonitization is examined using barometer of total Al content of amphibole. Furthermore, Ti content in amphibole is good indicator of metamorphic grade. The chemical composition of core and rim of matrix amphiboles and of core of amphibole included within plagioclase in the Joryu tonalite in the Oikawa and Hakusan Joryu tonalite, and in the Kimigano granodiorite in the Takehara district is measured. The results of the electron microprobe analysis are shown in Table 4, 5 and 6 and Fig. 43.

In the Oikawa district, the rim composition of matrix amphibole is measured near fractured space and pressure shadow. The total Al content (Al^T) in the core of matrix amphibole, which is averaged per sample, ranges from 1.58 to 1.65. The averaged Al^T in the rim of matrix amphibole ranges from 1.36 to 1.72. The averaged Al^T in the core of amphibole included with in plagioclase is 1.70. The averaged Ti content in the core and rim of matrix amphibole ranges from 0.22 to 0.27 and from 0.06 to 0.22 respectively. The Ti content in the rim of strongly mylonitized rocks tend to be lower than that in the less mylonitized rocks.

In Joryu tonalite of the Hakusan-Joryu district, difference of the averaged Al^T between the core and rim of matrix amphibole is small, ranging from 1.52 to 1.70. In many samples, the Al^T content in the rim is higher than that in the core. The averaged Ti content in the core and rim ranges from 0.22 to 0.28. The Ti content slightly decreases from the core (ca. 0.27) toward the rim (ca. 0.23).

In the Kimigano granodiorite Takehara district, the chemical composition of amphibole is measured for two samples (TA9D and KM304). The averaged Al^T content in the core and rim of matrix amphibole ranges from 1.44 to 1.72. The averaged Ti content in the matrix amphibole ranges from 0.10 to 0.26.

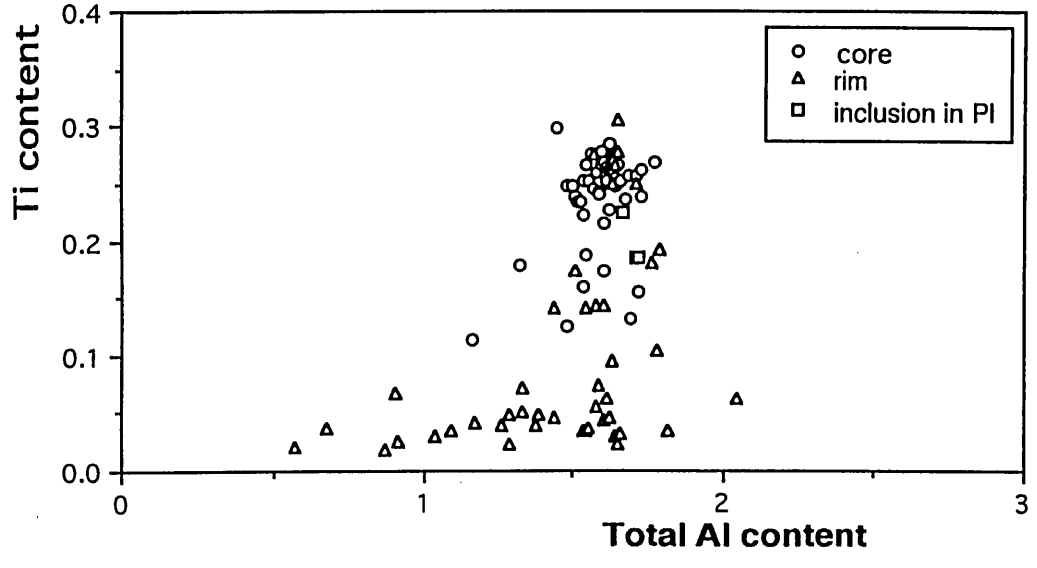

Fig. 43. Compositional variation in Al^T and Ti of amphibole in the Oikawa district. Pressure is calculated from Schmidt (1992).

Table 4. Representative chemical composition of amphibole of the Joryu tonalite in the Oikawa district.

Sample No.	AH12-a02 core	AH12-c03 core	AH3-b02 core	AH3-a04 rim	AH21-b02 core	AH21-b-06 rim	AH16-a11 core	Ah16-d09 rim
SiO_2 (wt%)	43.26	43.30	43.20	45.93	43.14	43.79	43.70	47.54
TiO_2	1.46	1.56	1.76	0.31	1.70	1.18	1.74	0.19
Al_2O_3	10.43	10.21	10.01	9.00	11.18	11.45	10.39	6.73
FeO	21.02	20.93	20.73	21.09	20.99	20.99	21.30	21.36
MnO	0.52	0.60	0.55	0.68	0.65	0.60	0.64	0.71
MgO	6.98	7.15	7.09	7.68	6.96	6.87	7.20	8.35
CaO	11.59	11.71	11.70	12.08	11.56	11.73	11.72	12.21
Na_2O	1.26	1.15	1.22	0.71	1.16	1.06	1.13	0.61
K_2O	1.40	1.37	1.32	0.61	1.44	1.22	1.41	0.50
Total	97.92	97.97	97.58	98.02	98.78	98.87	99.19	98.20
Si	6.723	6.724	6.739	7.072	6.647	6.727	6.699	7.298
Ti^C	0.227	0.242	0.275	0.048	0.262	0.180	0.266	0.029
Ti^T	0.000	0.000	0.000	0.000	0.000	0.000	0.000	0.000
Al^{IV}	1.277	1.276	1.261	0.928	1.353	1.273	1.301	0.702
Al^{VI}	0.343	0.309	0.300	0.457	0.370	0.486	0.292	0.332
Fe^{2+}	2.808	2.801	2.870	2.857	2.819	2.821	2.834	2.951
Fe^{3C}	0.459	0.448	0.364	0.390	0.416	0.402	0.434	0.328
Fe^{3T}	0.000	0.000	0.000	0.000	0.000	0.000	0.000	0.000
Mn	0.081	0.093	0.086	0.096	0.101	0.092	0.098	0.110
Mg	1.085	1.109	1.106	1.182	1.072	1.055	1.105	1.282
Ca	1.801	1.819	1.825	1.860	1.782	1.802	1.798	1.874
Na^B	0.196	0.178	0.175	0.109	0.179	0.160	0.173	0.094
Na^A	0.000	0.000	0.016	0.000	0.000	0.000	0.000	0.000
K	0.217	0.213	0.206	0.094	0.222	0.187	0.216	0.077
Total	15.217	15.213	15.222	15.094	15.222	15.187	15.216	15.077

Sample No.	Av. Al^T	Pressure (kb)
AH12 core	1.62	4.7
AH12 inc.in Pl	1.70	5.1
AH3 core	1.58	4.5
AH3 rim	1.51	4.2
AH21 core	1.65	4.8
AH21 rim	1.72	5.2
AH16 core	1.54	4.3
AH16 rim	1.36	3.5

Pressures are calculated by Schmidt (1992)'s equation.

4. Sense of shear

The kinematics of the ductile shear zone have been analyzed using the following microstructural kinematic indicators (see Simpson & Schmid 1983, and Cobbold *et al.* 1987):

(1) S-C relationships (Berthe *et al.* 1979, Lister & Snoke 1984) on both the microscopic and mesoscopic scales.

(2) Shear band foliation composed of recrystallized mica aggregates (C'-planes) (Ponce de Leon & Choukroune 1980, Platt & Vissers 1980, Dennis & Secor 1987).

(3) Asymmetric recrystallized tails around feldspar porphyroclasts (Simpson & Schmid 1983).

(4) Asymmetrical mica fish of biotite porphyroclasts (Eisbacher 1970, Simpson & Schmid 1983, Lister & Snoke 1984). The clasts-tail systems show σ-type geometry (Passchier & Simpson 1986) (Fig. 24c).

(5) Asymmetric quartz c-axis fabrics (Etchecopar 1977, Burg & Laurent 1978, Lister & Williams 1979, Lister & Hobbs 1980, Bouchez & Pecher 1981, Behrmann & Platt 1982)

(6) 'V'-shaped extensional fracturing (Hippertt 1993). It is reliable in case that fractured space shows large width or large number. However, the sense of shear determined from this microstructural criteria does not identical with that from the other microstructures in some specimens.

(7) Oblique foliation of elongate quartz subgrains and dynamically recrystallized grains (Brunel 1980, Simpson & Schmid 1983, Burg 1986).

(8) Asymmetrical boudinage of the xenolithic Ryoke metamorphic rocks in the older Ryoke granitic rocks on the mesoscopic scale (Goldstein 1988).

(9) Geometrical relationship between mesoscopic-scaled shear zone and foliation trajectory around this shear zone (Ramsay 1980).

In the Kasagi district, sense of shear is determined from criteria (1), (2), (3), (4) and (5) (Fig. 24c, Fig, 37). Oblique foliation in dynamically recrystallized quartz aggregates (Brunel 1980, Etchecopar & Vasseur 1987) is not significantly developed in all samples. Four localities distributed throughout Sakawa granodiorite of the studied

Table 5. Representative chemical composition of amphibole in the Joryu tonalite of the Hakusan-Joryu district

Sample No.	HA2-a15 core	HA2-b11 rim	HA4-c18 core	HA4-c28 rim	HA11-a6 core	HA11-c5 rim	HA7-b02 core	HA7-c6 rim
SiO_2 (wt%)	43.24	42.96	43.20	43.1	42.12	43.58	43.74	42.46
TiO_2	1.53	1.18	1.56	1.452	1.65	1.57	1.90	1.58
Al_2O_3	10.98	10.34	10.67	10.87	10.42	11.05	10.24	10.48
FeO	20.57	20.59	20.97	20.70	21.51	21.91	21.72	21.85
MnO	0.65	0.66	0.58	0.53	0.61	0.66	0.70	0.69
MgO	6.83	7.54	6.64	6.53	6.88	6.51	6.71	6.84
CaO	12.01	12.00	12.02	12.10	11.67	11.56	11.47	11.64
Na_2O	1.11	1.16	1.05	0.94	1.15	1.13	1.27	1.11
K_2O	1.45	1.30	1.46	1.47	1.23	1.25	1.18	1.19
Total	98.36	97.72	98.16	97.72	97.23	99.21	98.92	97.83
Si	6.708	6.707	6.716	6.740	6.528	6.672	6.712	6.590
Ti^C	0.237	0.184	0.242	0.227	0.258	0.241	0.292	0.245
Ti^T	0.000	0.000	0.000	0.000	0.000	0.000	0.000	0.000
Al^{IV}	1.292	1.293	1.284	1.260	1.418	1.328	1.288	1.410
Al^{VI}	0.412	0.321	0.375	0.438	0.211	0.364	0.283	0.216
Fe^{2+}	2.906	2.739	2.963	3.020	2.689	2.893	2.900	2.700
Fe^{3C}	0.285	0.475	0.297	0.214	0.672	0.463	0.433	0.692
Fe^{3T}	0.000	0.000	0.000	0.000	0.000	0.000	0.000	0.000
Mn	0.101	0.104	0.090	0.082	0.096	0.100	0.108	0.107
Mg	1.059	1.177	1.032	1.019	1.075	0.997	1.030	1.062
Ca	1.862	1.873	1.869	1.890	1.824	1.770	1.760	1.807
Na^B	0.318	0.127	0.131	0.110	0.176	0.172	0.194	0.172
Na^A	0.034	0.054	0.031	0.036	0.004	0.000	0.000	0.000
K	0.225	0.202	0.227	0.229	0.191	0.192	0.181	0.185
Total	15.259	15.256	15.259	15.265	15.195	15.192	15.181	15.185

Sample No.	$Av.Al^T$	Pressure (kb)
HA2 core	1.67	5.2
HA2 rim	1.62	4.7
HA4 core	1.65	4.8
HA4 rim	1.70	5.1
HA11 core	1.61	4.7
HA11 rim	1.70	5.1
HA8 core	1.52	4.2
HA8 rim	1.57	4.5
HA7 core	1.61	4.6
HA7 rim	1.64	4.8
HA5 core	1.61	4.6
HA5 rim	1.72	5.2

Pressures are calculated by Schmidt (1992)'s equation.

area display a top to the SE-ward directed sense of shear, although one localities display a NW-ward directed sense of shear and three locality no sense of shear (no or less rotational component of the finite strain) (Fig. 44).

Sense of shear for each samples in the Oikawa district is shown in Fig. 45. It is determined from criteria (4), (5), (6) and (7). In the strongly deformed sample (AH4), this microstructure is accompanied with the micro-heterogeneous shear zone (Fig. 27d).

The determined sense of shear is not regular throughout the Oikawa district, although top to the southward directed sense of shear dominate mylonitization. The problem if the bulk sense of shear is southward directed or conjugate shear zone system was developed under no rotational component of the bulk finite strain remains unsolved. However, asymmetry of the quartz LPOs indicates that ratio of simple shear and pure shear strain component (non-coaxiality) in the upper structural level (near the synform) is higher than that in the lower structural level. Therefore, magnitude of non-coaxiality intermittently increases toward the upper structural level. The center of the shear zone may be located near the synform or above the present exposure.

Sense of shear in the Hakusan-Joryu district is determined by criteria (2), (4), (5) and (7) (Fig. 45). Samples with retrogressive mylonitization (HK3, HA 38) shows a top to the SE-ward directed sense of shear with some component of vertical slip. In the other samples, the non-coaxiality is too low to determine the sense of shear. It is hypothetically suggested that non-coaxiality during the retrogressive mylonitization is higher than that before the mylonitization.

Table 6. Representative chemical compositions of amphiboles in the Kimiganogranodiorite of Takehara district

Sample No.	TA9D-c06 core	TA9D-c07 core	KM304-a03 core	KM304-b03 rim	KM43-c05 core	KM43-e06 rim
SiO_2 (wt%)	45.69	44.27	39.50	42.26	41.80	41.57
TiO_2	0.88	0.94	1.76	1.42	1.65	1.27
Al_2O_3	9.49	9.97	10.70	11.23	10.91	11.44
FeO	21.50	21.81	24.88	24.61	25.73	25.09
MnO	0.66	0.78	0.76	0.78	0.84	0.74
MgO	7.66	7.38	4.92	4.83	4.54	4.32
CaO	11.99	11.62	11.91	11.61	10.92	11.26
Na_2O	1.06	1.21	1.19	1.34	1.51	1.21
K_2O	1.04	1.10	1.43	1.35	1.46	1.48
Total	99.98	99.60	97.06	99.44	99.35	98.36
Si	6.926	6.778	6.222	6.462	6.405	6.435
Ti^C	0.133	0.143	0.278	0.218	0.253	0.196
Ti^T	0.000	0.000	0.000	0.000	0.000	0.000
Al^{IV}	1.074	1.222	1.685	1.538	1.595	1.565
Al^{VI}	0.365	0.304	0.000	0.180	0.076	0.207
Fe^{2+}	2.813	2.693	2.772	2.843	2.923	2.960
Fe^{3C}	0.446	0.647	1.055	0.921	1.020	0.924
Fe^{3T}	0.000	0.000	0.093	0.000	0.000	0.000
Mn	0.101	0.119	0.120	0.119	0.128	0.115
Mg	1.165	1.130	0.775	0.739	0.696	0.668
Ca	1.817	1.779	1.877	1.775	1.673	1.743
Na^B	0.160	0.185	0.123	0.205	0.231	0.187
Na^A	0.000	0.000	0.065	0.000	0.000	0.000
K	0.157	0.169	0.225	0.206	0.224	0.229
Total	15.157	15.169	15.290	15.206	15.224	15.229

Sample No.	Av. Al^T	pressure (kb)
TA9D	1.44	3.8
KM304 core	1.67	4.9
KM304 rim	1.72	5.2
KM43 core	1.68	5.0
KM43 rim	1.80	5.6

Pressure is calculated from Schmidt(1992)'s equation

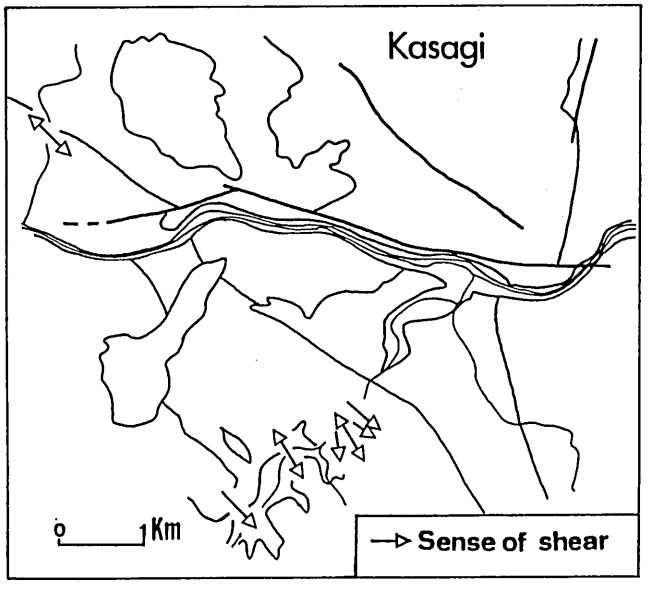

Fig. 44. Diagram showing sense of shear in the Kasagi district of the Ryoke inner shear zones. Arrows indicate relative displacement direction of the hanging wall.

The sense of shear of the ductile shear zone in the Takehara district have been determined using criteria (2), (3), (5), (8) and (9). The determined sense of shear is shown in Fig. 46. In the shear zone, at 6 localities the microstructures suggest a southward directed sense of shear (i.e. a southward displacement of the hanging wall of the shear zone), and at 6 locality a northward directed sense of shear. In the other localities, asymmetrical microstructure is not or weakly developed. The more strained samples which show c-axis maximum more than 10s, tend to indicate southward directed sense of shear. While, in the northern domain of this district a macroscopic drag fold of the Ryoke metamorphic rocks develops, indicating northward directed sense of shear. In the domain, sense of shear from the macroscopic structure shows good agreement with that from the mesoscopic to microscopic structures.

D. Discussion

1. Deformation condition

a. Deformation temperature estimated from microstructure and Lattice preferred orientation of quartz

As mentioned in chapter III.D.1, microstructure and lattice preferred orientation of quartz are good indicators of temperature. Quartz aggregates in the RISZ show variable

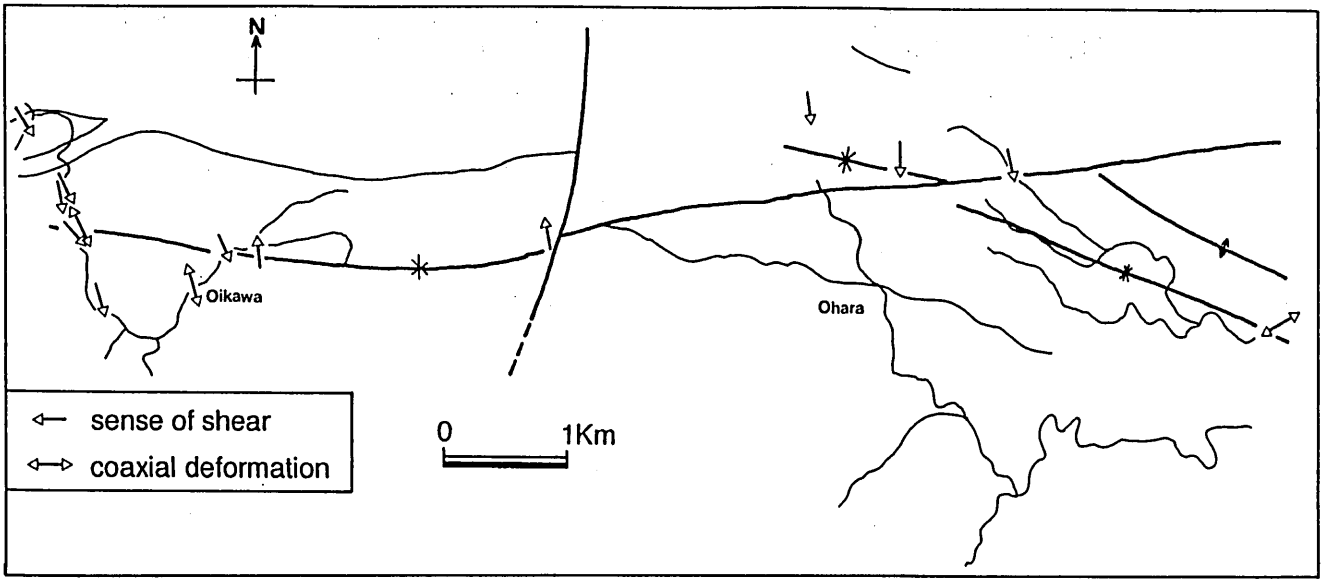

Fig. 45. Diagram showing sense of shear in the Oikawa and Hakusan-Joryu district.

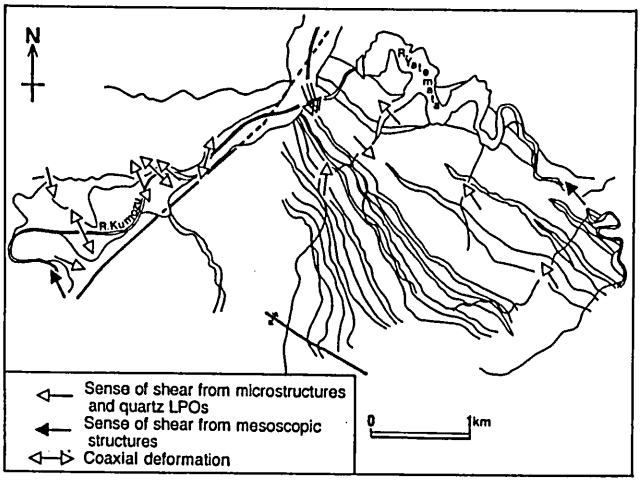

Fig. 46. Diagram showing sense of shear in the Takehara district.

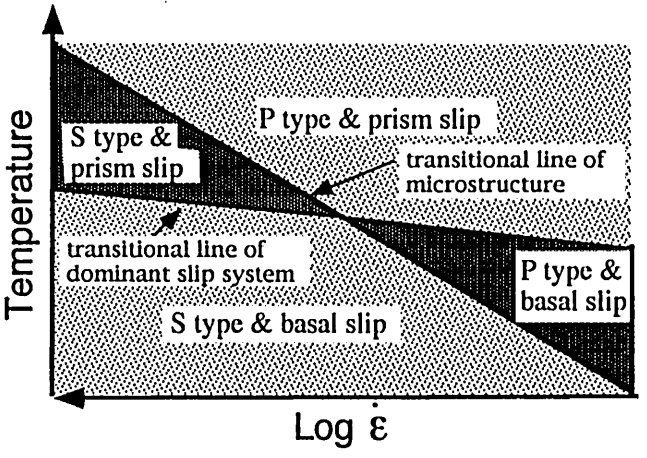

Fig. 47. The regions of each microstructural and LPO's pairs on temperature vs strain rate diagram.

microstructure; S type (resume 2) microstructure, P type (resume 3) microstructure irregular microstructure and duplex microstructure (Masuda & Fujimura 1981, Masuda *et al.* 1991 Hirth & Tullis 1992). These microstructural variation depends on temperature, strain rate and water content etc., since these factors control the mechanisms of dynamic recrystallization as recovery processes (Urai et al. 1986, Drury & Urai 1990). Further strictly speaking, the dislocation climb velocity (Vc)and the velocity of grain boundary migration (Vm) are function of temperature and stress (Gordon & Vandermeer 1966, Nicolas & Poirier 1977, Argon & Maffatt 1981, Poirier 1985), defined by

$$V_C = 2\pi\sigma\Omega D_0 \exp(-\Delta H_{SD}/kT)/kTl \qquad (1)$$

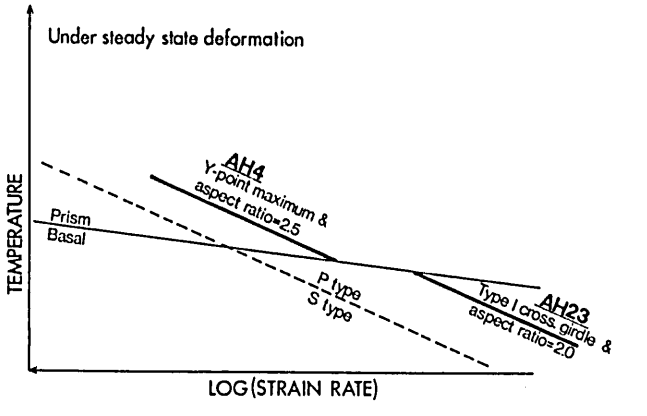

Fig. 48. Diagram showing variation in deformation temperature and strain rate. Microtextures and LPO patterns indicate that sample AH4 was deformed at higher temperature and faster strain rate than sample AH23.

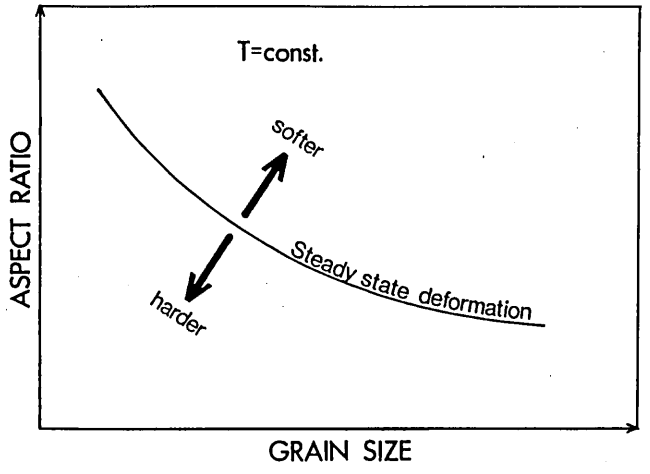

Fig. 49. Strain softening (or hardening) meter from the dynamically recrystallized grain size and aspect ratio. Assuming temperature is constant, there is a relationship between the dynamically recrystallized grain size and aspect ratio under steady state deformation.

$$V_M = FM = FM_0 \exp(-\Delta H_{GBM}/kT) \qquad (2)$$

respectively, where Ω is the atomic volume, σ is the differential stress, D_0 is a material constant with reference to self diffusion coefficient, l is the average distance from the dislocation at which the vacancy concentration is C_0, k is the Boltzmann's constant, ΔH_{SD} is the activation enthalpy for self diffusion, F is the driving force of grain boundary migration related to the difference in dislocation density between adjacent grains, M is the grain boundary mobility, Mo is the material constant with respect to the grain boundary mobility and ΔH_{GBM} is the activation enthalpy for grain boundary migration. Therefore, both velocities of dislocation climb and grain boundary migration exponentially increase with increasing temperature.

Also, strain rate indirectly affects both the velocities. Decrease in the velocity of dislocation climb results from decreasing strain rate ($\dot{\varepsilon}$) positively related to differential stress (σ) under steady state deformation: $\dot{\varepsilon} \propto A\sigma^n$. Previous results of experiments for the analogue materials empirically suggested that the driving force for a grain boundary migration (F) increases with increasing differential stress (Guillopé & Poirier 1979, Poirier & Guillopé 1979, Urai et al. 1986). And these experimental results suggested that the mechanism of dynamic recrystallization changes from subgrain rotation to grain boundary migration with increasing strain rate and consequently differential stress at given temperature (Guillopé & Poirier 1979, Tungatt & Humphreys 1981). However, in the case of dynamic recrystallization of quartz, the dominant mechanism of dynamic recrystallization changes from large scaled-grain boundary migration via subgrain rotation and finally to local grain boundary migration with increasing strain rate (Hirth & Tullis 1992). If the grain boundary migration produced by the experiments by Guillopé & Poirier (1979) and Tungatt & Humphreys (1981) are large scaled one, the strain rate (and/or differential stress) dependence on the transition of mechanism of dynamic recrystallization from subgrain rotation to grain boundary migration is obscure.

Around the center of the RISZ of the Kasagi, Oikawa and Hakusan-Joryu district, the microstructures of quartz are correlated to S type (resume 2) and P type (resume 3). The grain size is critically decreases down to 200-300 μm toward center of the shear zones. These features suggest that subgrain rotation dominates the recovery mechanism during dynamic recrystallization of quartz, although the subordinate mechanism is grain boundary migration in the Kasagi district. Therefore, deformation in these districts appears to be occurred at relatively low temperature (or faster strain rate). It is supported by dominant brittle deformation of plagioclase porphyroclasts (Tullis & Yund 1977, Pryer 1992, Fitz Gerald & Stünitz 1993).

The quartz LPO patterns in the Kasagi, Oikawa and Takehara district are correlated with type-I crossed girdle, type-II crossed girdle, Y-point maximum and cleft girdle. These patterns indicate that the prism<a> and basal<a> slips dominate deformation. Occurrence of prismatic subgrain boundary also implies that dominant slip direction is <a>. Dominant prism<a> and basal <a> slip implies that the mylonitization occurred at intermediate temperature around 500 °C and low temperature around 400 °C under general strain rate respectively (Schmid & Casey 1986, Mainprice & Bouchez 1987, Krohe & Eisbacher 1988). In these districts of RISZ, mylonitization occurred at intermediate and low temperature (MT and LT), as deduced from microstructures and LPO patterns of quartz.

As mentioned above, prism<a> slip is dominant at higher temperature than basal <a> slip (Blacic 1975). For example, in the Oikawa and Hakusan-Joryu district the transition of LPO patterns from type-I crossed girdle to Y-point maximum (Fig. 39 and 40), implying that deformation temperature is spatially different. However, concerning with the microstructure, there is also difference of strain rate as follows.

Masuda & Fujimura suggested that the microstructural transition from S type to P type depends on temperature and strain rate (or differential stress). S type microstructure is produced at faster strain rate or lower temperature than P type microstructure. Afterward, Hirth & Tullis (1991) suggested that distinct three microstructures (regime 1, 2 & 3) are produced at different strain rate and temperature (Fig. 18). Regime 2 microstructure corresponds to S type of Masuda & Fujimura (1981) and regime 3 microstructure to P type. The line of transition between S type and P type shows positive relationship between strain rate and temperature (Fig. 18).

On the other hand, many authors pointed out that LPO's transition resulted from variation in CRSS ratio between different slip systems, is associated with temperature changes (e.g. Hobbs 1985, Schmid & Casey 1986). Tullis *et al.* (1973) experimentally showed that transition of the quartz LPO between Z-point maximum and small circle girdle pattern depends on temperature and strain rate. Blacic (1975) also suggested that transition between basal and prismatic slip is dependent on temperature and strain rate. The transitional line between basal and prismatic slip is not parallel to the transitional line of the microstructures as shown Fig. 18. The non-parallelism is supported by the following facts. On Hirth & Tullis (1991)'s experiment the

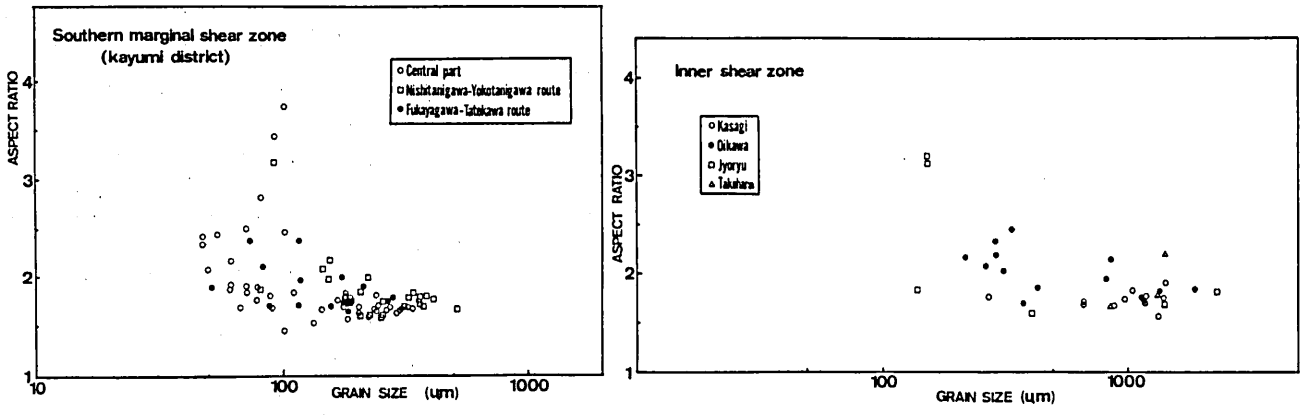

Fig. 50. Dynamically recrystallized grain size of quartz vs aspect ratio of quart from whole districts of the RSMSZ and the RISZ.

transition between basal and prismatic slip coincides with the microstructural transition between regime 1 and regime 2 microstructure. In natural deformation which commonly occurred at slower strain rate than that in the experiment the transition between basal and prismatic slip, the transition between Z-point maximum (or type-I crossed girdle) and Y-point maximum (or type-II crossed girdle) commonly occurs at near the microstructural transition between regime 2 and regime 3 microstructure (e.g. Koshiya 1988) or within resume 3 microstructure (e.g. Hobbs 1966, Sakakibara *et al.* 1990).

Therefore, there are four pairs of the combination between microstructures and slip systems in temperature vs strain rate diagram; S type & prismatic slip, S type & basal slip, P type & prismatic slip, P type & basal slip (Fig. 47). As shown Fig. 47, S type & prismatic slip pair occurs at higher temperature and faster strain rate than P type & basal slip pair, and P type & prismatic slip pair at higher temperature than S type & basal slip pair. For example, Mancktelow (1987) reported S type & prismatic slip pair (sample 7 in Fig. 2 of Mancktelow 1987) in the Simpson Fault zone. Sigemastu (Pers. Comm.) also described this pair in the Hatagawa shear zone. Its pair is produced at faster strain rate and higher temperature than P type & basal slip pair more commonly observed in deformed rocks (e.g. Hara *et al.* 1992). Furthermore, instead of microstructural transition, the aspect ratio is applicable for this method. It is assumed that in the temperature vs strain rate diagram the line of constant average aspect ratio that depend on temperature and strain rate is parallel to the line of the microstructural transition (Karato & Masuda 1989). In the Oikawa district, the quartz grains of sample AH4 exhibit a Y-point maximum pattern and average aspect ratio of 2.5. On the other hand, the grains of sample AH23 exhibit a type-I crossed girdle and aspect ratio of 2.0. As shown in Fig. 48, sample AH4 may be deformed at higher temperature and faster strain rate than sample AH23. Thus, strain rate and temperature in the shear zone are spatially not constant during the mylonitization.

For the use of this method, steady state deformation is assumed. Departure from steady state deformation could be evaluated by the relationship between dynamically recrystallized grain size and aspect ratio. The reason is as follows. Dynamically recrystallized grain size is directly related to differential stress, and depend on temperature and strain rate under steady state deformation. However, some authors suggest there is direct effect of temperature on the grain size through grain growth (Drury *et al.* 1985, Shimizu 1991).

On the other hand, one of characteristic difference between P type (regime 3) and S type (regime 2) microstructure appears to be the aspect ratio of dynamically recrystallized grains particularly under high strain (Karato & Masuda 1989). Dislocation climbing produces low angle grain boundary (subgrain boundary) and results in discontinually decreasing the aspect ratio as follows. Because the subgrain boundaries are perpendicular to the slip direction of dislocation and the slip direction crystallographic axis shows characteristic LPO pattern concentrating near bulk shear direction under simple shear deformation or X of the finite strain under general flattening to axial extension strain (or on the XY girdle under axial flattening strain) (Schmid & Casey 1986), the subgrain boundaries occur at high angle to the elongation direction. When the subgrain boundaries changes to the grain boundary associated with progressive increments of lattice misorientation due to increments of strain and dislocation climb, the aspect ratio on the XZ plane (and/or YZ plane for axial flattening strain) may be lowering with subgrain rotation. The recrystallized grains begin to elongate again such as 'Strain clock' model proposed by Lister & Snoke (1984). Grain boundary migration also allow to decrease the aspect ratio (Bons & Urai 1992), if the migration is not anisotropic. Therefore, the microstructural transition from S type (regime 2) to P type (regime 3), which is characterized by increase in aspect ratio associated with the transition of dominant recovery (dynamic recrystallization) mechanism (Hirth & Tullis 1992), depends on the ratio between strain rate and velocities of dislocation climb and grain boundary migration ($\dot{\varepsilon}/(V_C+V_M)$). As mentioned above, velocities of dislocation climb and grain boundary migration exponentially increase with increase in temperature at constant strain rate assuming steady state deformation. Consequently the microstructural transition

from S type (regime 2) to P type (regime 3) may occurs with increase in temperature and/or decrease in strain rate.

Therefore, the aspect ratio is also directly related to temperature and strain rate with assuming of steady state deformation. Therefore, at given temperature, there is a curve which relate the grain size with aspect ratio, assuming steady state deformation (Fig. 49). However, under non-steady state deformation, the aspect ratio is directly related to temperature, strain rate and stress, although the grain size is directly related to temperature and stress. Strain softening or hardening is regarded as the process that strain rate increases or decreases at constant temperature and stress. Since there is a direct relationship of strain rate only on the aspect ratio (and not on the grain size), aspect ratio under non-steady state deformation is departed from that under steady state deformation at constant temperature and stress. Distance from the curve in the diagram corresponds to the departure from steady state deformation. It may be depends on strain hardening coefficient defined by Poirier (1980). Evaluation of the departure from steady state deformation can be obtained from measurement of the grain size and aspect ratio. However, the relationship between the aspect ratio, temperature and strain rate is not quantitatively clarified (Karato & Masuda 1989). Present author expects that the relationship will be precisely clarified by experiments in future.

Fig. 50 shows the grain size and aspect ratio diagram from present study. These data do not lie on the line of the steady state deformation. These facts imply that in the shear zone strain softening or hardening which leads to the increase (or decrease) of strain rate without the change of differential stress took place, although if temperature during mylonitization is constant in the shear zone is uncertain. Consequently, estimation of departure from steady state deformation needs to estimate the deformation temperature which is obtained by the other method but the microstructure and LPO of quartz.

As mentioned in the above section, in the Hakusan-Joryu district the retrogressive reaction of sillimanite breakdown to muscovite occurs in the strongly mylonitized rocks. Assuming that the retrogressive pressure is 4 kb and P_{H2O} is 0.25, the retrogressive mylonitization in the metamorphic rocks could occur below 550 °C (Chatterjee & Johannes 1974). The metamorphic rocks without this reaction and no grain size reduction (sample HK7), which show dominant $\{10\bar{1}0\}[0001]$ slip systems and microstructure induced by grain boundary migration, were deformed above ca. 550 °C. The deformation temperature estimated from the chemical reaction shows a good agreement with that from LPO pattern (Blumenfeld *et al.* 1986, Mainprice & Bouchez 1987).

On the other hand, in the Takehara district, the dominant recovery mechanism is subgrain rotation, fast and slow grain boundary migration forming irregular microstructure. There is no or less decrease in grain size of quartz aggregates (500 μm). Dominant recovery mechanism of plagioclase is dislocation climb resulting in the formation of subgrain and new grain by subgrain rotation, implying that the deformation occurred at temperature greater than 400 °C (Pryer 1993, Fitz Gerald & Stünitz 1993). This is consistent with deformation temperature from quartz microstructures.

X-point maximum and type-II crossed girdle with higher half opening angle (ca. 50-60 degree) of quartz c-axis patterns and basal-prismatic subgrain boundary imply that prism<a> and prism[c] slip dominate intracrystalline plastic deformation (Lister 1981), although slip plane with [c] slip direction may be $\{11\bar{2}0\}$ from $<11\bar{2}0>$ pattern, which have been commonly reported from the experiments (see Table 1 in Linker *et al.* 1984). Mainprice & Bouchez (1987) suggested that Y-point maximum is produced at 500 °C and X-point maximum above 600 °C. These facts indicate that the deformation temperature is higher than that in the other district of the RISZ. The granitic rocks in the Takehara district correspond to the HT mylonite, according to Krohe & Eisbacher (1988). The intensity of development of the LPO patterns, which is related to strain magnitude (Lister & Hobbs 1980) is varied with space. The center of the shear zone estimated from the intensity is located in the zone linked by location of sample TA9, KM5 and KM302. Analogous patterns have been already reported by Hara (1962) from the metamorphic rocks in the sillimanite zone of the Kasagi district and Okudaira *et al.* (submitted) from the high grade metamorphic rocks in the Yanai district of the Ryoke belt.

b. Deformation temperature estimated from chemical composition of feldspars and amphiboles

The strain-related myrmekite occurs above 400 °C, as suggested by Simpson (1985) and Simpson & Wintsch (1989). As mentioned in the above section III-D, temperature during the mylonitization is estimated by feldspar-feldspar thermometer, using the myrmekitic plagioclase along the K-feldspar porphyroclasts and K-feldspar recrystallized in the pressure shadows around the host K-feldspar porphyroclasts from the Kimigano granodiorite (sample TA9D) in the Takehara district of the RISZ. The use of the feldspar pair with these microstructure has been proposed by Yamagishi (Pers. Comm.) in order to estimate temperature during deformation. The calculated temperatures from the averaged chemical composition range from 490 to 497 °C (Table 2), which correspond to the lower limit of the temperature estimated from the quartz LPO patterns. These values are slightly higher than those from the USL of the Kayumi district in the southern marginal shear zone. It could be concluded that the mylonitization in the Takehara district occurred at higher temperature (ca. 500 °C≤).

In the Oikawa district, the averaged Ti content (ca. 0.10) of rim of fractured matrix amphibole in the strongly mylonitized samples of the Joryu tonalite is significantly lower than that of the core (ca. 0.26) (Table 4). Rasse (1974) suggested that the Ti content of the amphibole is positively related to the metamorphic grade (temperature). Some of the rims indicate actinolitic compositions. According to Rasse (1974), the tonalite was crystallized at granulite facies (above 600 °C) and mylonitized at lower amphibolite facies (450-500 °C). The estimated temperature during the mylonitization based on the Ti content roughly agrees with that from the LPO's analysis and with the fact that in the Hakusan-Joryu district sillimanite was broken-down to muscovite during mylonitization. Since the Ti content of the rim at side of extensional fracture is lower than that of the core, the mylonitization appears to be

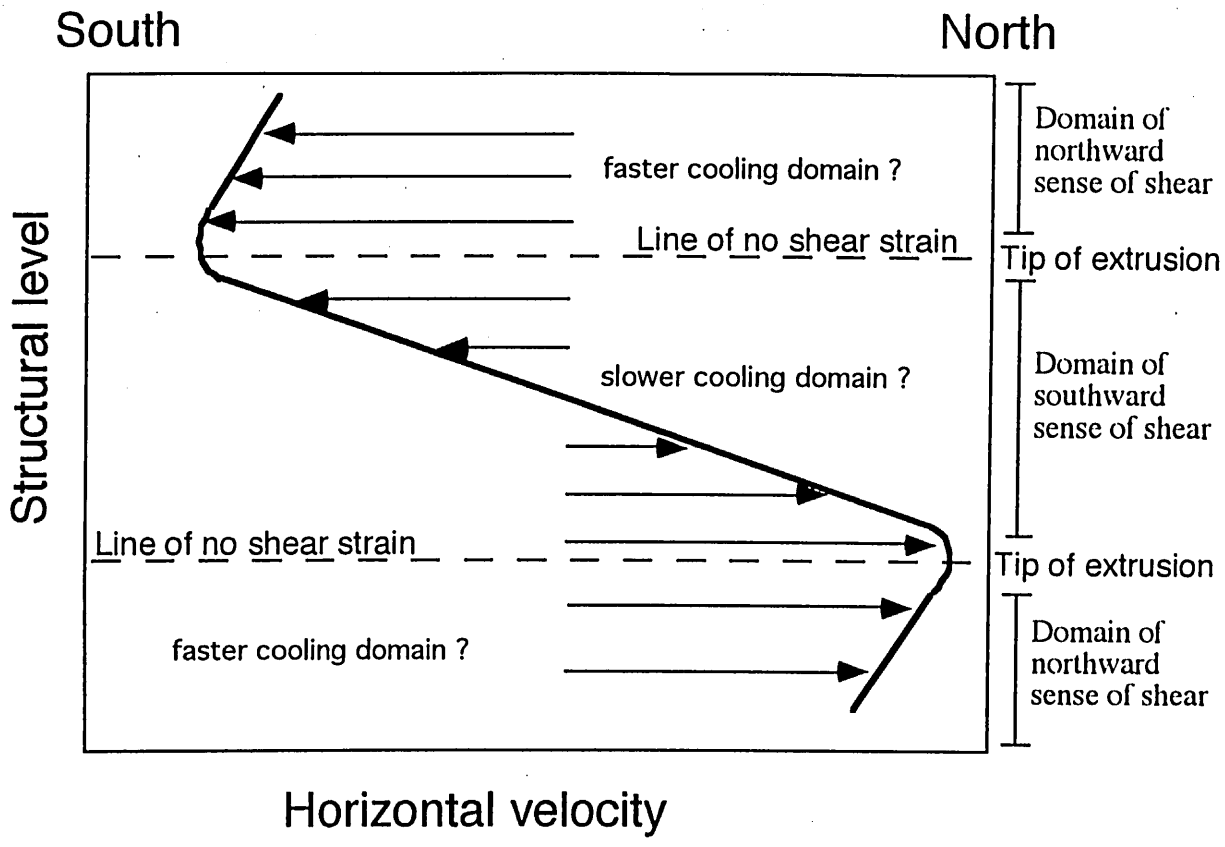

Fig. 51. Schematic velocity profile from the quartz LPO patterns in the Takehara district.

occurred during the retrogressive stage related to cooling of the Joryu tonalite. On the other hand, in the Takehara district, difference in the Ti content between in the rim and core in the Kimigano granodiorite is small. It suggests that in the Takehara district retrograde mylonitization is not or slightly occurred.

Pressure during crystallization of the tonalite and the mylonitization has been examined using barometer of total Al content of amphibole. Hamarstrom & Zen (1984) suggested that there is a linear relationship between the total Al content of amphibole and pressure during the crystallization. Afterward, this relationship has been confirmed by many authors (Hollister *et al.* 1987, Rutter *et al.* 1989, Schmidt 1992). The result of the electron microprobe analysis and calculated pressure in the Oikawa, Hakusan-Joryu and Takehara district are shown in Table 4 ,5 & 6 and Fig. 43. These values from the core in the all analyzed samples, from rim in the strongly deformed sample during LT and MT phase (sample AH3 and AH16) and from core of inclusion in the plagioclase (sample AH12) corresponds to the pressure of 3.8-5.2 kb, 3.5-4.2 kb and 5.1 kb in pressure respectively, according to Schmidt (1992). Chemical composition of the core of amphibole included in plagioclase grains could be frozen at earlier stage of the crystallization of the tonalite than that of the core of matrix amphibole. The composition of the rim of matrix amphibole may be reequilibrated during the mylonitization due to effect of the strain energy on the chemical reaction, as pointed out by Wintsch & Dunning (1985). Therefore, it is suggested that the Joryu tonalite ascended during the crystallization from the melt, and also during a cooling stage (accompanied by the mylonitization) after the crystallization and at closing stage of the mylonitization.

2. Kinematics

In the RISZ except for the Takehara district (retrogressive shear zone), the southward and southeastward directed sense of shear with some vertical component dominate the mylonitization. However, non-coaxiality from the quartz LPO patterns is relatively low as whole, although it is widely varied in the shear zones. Three dimensional shape of the finite strain in the RISZ with exception of the Takehara district is varied from constrictive to plane strain (Fig. 20), as illustrated by geometry of quartz c-axis patterns (Hara 1971, Schmid & Casey 1986).

On the other hand, there are partitionings of sense of shear (positive or negative of vorticity) in the Takehara district (HT shear zone) (Fig. 46). The schematic velocity profile inferred from sense of shear and strain magnitude based on LPO patterns of quartz is illustrated in Fig. 51. The sense of shear for each structural domain (level) is spatially partitioned. This heterogeneous flow as several extrusions (and/or intrusions) of ductile flow, alternating the domains of northward and southward directed sense of shear, may be caused by spatial heterogeneity of rheological behavior between the Kimigano granodiorite, Fukudayama

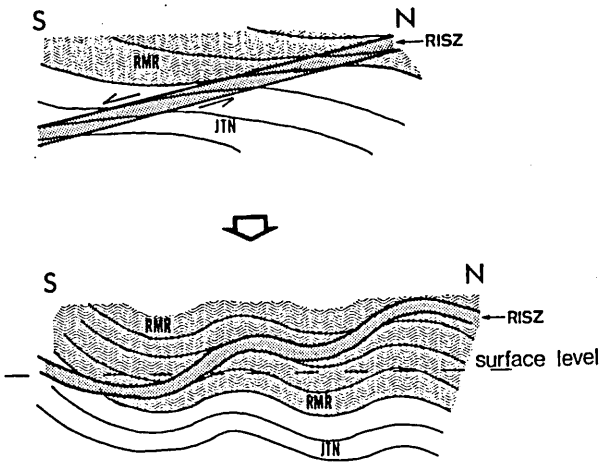

Fig. 52. Geometrical relationship between RISZ, H-T phase gneissosity and boundary between the Ryoke metamorphic rocks (RMR) and Joryu tonalite (JTN). Followed upright folding accommodated initial shear zone geometry.

granodiorite and Ryoke metamorphic rocks, or within the Kimigano granodiorite. In the later case, heterogeneous cooling within the Kimigano granodiorite results in the spatial heterogeneity of rheological behavior. Merle and Guillier (1989) produced the analogous kinematic environments on scaled experiments, although this procedure was accompanied with recumbent folding. The natural analogous environment have been reported by Schmid et al. (1988) and Ratschbacher et al. (1991) on macroscale, and by Krohe (1990) on microscopic scale. In these cases, heterogeneous flow may be controlled by heterogeneity of rheological behavior within deformed masses. The bulk sense of shear in the Takehara district can not be determined, since there is wide variation of flow partitioning pattern depending on angle between shear direction and boundary between layers with different viscosities (Ishii 1992).

3. Tectonic implication

In the inner region of the Ryoke metamorphic terrane, the shear zone is divided into HT zone in the Takehara district and MT-LT zone in the other district. The Ryoke metamorphic rocks around the RISZ is bearing sillimanite, implying that the peak metamorphism was reached at the grade of higher amphibolite facies (ca. 550 °C ≤) (Seo 1983). Therefore, the HT mylonitization occurred during or just after the peak metamorphism. Since the MT and LT mylonitization occurred during retrogressive metamorphism, the HT mylonitization was followed by the MT and LT mylonitization. The microstructures and LPOs in the Takehara district, which was produced during the HT mylonitization, was frozen during the MT and LT mylonitization, since strain localization was transferred to the other district during MT and LT mylonitization. The so-called "penetrative gneissosity" in the older Ryoke granitic rocks was produced in the lower strained region during the HT phase. However, the stretching direction was oriented to NS or SE-NW direction throughout the HT, MT and LT mylonitization. Upright folding bending the mylonitic foliation during the MT and LT phase developed after MT and LT mylonitization.

The geometrical relationship between the HT foliation and MT-LT mylonitic foliation is examined as follows. The retrogressive shear zone in the Ryoke metamorphic rocks of the Hakusan-Joryu district may be linked with the shear zone in the Oikawa district, because of the existence of the upright folds, the similarity of the microstructure and LPO patterns and no-existence of strongly deformed zone in the Joryu tonalite of the Hakusan-Joryu district, although the structural level of the shear zone in the Oikawa district apparently different to that in the Hakusan-Joryu district. It is due to NS striking fault movement following development of retrogressive shear zone. Probably, the retrogressive shear zone develops oblique to the boundary between the Joryu tonalite and Ryoke metamorphic rocks and to the H-T penetrative gneissosity of the Joryu tonalite and Ryoke metamorphic rocks. The geometrical relationship between the retrogressive shear zone, gneissosity and mass boundary between the Joryu tonalite and Ryoke metamorphic rocks is illustrated in Fig. 52. Any M-T and L-T shear zone have not been discovered in the north of this district (e.g. Aoyama highland district) yet. The retrogressive shear zone may be located in the upper level than the surface. The shear zone was initially developed with gently southward dipping, while the gneissosity of tonalite and metamorphic rocks formed during H-T phase horizontally dips. Upright folding developed after retrogressive shear zone, modifying the initial structural geometry (Fig. 52). This initial relationship is compatible with southward directed sense of shear from the retrogressive shear zone. This structural relationship apparently similar to typical extensional shear zone with doming of basement as well as in the metamorphic core complex suggested by Lister & Baldwin (1991).

E. Conclusions

The new information about tectonics in the Ryoke metamorphic terrane is obtained by present study, as followings.

(1) In the he Ryoke inner shear zone, the mylonite zone is divided into two zone; high temperature zone in the Takehara district (ca. 500 °C ≤) and intermediate-low temperature zone in the Kasagi, Oikawa and Hakusan-Joryu district (ca. 500 °C ≥). The HT mylonitization occurred during or just after the peak metamorphism of the Ryoke terrane. Afterward, the MT-LT mylonitization occurred during the retrogressive metamorphism.

(2) The stretching direction in the RISZ was oriented to N-S and NW-SE direction throughout phase of the mylonitization. During the HT mylonitization, sense of shear in the Takehara district was heterogeneously partitioned. While, southward directed sense of shear dominate the MT-LT mylonitization, although the non-coaxiality is relatively low under from general constrictive strain to plane strain.

(3) In the MT-LT shear zone of the Oikawa and Hakusan-Joryu district, there are spatial differences of deformation temperature and strain rate. The microstructure-LPO pair possible to be a useful indicator of temperature

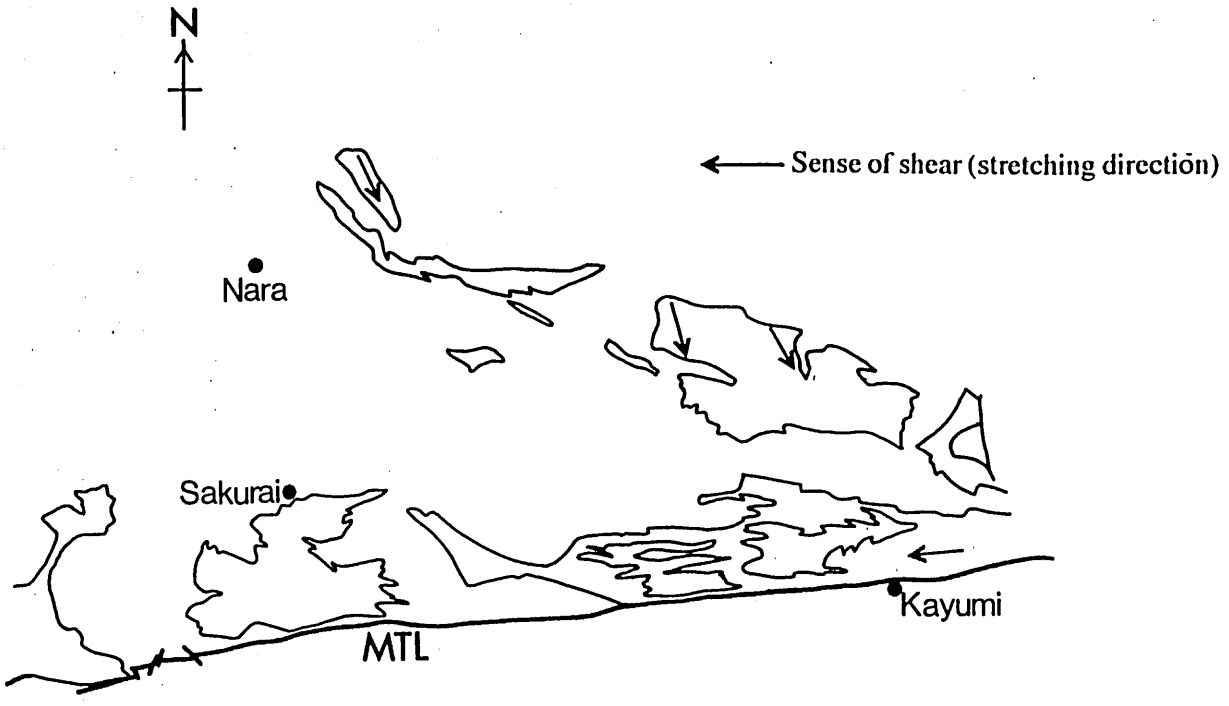

Fig. 53. Representative sense of shear and stretching direction during M-T and L-T deformation for each district in the Kinki Province.

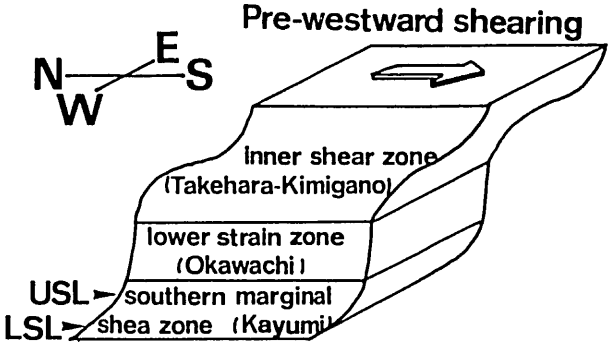

Fig. 54. Schematic diagram showing variation in strain magnitude during H-T mylonitization.

and strain rate, although some uncertainties are remained.

(4) The older Ryoke granitic rocks in the inner region of the terrane was crystallized at pressure of 3.8-5.2 kb (14-18 km in depth). On the other hand, the MT-LT mylonitization occurred at pressure of 3.5-4.2 kb (13-16 km in depth). The inner zone was slightly exhumed during the MT-LT mylonitization.

V. Synthetic discussion

A. Kinematic model of the shear zone system developed in the Kinki Province of the Ryoke belt

In the above sections, various structural element of the shear zones in the Kinki Province of the Ryoke belt have been described. The structural evolution of the these shear zone may depend on the variations in temperature, magnitude of differential stress and stress configuration. These factors result in the variations in strain rate, non-coaxiality, strain magnitude and three dimensional shape of the finite strain. In the following section, the timing of the formation of the shear zones and the strain path partitioning between the each shear zones will be discussed

1. Timing of the formation of the shear zones

The Ryoke southern marginal shear zone in the Kayumi district was developed at ca. 460 °C in the USL and ca. 400 °C in the LSL. As mentioned in section III-D, the chronological data reported by Takagi *et al.* (1989), suggest that the southern marginal shear zone of the Kayumi district has been formed during 83-60 Ma at most.

While, in the Ryoke inner shear zone (RISZ) mylonitization mainly occurred at MT (≤ 500 °C) to LT (ca. 450-350 °C), except for the Takehara district in which the mylonitization developed at higher temperature (≥ 500 °C). There is no datum for mineral age in the RISZ. Assuming that the older Ryoke granitic rocks in the RSMSZ and RISZ of the Kinki Province intruded at same time and were cooled at same rate as whole, the development of the RISZ characterized by the MT and LT mylonitization is coeval with the development of the RSMSZ. On the other hand, the mylonitization in the Takehara district of the RISZ occurred before the formation of the RSMSZ (83 Ma). This assumption may be supported by the fact that the spatial variation in the age for the granitic rocks in the Ryoke belt toward the north is not

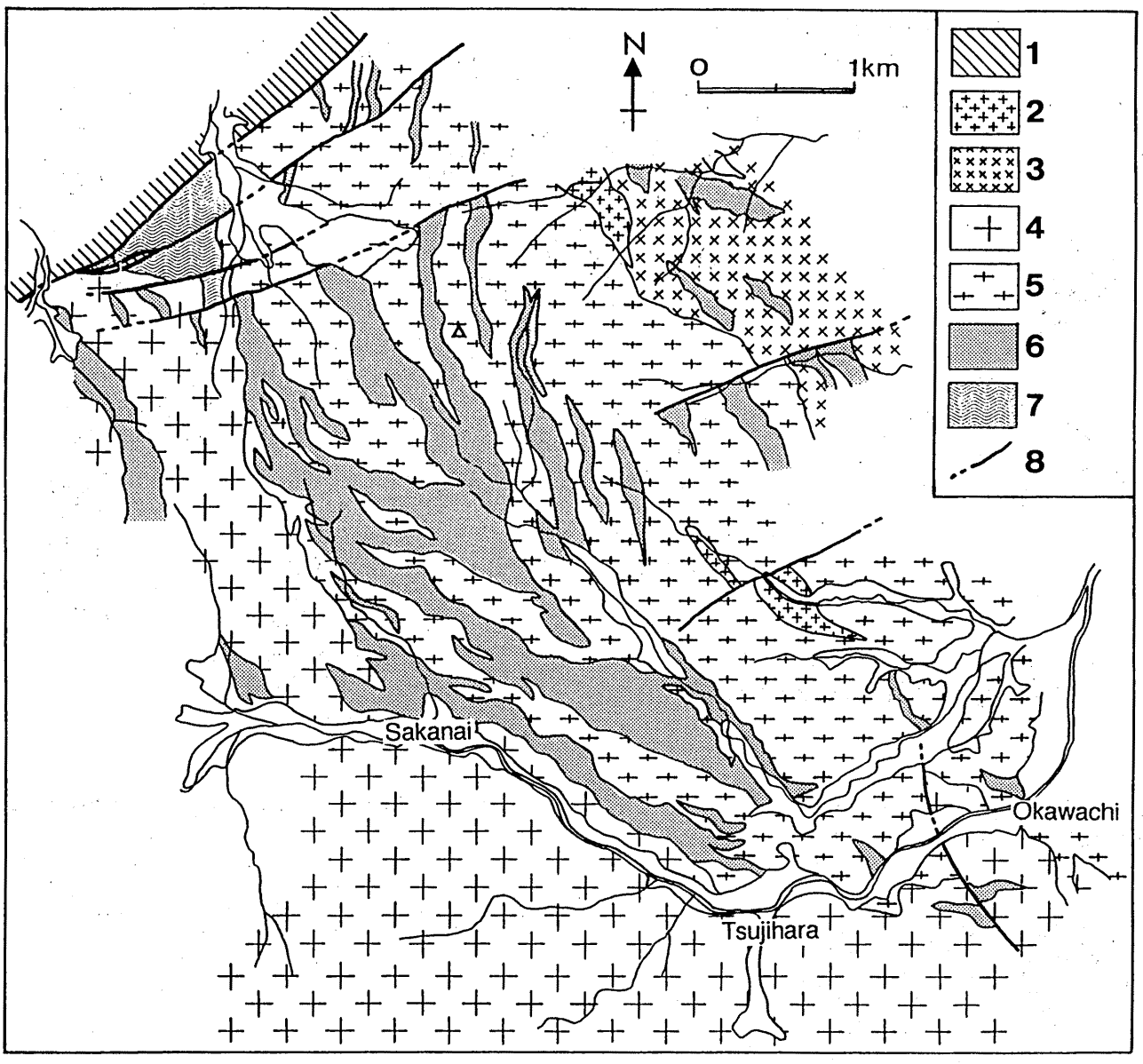

Fig. 55. Geological map of the Okawachi district. 1: Tertiary, 2: Aho granite, 3: Nishino granite, 4: Misugi tonalite, 5: Kimigano granodiorite, 6: Yokono granodiorite, 7: Hatai tonalite, 8: Basic gneiss, 9: Pelitic, psammitic and siliceous gneiss.

significant than that toward the east in the southwest Japan (Kinoshita & Ito 1986, 1988, Nakajima 1990). The following discussion is based on this assumption.

The HT mylonitization is possibly regarded as III or IV phase after Seo & Hara (1980) and Seo (1985) and D_2 phase after Ohtomo (1993), and the MT and LT mylonitization as D_3 or D_4 phase after Ohtomo (1988, 1993).

2. Strain path partitioning between the RSMSZ and RISZ

The data from the LPO and strain analysis imply that the NS stretching occurred before the EW stretching under the MT to LT mylonitization in the Kayumi district of the RSMSZ. In the RISZ, the NS (or NW-SE) stretching dominate the HT to LT mylonitization (Fig. 53). Therefore, the deformation during H-T stage throughout the Kinki Province of the Ryoke belt is characterized by the NS stretching without spatial partitioning of stretching direction. Afterward, the change of stretching direction took place in the Kayumi district of the RSMSZ during the retrogression of the Ryoke metamorphism. The spatial partitioning of the stretching direction between the RISZ and RSMSZ may be synchronously developed during M-T and L-T phase of the mylonitization.

Partitionings of the stretching direction on large scale have been reported by some authors (Darot 1974, Harris 1985a & b, Bale & Brun 1989, Neubauer 1993). These studies suggested that the stretching direction (shear direction) is varied with structural level. Therefore, there are variations in (shear) strain magnitude for two principle axes which are mutually perpendicular. Assuming that the

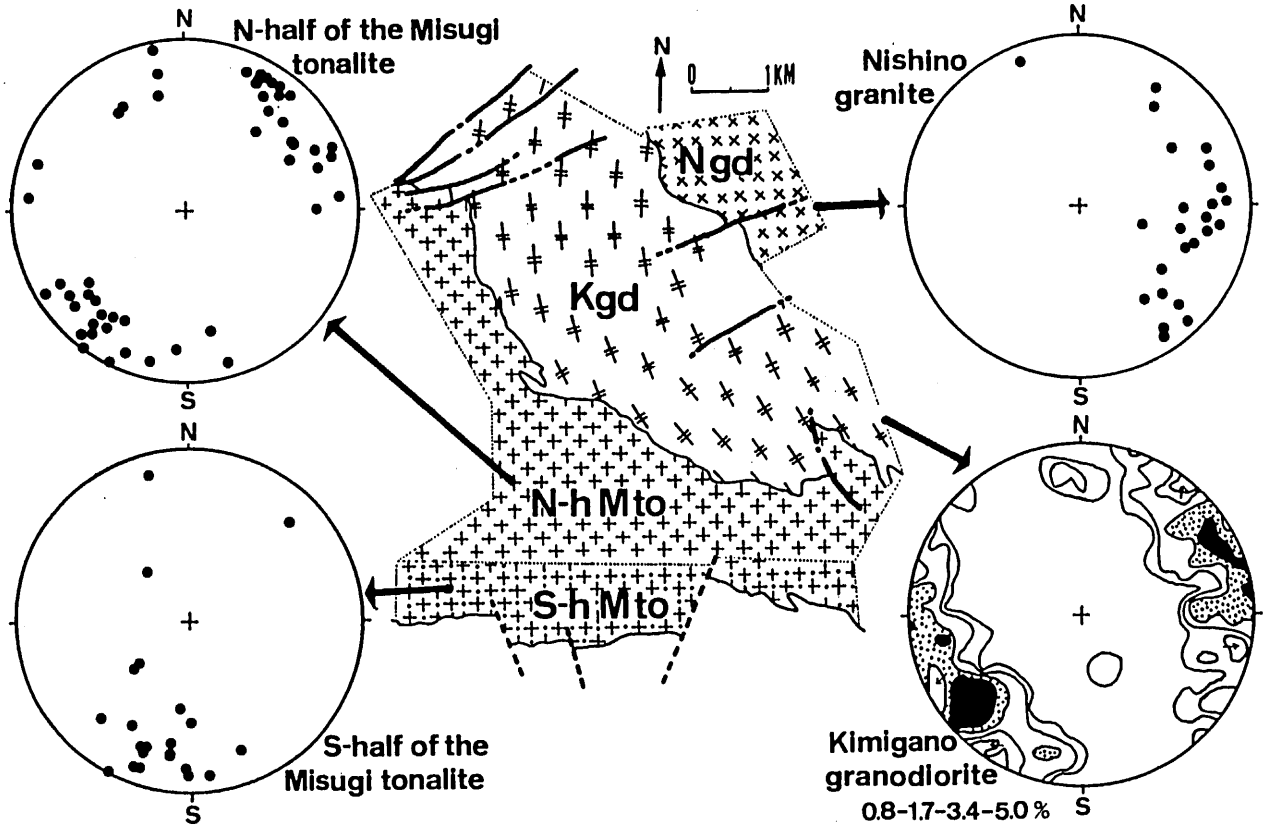

Fig. 56. Equal area plots showing the orientation data for foliation of the Kimigano granodiorite, Misugi tonalite and Nishino granite in the Okawachi district.

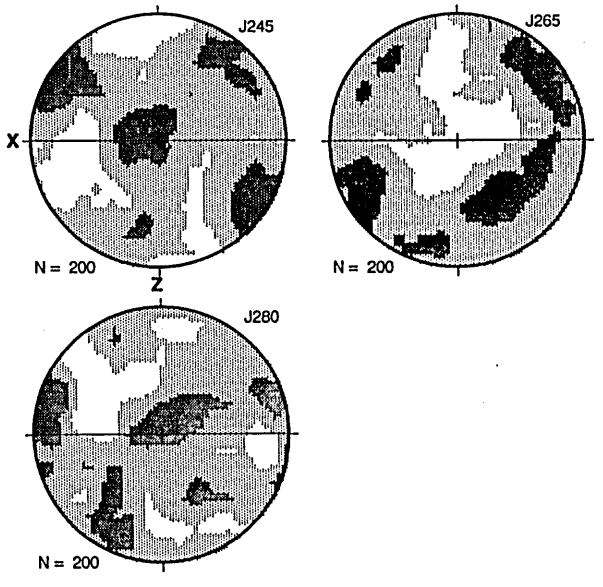

Fig. 57. Quartz c-axis fabrics from the Kimigano granodiorite in the Okawachi district. Contour interval: 2σ, n = number of c-axes.

mylonitic foliation developed throughout the Kinki Province of the Ryoke belt dips north at low angle as whole, the RSMSZ is located at lower structural level than the RISZ. It is suggested that during the L-T and M-T mylonitization, the EW stretching predominate in the lower structural level, and NS stretching in the upper structural level in the Ryoke belt. It appear that the temporal change of stretching direction from NS to EW in the Kayumi district of the RSMSZ coincides with the descending stage estimated from chemical variation within the matrix amphibole.

The variation in strain magnitude before the EW stretching in term of the formation of the RSMSZ is illustrated in Fig. 54. It is based on the results from the above section (III-C and IV-C) and the microstructural and LPO's data from the Okawachi district. It is inferred that the strain magnitude before the EW stretching in the Kayumi district decreases toward the upper structural level. While, in the Okawachi district which is located in the north (and/or upper structural level) of the Kayumi district, the alternation of the basic rocks and the Kimigano granodiorite is tightly folded with the vertical axis plunging toward NW-NS (Fig. 55 & 56). In the Okawachi district, quartz c-axis patterns show a random orientation, although preferred dimensional orientation of biotite which define the foliation is significantly developed without quartz grain size reduction and development of mica fish structure (Fig. 57). And the grain size of quartz is too large (>1000 μm) to result in 'grain boundary sliding' (Behrmann 1985) (Fig. 58). The slightly elongate xenoliths of basic rocks, whose long axis is parallel to the foliation of Kimigano granodiorite, is observed in the Kimigano granodiorite.

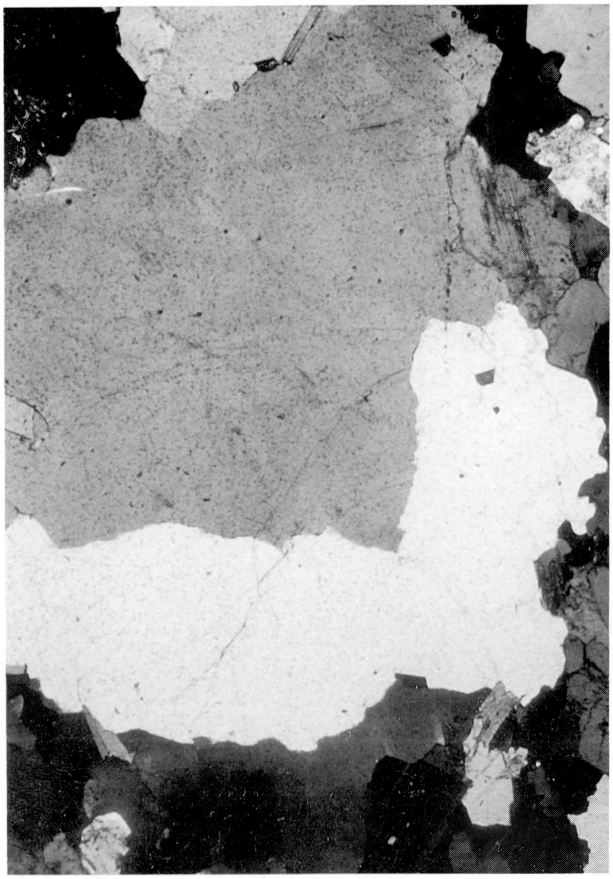

Fig. 58. Microphotograph of quartz grains of the Kimigano granodiorite in the Okawachi district, showing no deformational feature.

These facts imply that the strain magnitude in the Okawachi district is very small, although development of the large scaled fold need considerable strain increments. Therefore, it is suggested that this fold was developed during magmatic stage, according to Paterson *et al.* (1989). The EW compression occurred in the Kimigano granodiorite of the Okawachi district during the magmatic stage. Then, no or less solid state deformation occurred in the Okawachi district. The NS stretching in the Takehara district were closed at higher temperature. The strain localization (development of the shear zone) by the successive NS stretching transfers into the other district of the RISZ during the MT and LT stage. The MT and LT stage mylonitization in the RISZ resulted from ductile thrusting with southward directed sense of shear under lower bulk non-coaxiality. In the Kayumi district the RSMSZ developed as subhorizontal ductile shear zone with westward directed sense of shear. The variations in sense of shear and its direction, which is comparable with Harris (1985) in the in Alpine Corsica, indicate that the heterogeneous ductile flow on large scale occurred in the Kinki Province of the Ryoke belt.

The younger Ryoke granitic rocks (the Misugi tonalite) intruded into the older rocks at ca. 3.0 kb after the LT and MT mylonitization in the RSMSZ and RISZ. Therefore, in the Kayumi district the older rocks were exhumed from 4.5 kb to ca. 3.0 Kb during the intrusion of the younger granitic rocks (Fig. 59). Hara *et al.* (1990) suggested that intrusion of the younger Ryoke granitic rocks took place during or after the upright folding. It is hypothetically suggested that this exhumation coincides with the upright folding.

B. Tectonic implication

The partitioning of stretching direction between the RSMSZ and RISZ is not only developed in the Kinki province, but also in the Chubu district, implied by Ohtomo (1993) and Toriumi & Kuwahara (1988)'s works. However, in the Chugoku, Shikoku and Kyushu district of the Ryoke belt the lineations of the metamorphic rocks and older granitic rocks show EW trend in both the inner zone and southern marginal zone (Okamura 1960, Nureki 1960, Toriumi & Masui 1986, Okamoto *et al.* 1989, Okudaira 1992MS, Takahashi (Pers. Comm.), indicating that the EW stretching dominate ductile deformation. The elements of the RSMSZ is intermittently exposed westward from the Kishiwada district (Takagi *et al.* 1987) of the Kinki Province, in the Awaji island (Takahashi 1992) and the Shodo island (Kutsukake *et al.* 1979). The RSMSZ which is lower structural level than the RISZ is shifted toward north in the eastern part of the Chugoku district. As mentioned in the above section, the partitioning of the stretching direction depend on structural level of the belt. Since the western part of the Ryoke belt correspond to the relatively lower structural level, the EW stretching dominate the M-T and L-T deformation Fig. 60.

In the Kayumi district of the RSMSZ, the stretching direction changed from NS to EW before 83 Ma. Then, the LT and MT mylonitization occurred at 83-70 Ma. Darmyer & Takasu (1992) suggested that the mylonitization in the southern marginal shear zone of the Chubu district occurred at 62-63 Ma, assuming the mylonitization occurred at ca. 300 °C. The RSMSZ in the Chubu district was developed at grade of epidote-amphibolite facies (Takagi 1986, Hara Pers. Com.) (> 400 °C). Therefore, temperature during the mylonitization and also the age of mylonitization, suggested by Darmyer & Takasu (1992), appear to be underestimated. Ohtomo (1993) suggested that the mylonitization occurred before 72 Ma in the shear zone of the Mikawa-Toei area. On the other hand, in the Awaji island, Takahashi (1992) pointed out that the mylonitization developed before 87.7 Ma. These spatial variation in the age of the mylonitization implies that the LT and MT mylonitization in western part of the RSMSZ has been closed at earlier than in the eastern part. The isotherm of 350 °C at which the LT mylonitization was closed, were cut by the RSMSZ (Fig. 61). This foot wall geometry is comparable with model A of Passchier (1984), assuming normal thermal gradient.

During 88-62 Ma, at which the stretching direction changed from NS to EW in the RSMSZ, the subduction direction of the Izanagi plate perpendicular to the trench has been transferred to that of the Kula-Pacific plate oblique to the trench at low angle (Engebreston 1982, Maruyama & Seno 1986). This change of the subduction direction is responsible for changing the stretching direction in the RSMSZ (Fig. 62). In the Sambagawa belt which was located in the lower structural level than the Ryoke belt, stretching direction has been changed from NS for the Bic

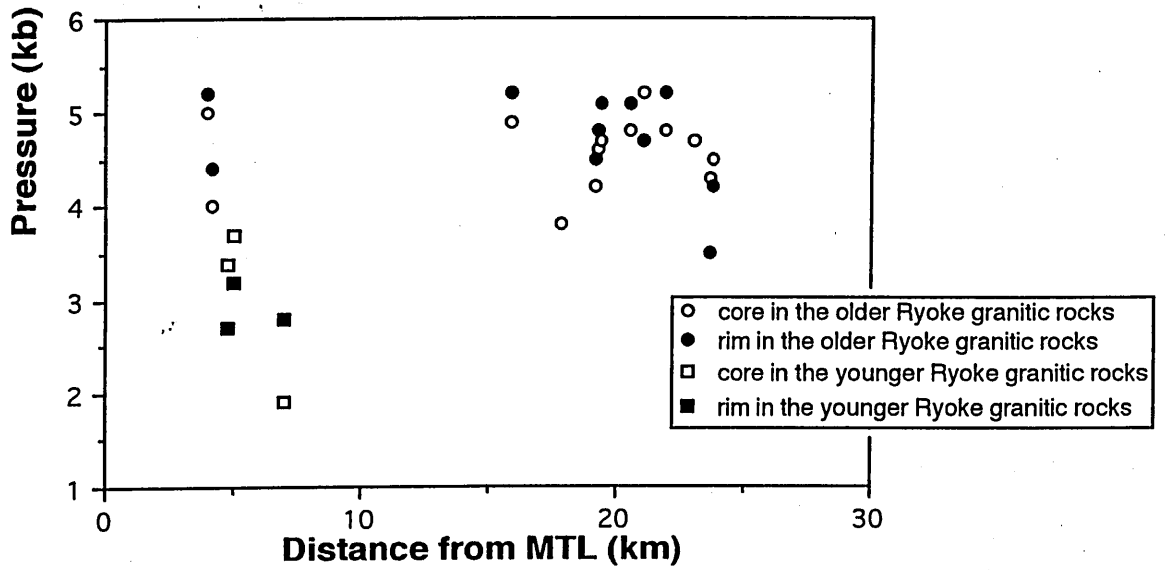

Fig. 59. Diagram showing relationship between pressure estimated from chemical analyses of amphibole and the distance from MTL in the Kinki Province.

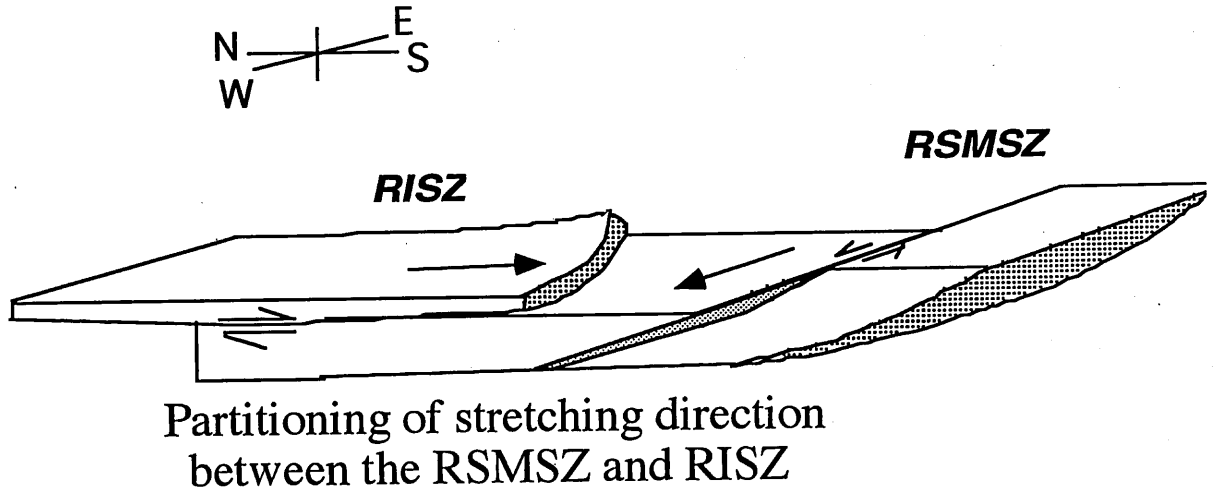

Fig. 60. Schematic diagram showing partitioning of stretching direction and sense of shear during M-T and L-T phase between the RSMSZ and RISZ in the Ryoke metamorphic terrane of the Kinki province.

and Sim-Bim phase to EW for the Sb_1 and Sb_2 phase (Kaikiri *et al.* 1991, Hara *et al.* 1992), as well as in the RSMSZ. However, the reason for no change of the stretching direction in the RISZ is unresolved.

Yokoyama (1979) and Hara *et al.* (1980) suggested that the orientations of the minimum principle stress axis (σ_3) inferred from dyke orientation in the Chugoku-Setouchi district were varied from NS at first stage to EW at second, third and forth stage, and that σ_3 tend to be oriented to EW in the southern part and to NS in the northern part. This spatial and tidal variation in σ_3 is entirely identical with that in the stretching direction (Fig. 62). Ductile flow in the low P/T metamorphic belt with syntectonic intrusion of granitic rocks was non-uniform in term of the stretching direction due to non-uniform stress configuration, depending on structural level of the belt.

The partitioning of stretching direction (e.g. Harris 1985, Balé & Brun 1989, Ring 1992, present study), non-coaxiality (e.g. Law *et al.* 1986, Lee *et al.* 1987, Ratschbacher *et al.* 1991), sense of shear (e.g. Harris 1985, Mancel & Merle 1987, Schmid & Hass 1989, Ratschbacher et al 1991) and three dimensional shape of the finite strain (e.g. Siddans 1983, Toriumi 1985, Holst 1985, Paterson *et al.* 1989, Schulz-Ela & Hudleston 1991) on large scale should be compared with theoretical and experimental works (e.g. Sanderson 1982, Hudleston 1983, Ingles 1983,

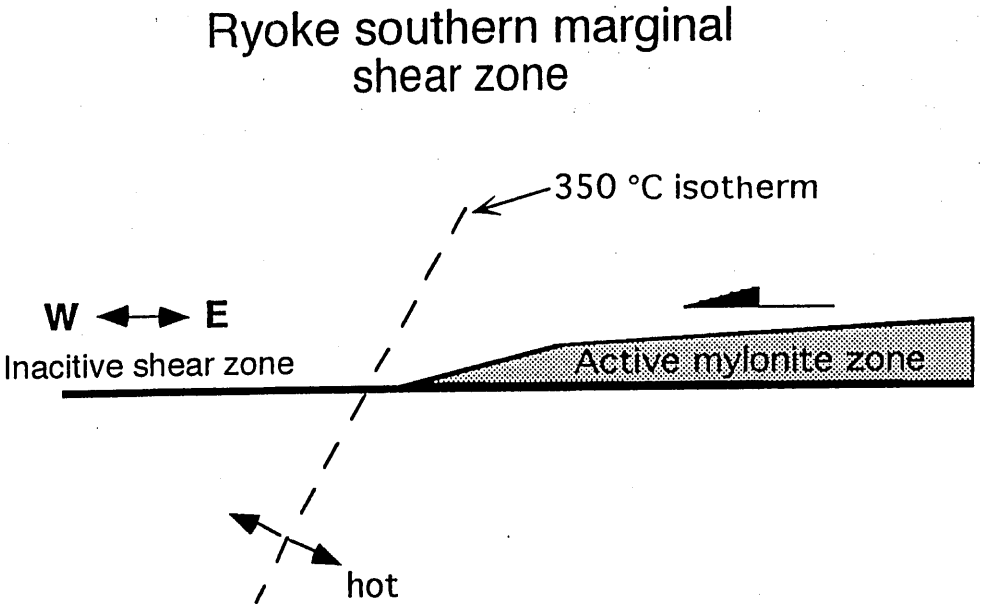

Fig. 61. Diagram showing foot wall geometry, which the Ryoke southern marginal shear zone cuts isotherm of ca. 350 °C.

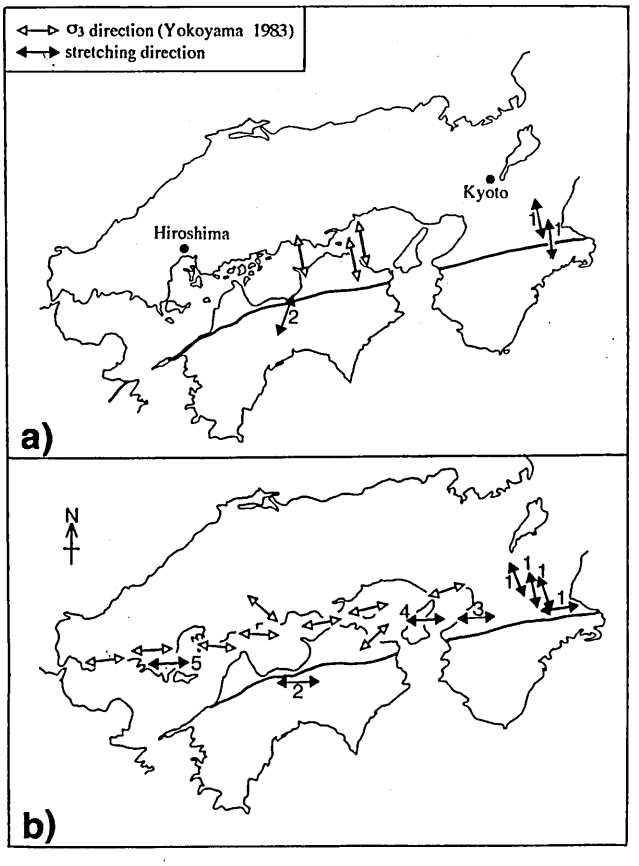

Fig. 62. Variation in stretching direction and principle minimum stress direction in the southwest Japan, compiled from (1) this study, (2) Kaikiri et al. (1991), (3) Takagi et al. (1988), (4) Takahashi (Person. Commun.), (5) Okamura (1959) and Yokoyama (1983). a) HT phase. b) MT-LT phase.

Means 1989, Merle 1989, Merle & Guillier 1989, Otsuki 1992, Weijamars 1991 & 1992, Ishii 1992), in order to clarify the contributors to the development of various structural patterns for the crustal deformation. For example, numerical experiments for deformation of continental lithosphere in the collision zone have produced variations in principle stress direction and stretching direction (strain configuration) (e.g. Houseman & England 1986, Cohen & Morgan 1986, Stefanick & Jurdy 1992). In natural studies, variation in stress direction has been reported by some authors (e.g. Molnar and Deng. 1984, England & Houseman 1986, Tsukahara & Ikeda 1991). The produced structure is appeared to be controlled by difference in rheological behavior between each geological bodies and shape factor (geometrical relationship between each geological bodies). In the Ryoke metamorphic terrane, spatially heterogeneous ductile flow during M-T and L-T phase, which is caused by heterogeneous stress configuration, suggesting that there are some huge invisible rigid masses controlling stress configuration.

VI. Conclusions

In the Ryoke metamorphic terrane of the Kinki province, the ductile deformation of the older Ryoke granitic rocks during the HT phase (≥ ca. 500 °C) is characterized by N-S stretching. The HT shear zone in the inner region of the Ryoke metamorphic terrane developed with heterogeneous strain gradient at pressure of 4-5 kb. Afterward, stretching direction was spatially partitioned into EW direction in the RSMSZ and NS direction in the RISZ during the MT-LT deformation. Sense of shear in the RSMSZ and RISZ is a top toward the west and south respectively. Thus, in the RSMSZ, stretching direction was temporally changed. This change of stretching direction occurred at ca. 83 Ma, which coincided with temporal change of subduction direction of oceanic plate

from NS direction in the Izanagi plate to EW direction in the Kula plate at 85 Ma. Although subduction direction changed at that time, stretching direction in the RISZ was not changed and remained NS direction. This spatial partitioning between RSMSZ and RISZ during MT-LT mylonitization may depend on the structural level, supported by some of theoretical and natural works. After the MT-LT mylonitization, the younger Ryoke granitic rocks intruded into the older Ryoke granitic rocks and Ryoke metamorphic rocks at pressure of ca. 3 kb.

Acknowledgments

I wish to my sincere thanks to Professor Ikuo Hara of Hiroshima University for many useful discussions and reasonable suggestions, and for his critical reading of the manuscript. Special thanks are due to Dr. Toru Takeshita of Hiroshima University for his helpful advices and critical reading of the manuscript, and Dr. Yasutaka Hayasaka of Hiroshima University for useful advices in electron microprobe analysis. I am also indebted to Professor Yuji Okimura, Professor Setsuo Takeno, Professor Satoru Honda and Professor Yuji Sano of the Hiroshima University. Thanks are also due to Professor Toshihiko Shimamoto of Earthquake Research Institute, University of Tokyo, Professor Tetsuo Yamada of the Shinshu University Dr. Tsuyoshi Toyoshima of Niigata University, Dr. Yukiko Ohtomo of Earthquake Research Institute, University of Tokyo, Mr. Kazuaki Okamoto of Tokyo Institute of Technology and Mr. Yasuhiro Sakurai for helpful advices and encouragement. I also wish to thanks Dr. Ichiko Shimizu of University of Tokyo and Dr. Kyuichi Kanagawa of Chiba University for their technical advices in the operation of X-ray texture goniometer and useful discussions about the microstructures of quartz. I would like to thank the member of the Petrologist Club of Hiroshima University for their helpful discussions and advices, and Mr. Asao Minami for his helpful technical assistance and advices in EPMA analysis, and Mr. Akito Magai and Mr. Kazuo Uemura for preparing thin sections. I thank Mr. Hirokazu Tabata and Mr. Hiraku Yamagishi of University of Tokyo for their helpful advices and kindful assistance in my staying for a long time in Tokyo, and Mr. Takamoto Okudaira, Mr. Masahiko Tagami, Miss. Yasuko Suzuki, Mr. Keisuke Naomoto, Mr. Kiyoshi Ise, Mr. Toshihiko Sakashima and Mr. Shintaro Kida of Hiroshima University for their help with preparation of this thesis. I am grateful to my parents for their hearty education and financial support throughout the course of this work.

References

Argon, A. S. and Maffatt, W. C. 1981: Climb of extended edge dislocations. *Acta Metal.*, **29**, 293-299

Balé, P. and Brun J.-P. 1989: Late Precambrian thrust and Wrench zones in northern Brittany (France). *Jour. Struct. Geol.*, **11**, 391-405.

Behrmann, J. H., 1985: Crystal plasticity and superplasticity in quartzite: a natural example. *Tectonophysics*, **115**, 101-129.

Behrmann, J. H. and Mainprice, D., 1987: Deformation mechanisms in a high-temperature quartz-feldspar mylonite: evidence for superplastic flow in the lower continental crust. *Tectonophysics*, **140**, 297-305.

Behrmann, J. H. and Platt, J. P., 1982: Sense of nappe emplacement from quartz c-axis fabrics: an example from the Betic Cordillera (Spain). *Earth Planet Sci. Lett.*, **59**, 208-215.

Berthé, D., Choukroune, P. and Jegouzo, P., 1979: Orthogneiss, mylonites and non-coaxial deformation of granites: the example of the South Armorican shear zone. *Jour. Struct. Geol.*, **1**, 31-43.

Blacic, J. D., 1975: Plastic deformation mechanisms in quartz: the effect of water. *Tectonophysics*, **27**, 271-294.

Blumenfeld, P., Mainprice, D. and Bouchez, J.-L. 1986: C-slip in quartz from subsolidus deformed granite. *Tectonophysics*, **127**, 97-115.

Bons, P. D. and Urai, J. L. 1992: Syndeformational grain growth: microstructures and kinetics. *Jour. Struct. Geol.*, **14**, 1101-1109.

Bouchez, J. L., Lister, G. S. and Nicolas, 1983: Fabric asymmetry and shear sense in movement zones. *Geol. Rdsch*, **72**, 401-419.

Bouchez, J. L., Mainprice, D. H., Trepied, L. and Doukhan, J. L., 1984: Secondary lineation in a high-T quartzite (Galicia, Spain): an explanation for an abnormal fabric. *Jour. Struct. Geol.*, **6**, 159-165.

Bouchez, J. L. and Pecher, A., 1981: The Himalayan main central thrust pile and its quartz-rich tectonites in central Nepal. *Tectonophysics*, **78**, 23-50

Brun, J.-P. & Cobbold, P. R., 1980: Strain heating in shear zones. *Jour. Struct. Geol.*, **2**, 149-158.

Brun, J.-P. and Pons, J., 1981: Strain patterns of pluton emplacement in a crust under going non-coaxial deformation, Sierra Morena, Southern Spain. *Jour. Struct. Geol.*, **3**, 219-230.

Brunel, M., 1980: Quartz fabrics in shear-zone mylonite: Evidence for a major imprint due to late strain increments. *Tectonophysics*, **64**, T33-T44.

Burg, J.-P., 1986: Quartz shape fabric variations and c-axis fabrics in a ribbon-mylonite: arguments for an oscillating foliation. *Jour. Struct. Geol.*, **8**, 123-131.

Burg, J.-P. and Laurent, P., 1978: Strain analysis of a shear zone in a granodiorite. *Tectonophysics*, **47**, 15-42.

Castro, A., 1986: Structural pattern and ascent model in the Central Extramadura batholith, Hercynian belt, Spain. *Jour. Struct. Geol.*, **8**, 633-645.

Chatterjee, N. D. and Johannes, W., 1974: Thermal stability and standard thermodynamic properties of synthetic 2 M1-muscovite, KAl_2 $[AlSi_3O_{10}(OH)_2]$. *Cont. Mineral. Petrol.*, **48**, 89-114.

Christie, J. M. and Ord, A., 1980: Flow stress from microstructures of mylonites: example and current assessment. *Jour. Geophys. Res.*, **85**, 6253-6262.

Cohen, S. C. and Morgan, R. C., 1986: Intraplate deformation due to continental collisions: a numerical study of deformation in a viscous sheet. *Tectonophysics*, **132**, 247-259.

Corsini, M., Vauchez, A., Archanjo, C. and de Sa, E. F. J.. 1991: Strain transfer at continental scale from a transcurrent shear zone to a transpressional fold belt: The Patos-Serido system, northeastern Brazil. *Geology*. **19**, 586-589.

Coward, M. P., 1983: Thrust tectonics, thin skinned or thick skinned, and the continuation of thrusts to deep in the crust. *Jour. Struct. Geol.*, **5**, 113-123.

Coward, M. P., 1984: The strain and textural history of thin-skinned tectonic zones: examples from the Assynt of the Moine thrust zone, NW Scotland. *Jour. Struct. Geol.*, **6**, 89-99.

Coward, M. P. and Kim, J. H., 1981: Strain within thrust sheets. In "*Thrust and Nappe Tectonics. Spec. Publ., Geol. Soc. London*, **9**, 275-292.

Cumbest, R. J., Drury, M. R., van Roermund, H. L. M. and Simpson, C., 1989: Dynamic recrystallization and chemical evolution of clinoamphibole from Senja, Norway. *Cont. Miner. Petrol.*, **101**, 319-349.

Dallmeyer, R. D. and Takasu, A., 1992: Middle Paleocene terrane juxtaposition along the Median Tectonic Line, southwest Japan: evidence from $^{40}Ar/^{39}Ar$ mineral ages. *Tectonophysics*, **200**, 281-297.

Darot, M., 1974: Cinématique de l'extrusion, a partir du manteau, des peridotites de la Sierra Bermejia (Serrania de Runda, Espagne). *C. R. Acad. Sci. Paris*, **278**, 1673-1676.

Dell'Angelo, L. N. and Tullis, J., 1989: Fabric development in experimentally sheared quartzites. *Tectonophysics*, **169**, 1-21.

Dennis, A. J. and Secor, D. T., 1987: A model for the development of crenulations in shear zones with applications from the Southern Appalachian Piedmont. *Jour. Struct. Geol.*, **9**, 809-817.

Dietrich, D. and Song, H. 1984: Calcite fabrics in a natural shear environment, the Helvetic nappes of western Switzerland. *Jour. Struct. Geol.*, **6**, 19-32.

Dillamore, I. L., Roberts, J. G. & Bush, A. C., 1979: Occurrence of shear bands in heavily rolled cubic metals. *Metal. Sci. Jour.*, **13**, 73-77.

Dodson, M., 1973: Closure temperature in cooling geochronological and petrological systems. *Contrib. Mineral. Petrol.*, **40**, 259-274.

Drury, M. R. and Humphreys, F. J., 1988: Microstructural shear criteria associated with grain-boundary sliding during ductile deformation. *Jour. Struct. Geol.*, **10**, 83-89.

Drury, M. R., Humphreys, F. J. and White, S. H., 1985: Large strain deformation studies using polycrystalline magnesium as a rock analogue. Part II: dynamic recrystallization mechanisms at high temperatures. *Phys. Earth Planet. Inter.*, **40**, 208-222.

Drury, M. R. and Urai, J., 1990: Deformation-related recrystallization processes. *Tectonophysics*, **172**, 235-253.

Echigo, H. and Kimura, T., 1973: Minor geologic structures of the cataclastic rocks, including mylonites, along the Median Tectonic Line in the eastern Kii Peninsula, Southwest Japan. In " *The Median Tectonic Line*", ed. by Sugiyama, R., Tokai University press, 115-137.

Eisbacher, G. H., 1970: Deformation mechanisms of mylonitic rocks and fractured granites in the Cobequid Mountains, Nova Scotia, Canada. *Geol. Soc. Am. Bull.*, **81**, 2009-2020.

Engebreston, D. C., Cox, A. and Gordon, R. G., 1985: Relative motions between oceanic and continental plates in the Pacific basin. *Geol. Soc. Am. Spec. Pap.* 206 pp.

England, P. and Houseman, G., 1986: Finite strain calculations of continental deformation 2. Comparison with the India-Asia collision zone. *Jour. Geophys. Res.*, **91**, 3664-3676.

Etchecopar, A., 1977: A plane kinematic model of fabric development in polycrystalline aggregates: comparisons with experimental and natural examples. *Tectonophysics*, **39**, 121-139.

Etchecopar, A. and Vasseur, G., 1987: A 3-D kinematic model of fabric development in polycrystalline aggregates: comparisons with experimental and Natural examples. *Jour. Struct. Geol.*, **9**, 705-717.

Ferguson, C. C. and Lloyd, G. E., 1982: Paleostress and strain estimates from boudinage structure and their beginning on the evolution of a major Variscan fold —Thrust Complex in southwest England. *Tectonophysics*, **88**, 269-289.

Fitz Gerald, J. D. and Stünitz, H., 1993: Deformation of granitoids at low metamorphic grade. I: Reactions and grain size reduction. *Tectonophysics*, **221**, 269-297.

Flinn, D., 1962: On folding during three dimensional progressive deformation. *Q, Jl Geol. Soc. Lond.* **188**, 358-428.

Fossen, H. and Tikoff, B., 1993: The deformation matrix for simultaneous simple shearing and volume change, and its application to transpression-transtension tectonics. *Jour. Struct. Geol.*, **15**, 413-422.

Fyfe, W. S., Price, N. J. & Thompson, A. B., 1978: *Fluids in the Earth's Crust*. Elsevier, Amsterdam.

Gapais, D., 1989: Shear structures within deformed granites: Mechanical and thermal indicators. *Geology*, **17**, 1144-1147.

Gapais, D., Balè, P., Choukroune, P., Cobbold, P. R., Mahjoub, Y. and Marquer, D., 1987: Bulk kinematics from shear zone patterns: some field examples. *Jour. Struct. Geol.*, **9**, 635-646.

Gapais, D. and Barbarin, B., 1986: Quartz fabric transition in a cooling syntectonic granite (Hermitage Massif, France). *Tectonophysics*, **125**, 357-370.

Goetze, C., 1975: Sheared lherzolites: from the point of view of rocks mechanics. *Geology*, **3**, 172-173.

Goldstein, A. G., 1988: Factors affecting the kinematic interpretation of asymmetric boudinage in the shear zone. *Jour. Struct. Geol.*, **10**, 707-715.

Gordon, P. and Vandermeer, R. A. 1966: Grain boundary migration. In "*Recrystallization, Grain Growth and Textures*", 295-266. Am. Soc. Metals, Metal Park, Ohio.

Guglielmo, G., Jr., 1993: Interference between pluton expansion and non-coaxial tectonic deformation: three-dimensional computer model and field implications. *Jour. Struct. Geol.*, **15**, 593-608.

Guillopè, M. and Poirier, J. P., 1979: Dynamic recrystallization during creep of single-crystalline halite: An experimental study. *Jour. Geophys. Res.*, **84**, 5557-5567.

Hacker, B. R., Yin, A. and Christie, M., 1992: Stress magnitude, strain rate, and rheology of extended middle continental crust inferred from quartz grain sizes in the Whipple Mountains, California. *Tectonics*, **11**, 36-46.

Hammarstrom, J. M. and Zen, E-an., 1986: Aluminum in hornblende: An empirical igneous geobarometer. *Am. Mineralogist*, **71**, 1297-1313.

Hara, I., 1962: Studies on the structure of the Ryoke metamorphic rocks of the Kasagi district, southwest Japan. *Jour. Sci. Hiroshima Univ. Ser. C*, **4**, 163-224.

Hara, I., 1971: An ultimate steady-state pattern of c-axis fabric of quartz in metamorphic tectonites. *Geol. Rundsch.*, **60**, 42-73.

Hara, I., Sakurai, Y., Arita, S. and Paulitsch 1980a: Distribution pattern of quartz in granites —evidence of their high-temperature deformation during cooling. *N. Jb. Miner. Mh. H.*, **1**, 20-30.

Hara, I., Sakurai, Y., Okudaira, T., Hayasaka, Y., Ohtomo, Y. and Sakakibara, N., 1991: Tectonics of the Ryoke belt. *Excursion guide book in 98th Ann. Meet. Geol. Soc. Japan*, 1-20.

Hara, I., Shiota, T., Hide, K., Kanai, K., Goto, M., Seki, S., Kaikiri, K., Takeda, K., Hayasaka, Y., Miyamoto, T., Sakurai, Y. and Ohtomo, Y., 1992: Tectonic evolution of the Sambagawa schists and its implications in convergent margin processes. *Jour. Sci. Hiroshima Univ.*, **9**, 495-595.

Hara, I., Shiota, T., Takeda, K., Okamoto, K. and Hide, K., 1990: Sambagawa Terrane. In "*Pre-Cretaceous Terranes of Japan*" eds. by Ichikawa, K., Mizutani, S., Hara, I., Hada, S. and Yao, A., Publ. IGCP Proj., 137-163.

Hara, I., Shoji, K., Sakurai, Y., Yokoyama, S. and Hide, K. 1980b: Origin of the Median Tectonic Line and its initial shape. *Mem. Geol. Soc. Japan*, **18**, 27-49.

Hara, I., Yamada, T., Yokoyama, S., Arita, M and Hiraga, Y., 1977: Study on the southern marginal shear belt of the Ryoke metamorphic terrain-Initial movement picture of the Median Tectonic Line. *Earth Sci. (Chikyu Kagaku)*, **31**, 204-217.

Hara, I. and Yokoyama, S., 1974: Deformation of Ryoke granitic rocks during the generation of the Median Tectonic Line. *Basement Complex*, **1**, 9-14.

Harada, T. 1890: Die japanishen Inseln, ein topographische geologische Uberschet. Verlag von Paul Parey, 126p.

Harris, L. B., 1985a: Direction changes in thrusting of the schistes Lustrés in Alpine Corsica. *Tectonophysics*, **120**, 37-56.

Harris, L. B., 1985b: Progressive and polyphase deformation of the Schistrés in Cap Corse, Alpine Corsica. *Jour. Struct. Geol.*, **7**, 637-650.

Harrison, T. M., Duncan, I. and McDougall, I., 1985: Diffusion of ^{40}Ar in biotite: Temperature, pressure and compositional effects. *Geochem. Cosmo. Acta*, **49**, 2461-2468.

Haselton, T. H. Jr., Hovis, G. L., Hemingway, B. S. and Robie, R. A. 1983: Calorimetric investigation of the excess entropy of mixing in analbite-sanidine solid solutions: lack of evidence for Na, K Short-range order and implications for two-feldspar thermometer. *Am. Mineralogist*, **68**, 398-413.

Hayama, Y., Miyagawa, K., Nakajima, W. and Yamada, T., 1963: The Kashio Tectonic Zone, Urakawa to Wada area, Central Japan. *Chikyu Kagaku (Earth Science)*, **66**, 23-31.

Hayama, Y. and Yamada, T., 1973: Some considerations on the Median Tectonic Line of the Kashio phase in the light of the Ryoke plutonic history. In "*The Median Tectonic Line*" ed. by Sugiyama, R., Tokai Univ. Press, 1-7.

Hayama, Y. and Yamada, T., 1980: Median Tectonic Line at the stage of its origin in relation to plutonism and mylonitization in the Ryoke Belt. *Mem. Geol. Soc. Japan*, **No. 18**, 5-26.

Hayama, Y., Yamada, T., Ito, M., Kutsukake, T., Masaoka, K., Miyakawa, K., Mochizuki, Y., Nakai, Y., Tainosho, Y., Yoshida, M., Kawaharabayashi, I. and Tsumura, Y., 1982a: Geology of the Ryoke Belt in the eastern Kinki District, Japan — The phase divisions and the mutual relations of the granitic rocks. *Jour. Geol. Soc. Japan*, **88**, 451-466.

Hayama, Y., Yamamoto, H. and Yamada, T., 1982b: Mode of occurrence and genesis of crystalline schists in the Ryuhozan Belt, West Kyushu. *Jour. Geol. Soc. Japan*, **88**, 535-540.

Hayasaka, Y., Hara, I. and Yoshigai, T., 1989: Nappe structure of the Asaji metamorphic rocks , with special reference to geological structure of the basement complexes in Kyushu. *Mem. Geol. Soc. Japan*, **No. 33**, 177-186.

Hayashi, T. and Takagi, H. 1987: Shape fabric of recrystallized quartz in the mylonites along the Median Tectonic Line, southern Nagano Prefecture. *Jour. Geol. Soc. Japan*, **93**, 349-359.

Head, H. C. and Cater, N. L., 1968: Experimentally induced "Natural" intragranular flow in quartz and quartzite. *Am. Jour. Sci.*, **20**, 1-42.

Hippertt, J. F. M., 1993: 'V'-pull-apart microstructures: a new shear-sense indicator. *Jour. Struct. Geol.*, **15**, 1393-1403.

Hirth, G. and Tullis, J., 1992: Dislocation creep regimes in quartz aggregates. *Jour. Struct. Geol.*, **14**, 145-159.

Hobbs, B. E., 1966: Microfabric of Tectonites from the Wyangala Dam Area, New south Wales, Australia. *Geol. Soc. Am. Bull.*, **77**, 685-706.

Hobbs, B. E., 1985: The geological significance of microfabric analysis. In "*Preferred orientation in deformed materials and rocks*", ed. by H.-R. Wenk, Academic Press inc., 463-479.

Hobbs, B. E. and Ord, A., 1989: Plastic instabilities: Implications for the origin of intermediate and deep focus earthquakes. *Jour. Geophys. Res.*, **93**, 10521-10540.

Hollister, L. S. and Crawford, M. L., 1986: Melt-enhanced deformation: A major tectonic process. *Geology*, **14**, 558-561.

Hollister, L. S., Grissom, G. C., Peters, E. K., Stowell, H. H. and Sissopn, V. B., 1987: Confirmation of the empirical correlation of Al in hornblende with pressure of solidification of calc-alkaline plutons. *Am. Mineralogist*, **72**, 231-239.

Holst, T. B., 1985: Implications of a large flattening strain for the origin of a bedding-parallel foliation in the Early Proterozoic Thomson Formation, Minnesota. *Jour. Struct. Geol.*, **7**, 375-383.

Holst, T. B. and Fossen, H., 1987: Strain distribution in a fold in the West Norwegian Caledonides. *Jour. Struct. Geol.*, **9**, 915-924.

Houseman, G. and England, P., 1986: Finite strain calculations of continental deformation 1. method and

general results for convergent zones. *Jour. Geophys. Res.*, **91**, 3651-3663.

Hudleston, P. J. 1983: Strain patterns in an ice cap and implications for strain variations in shear zones. *Jour. Struct. Geol.*, **5**, 455-463.

Hutton, D. H. W., 1982: A tectonic model for the emplacement of the Main Donegal Granite, NW Ireland. *Jour. Geol. Soc. London*, **139**, 615-631.

Hutton, D. H. W., 1988a: Granite emplacement mechanisms and tectonic controls: inferences from deformation studies. *Trans. R. Soc. Edinb. Earth Sci.*, **79**, 245-255.

Hutton, D. H. W., 1988b: Igneous emplacement in a shear-zone termination: The biotite granite at Stroutian, Scotland. *Geol. Soc. Am. Bull.*, **100**, 1392-1399.

Hutton, D. H. W., Dempster, T. J., Brown, P. E. and Becher, S. D., 1990: A new mechanism of granite emplacement: intrusion in active extensional shear zones. *Nature*, **343**, 452-455.

Iglesias Pons de Leon, M. and Choukroune, P., 1980: Shear zones in the Iberian Arc. *Jour. Struct. Geol.*, **2**, 63-68.

Ingles, J., 1983: Theoretical strain patterns in ductile zones simultaneously undergoing heterogeneous simple shear and bulk shortening. *Jour. Struct. Geol.*, **5**, 369-381.

Inoue, T., 1977: Geological studies on the Ryoke metamorphic and granitic rocks in Hakusan-cho, Ichisi-gun, Mie Prefecture. Graduation thesis of Hiroshima university.

Inoue, T., 1979: Petrological studies on the Ryoke metamorphic and granitic rocks in southern part of Nunobuki Mountains, Mie Prefecture. Master thesis of Hiroshima University.

Ishii, K., 1992: Partitioning of non-coaxiality in deforming layered rock masses. *Tectonophysics*, **210**, 33-43.

Ito, M., 1978: Granitic rocks and mylonitization in the Kayumi district Mie Prefecture. *MTL*, **3**, 99-101.

Jaoul, O., Tullis, J. and Kronenberg, A., 1984: The effect of varying water contents on the creep behavior of Heavitree quartzite. *Jour. Geophys. Res.*, **89**, 4298-4312.

Jessell, M. W. 1986: Grain boundary migration and fabric development in experimentally deformed octa-chloropropane. *Jour. Struct. Geol.*, **8**, 527-542.

Jessell, M. W., 1988: Simulation of fabric development in recrystallizing aggregates —II. Example model runs. *Jour. Struct. Geol.*, **10**, 779-793.

Kaikiri, K., Hara, I., Shiota, T., Okamoto, K. and Hide, K., 1991: Strain picture variation in folding history of the Sambagawa belt, central Shikoku. *Abst. 98th Ann. Meet. Geol. Soc. Japan*, 442.

Kanaori, Y., 1990: Late Mesozoic-Cenozoic strike-slip and block rotation in the inner belt of Southwest Japan. *Tectonophysics*, **177**, 381-399.

Kanaori, Y., Yairi, K. and Miyakoshi, K., 1988: Deformation microstructures and their genetic processes of granitic rocks in the northern region of the Atotsugawa fault, central Japan. *Jour. Geol. Soc. Japan*, **94**, 51-55.

Karato, S. and Masuda, T., 1989: Anisotropic grain growth in quartz aggregates under stress and its implication for foliation development. *Geology*, **17**, 695-698.

Katada, M., Isomi, H., Yamada, N., Murayama, M. and Kawada, K., 1968: Geology of Japanese central Alps and its western area. (3). *Chikyu Kagaku (Earth Science)*, **57**, 12-23.

Kerrich, R. and Starkey, J., 1979: Chemical removal of feldspar and layer silicates from quartz-bearing rocks fro X-ray petrofabric studies. *Am, mineralogist*, **64**, 452.

Kholstedt, D. C. and Weathers, M. S., 1980: Deformation-induced microstructures, paleopiezometers and differential stresses in deeply eroded fault zones. *Jour. Geophys. Res.*, **85**, 6269-6285.

Kinoshita, O. and Ito, H., 1986: Migration of Cretaceous magmatism in Southwest Japan related to ridge subduction. *Jour. Geol. Soc. Japan*, **92**, 723-735.

Kinoshita, O. and Ito, H., 1988: Cretaceous magmatism in Southwest and Northeast Japan related to two ridge subduction and Mesozoic magmatism along East Asia continental margin. *Jour. Geol. Soc. Japan*, **94**, 925-944.

Knipe, R. J., 1989: Deformation mechanisms — recognition from natural tectonites. *Jour. Struct. Geol.*, **11**, 127-146.

Knipe, R. J., 1990: Microstructural analysis and tectonic evolution in thrust systems: examples from the Assynt region of the Moine Thrust Zone, Scotland. In *"Deformation Mechanisms in Rocks and Ceramics"*, ed. by Barber, D. J., 228-261, Allen and Unwin.

Kobayashi, T. 1941: The Sakawa orogenic cycle and its bearing on the origin of the Japanese Islands. *Jour. Fac. Sci., Imp. Univ. Tokyo*, (2), **5**, 219-578.

Koch, P. S. and Christie, J. M., 1981: Spacing of deformation lamellae as a paleopiezometer. *Abst. EOS trans. Am., Geophys. Un.*, **62**, 130.

Kocks, P. S., Christie, J. M., Ord, A. and George Jr., R. P., 1989: Effect of water on the rheology of experimentally deformed quartzite. *Jour. Geophys. Res.*, **94**, 13975-13996.

Koshiya, S., 1988: Quartz c-axis fabric and microstructure in mylonite — An application to the Hatagawa Shear Zone, northeast Japan. Jour. *Tectonic Research Group Japan*, **33**, 13-32.

Krohe, A., 1990: Local variations in quartz [c]-axis orientations in non-coaxial regimes and their significance for the mechanics of S-C fabrics. *Jour. Struct. Geol.*, **12**, 995-1004.

Krohe, A. and Eisbacher, G. H., 1988: Oblique crustal detachment in the Variscan Schwarzwald, southwestern Germany. *Geol. Rundsch.*, **77**, 25-43.

Kutsukake, T., Hayama, Y., Honma, H., Masaoka, K., Miyakawa, K., Nakai, Y., Yamada, T. and Yoshida, M., 1979: Geology and petrography of the Ryoke belt in the Shodo-shima Island and the eastern Sanuki region. *Mem. Geol. Soc. Japan*, **No. 17**, 47-68.

Lacassin, R. and Van den Driessche, J., 1983: Finite strain determination of gneiss: application of Fry's method to porphyroid in the southern Massif Central (France). *Jour. Struct. Geol.*, **5**, 245-253.

Law, R. D., Casey, M. and Knipe, R. J., 1986: Kinematic and tectonic significance of microstructures and crystallographic fabrics within quartz mylonites from the Assynt and Eriboll regions of the Moine thrust zone, NW Scotland. *Trans. Roy. Soc. Edinb.: Earth Sci.*, **77**, 99-125.

Law, R. D., Knipe, R. J. and Dyan, H. 1984: Strain path partitioning within thrust sheets: microstructural and petrofabric evidence from the Moine thrust zone at Loch Eriboll, North-West Scotland. *Jour. Struct. Geol.*, **12**, 29-45.

Lee, J., Miller, E. L. and Sutter, J. F., 1987: Ductile strain and metamorphism in an extensional tectonic setting: a case study from the northern Snake Range, Nevada. In "*Continental Extensional Tectonics*" eds. by Coward, M. P., Dewey, J. F. and Hancock, P. L., Geol. Soc. Spec. Publ., **28**, 267-298.

Linker, M. F., Kirby, S. H., Ord, A. and Christie, J. M., 1984: Effects of compression direction on the plasticity and rheology of hydrolytically weakened synthetic quartz crystals at atmospheric pressure. *Jour. Geophys. Res.*, **89**, 4241-4255.

Lisle, R. J., 1984: Strain discontinuities within the Seve-Köli Nappe Complex, Scandinavian Caledonides. *Jour. Struct. Geol.*, **6**, 101-110.

Lister, G. S. 1977: Discussion: Crossed girdle c-axis fabrics in quartzites plastically deformed by plane strain and progressive simple shear. *Tectonophysics*, **39**, 51-54.

Lister, G. S., 1981: The effect of the basal prism mechanism switch on fabric development during plastic deformation of quartzite. *Jour. Struct. Geol.*, **3**, 67-75.

Lister, G. S. and Baldwin, S. L., 1993: Plutonism and the Origin of metamorphic core complexes. *Geology*, **21**, 607-610.

Lister, G. S. and Dornsiepen, U. F., 1982: Fabric transition in the Saxony Granulite terrain. *Jour. Struct. Geol.*, **4**, 81-92.

Lister, G. S. and Hobbs, B. E., 1980: The simulation of fabric development during plastic deformation and its application to quartzite: the influence of deformation history. *Jour. Struct. Geol.*, **2**, 355-370.

Lister, G. S., Paterson, M. S. and Hobbs, B. E., 1978: The simulation of fabric development in plastic deformation and its application to quartzite: the model. *Tectonophysics*, **45**, 107-158.

Lister, G. S. and Price, G. P., 1978: Fabric development in a quartz-feldspar mylonite. *Tectonophysics*, **49**, 37-78.

Lister, G. S. and Snoke, A. W., 1984: S-C mylonite. *Jour. Struct. Geol.*, **6**, 617-638.

Lister, G. S. and Williams, P. F., 1979: Progressive development of quartz fabrics in a shear zone from Monte Mucrone, Sesia-Lanze zone, Italian Alps. *Jour. Struct. Geol.*, **1**, 43-52.

Lloyd, G. E., Ferguson, C. C. and Reading , K., 1982: As tress-transfer model for the development of extension fracture boudinage. *Jour. Struct. Geol.*, **4**, 355-372.

Lloyd, G. E., Law, R. D., Mainprice, D. and Wheeler, J., 1992: Microstructural and crystal fabric evolution during shear zone formation. *Jour. Struct. Geol.*, **14**, 1079-1100.

Mainprice, D. and Bouchez, J.-L., 1987: Characterization of slip systems in naturally deformed quartz by microstructural, X-ray texture goniometry and transmission electron microscopy studies: application to simple fabric types as a function of temperature. In Conference report "*Crystallographic fabrics and deformation histories*", reported by Law, R. D., *Jour. Geol. Soc. Lond.*, **144**, 677. (Abstract)

Mainprice, D. and Nicolas, A., 1989: Development of shape and lattice preferred orientations: application to the seismic anisotropy of the lower crust. *Jour. Struct. Geol.*, **11**, 175-189.

Mancktelow, N. S. 1987: Quartz textures from the Simpson Fault Zone, southwest Switzerland and north Italy. *Tectonophysics*, **135**, 133-153.

Mancel, P. and Merle, O., 1987: Kinematics of the northern part of the Simplon line (Central Alps). *Tectonophysics*, **135**, 265-275.

Maruyama, S. and Seno, T., 1986: Orogeny and relative plate motions-an example of the Japanese islands. *Tectonophysics*, **127**, 1-25.

Masaoka, K., 1987: Structure of granitic rocks of the southern Ryoke belt, Kinki district, Japan. *Jour. Min. Petrol. Econ. Geol.*, **82**, 60-74.

Masuda, T. and Fujimura, A., 1981: Microstructural development of fine-grained quartz aggregates by syntectonic recrystallization. *Tectonophysics*, **72**, 105-128.

Masuda, T., Koike, T., Yuko, T. and Morikawa, T., 1991: Discontinuous grain growth of quartz in metacherts: influence of mica on a microstructural transition. *Jour, Metamorphic Geol.*, **9**, 389-402.

Masuda, T. and Kuriyama, M., 1988: Successive "mid-point" fracturing during microboudinage: an estimate of the stress-strain relation during a natural deformation. *Tectonophysics*, **147**, 171-177.

Means, W. D., 1989: Stretching faults. *Geology*, **17**, 893-896.

Means, W. D., Hobbs, B. E., Lister, G. S. and Williams, P. F., 1980: Vorticity and non-coaxiality in progressive deformation. *Jour. Struct. Geol.*, **2**, 371-378.

Mercier, J. C., Anderson, D. A. and Carter, N. L., 1977: Stress in the lithosphere: Inferences from steady state flow of rocks. *Pure Appl. Geophys.*, **115**, 199-226.

Merle, O., 1989: Strain models within spreading nappes. *Tectonophysics*, **165**, 57-71.

Merle, O. and Guillier, B., 1989: The building of the Central Swiss Alps: An experimental approach. *Tectonophysics*, **165**, 41-56.

Michibayashi, K. and Masuda, T., 1993: Shearing during progressive retrogression in granitoids: abrupt grain size reduction of quartz at the plastic-brittle transition for feldspar. *Jour. Struct. Geol.*, **222**, 151-164.

Miyashiro, A., 1973: Metamorphism and Metamorphic Belts. Allen and Unwin, London.

Molnar, P. and Deng., 1984: Faulting associated with large earthquakes and the average rate of deformation in central and eastern Asia. *Jour. Geophys. Res.*, **89**, 6911-6917.

Nadai, A., 1963: *Theory of Flow and Fracture of Solids*, Engineering Societies Monographs. McGraw-Hill, New York.

Nakajima, T., Shirahase, T. and Shibata, K., 1990: Along-arc lateral variation of Rb-Sr and K-Ar ages of Cretaceous granitic rocks in Southwest Japan. *Cont. Min. Petrol.*, **104**, 381-389.

Nakajima, W., 1960: Geology of the northern margin of the Ryoke zone in the Yamato Plateau. *Chikyu Kagaku (Earth Science)*, **49**, 1-14.

Neubauer, H. F., 1993: Kinematics of crustal stacking and dispersion in the south-eastern Bohemian Massif. *Geol. Rundsh.*, **82**, 556-565.

Nicolas, A. and Poirier, J. P. 1977: *"Crystalline Plasticity and Solid State Folow in Metamorphic rocks"*. Wiley, New York.

Nureki, T., 1960: Structural investigation of the Ryoke metamorphic rocks of the area between Iwakuni and Yanai, southwestern Japan. *Jour. Sci. Hiroshima. Univ. Ser. C*, **3**, 69-141.

Ohira, Y., 1982: Geology of the Ryoke Belt in the northern area of Mt. Takami, central Kii Peninsula, Japan. *Jour. Geol. Soc. Japan*, **88**, 467-481.

Ohtomo, Y. 1987: Structure of the shear zone around the Median Tectonic Line of Sakuma district. *Abst. 94th Ann. Meet. Geol. Soc. Japan*, 314.

Ohtomo, Y. 1988: Mylonitization of the Tenryukyo Granite in the Ryoke metamorphic belt, Central Japan. *Abst. 95th Ann. Meet. Geol. Soc. Japan*, 470.

Ohtomo, Y. 1989: Nappe structures along southern margin of the Ryoke belt around the Aichi-Shizuoka Prefecture border. *Abst. 96th Ann. Meet. Geol. Soc. Japan*, 394.

Ohtomo, Y. 1990: Deformation styles and tectonics of granitic rocks of the Ryoke belt (V) Cataclasite of the Median Tectonic Line. *Chikyu Monthly*, **12**, 473-477.

Ohtomo, Y., 1991: Tectonics of the Ryoke metamorphic belt produced the formation of mylonite zone. *Abst. 98th Ann. Meet. Geol. Soc. Japan*, 314.

Ohtomo, Y. 1993: Origin of the Median Tectonic Line. *Jour. Sci. Hiroshima Univ. Ser. C*, **9**, 611-699.

Okamoto, K., Hara, I. and Suzuki, M. 1989: A preliminary report on geological structure on the Manotani-Higo Metamorphic rocks of the Kosa district, Kyushu. *Mem. Geol. Soc. Japan*, **No. 33**, 187-198.

Okamura, Y., 1960: Structural and Petrological studies on the Ryoke gneiss and granodiorite complex of the Yanai district, southwest Japan. *Jour. Sci. Hiroshima Univ. Ser. C*, **3**, 143-213.

Okudaira, T., Hara, I., Sakurai, Y., Hayasaka, Y. and Sakakibara, N., 1991: Structural analysis of the Ryoke belt in the Iwakuni-Yanai district, Yamaguchi prefecture. *Abst. 97th. Ann. Meet. Geol. Soc. Japan*, 310.

Okudaira, T., Hara, I., Sakurai, Y. and Hayasaka, Y., 1992: Tectonic evolution of the Ryoke belt in the Iwakuni-Yanai district, southwest Japan. *Abst. 98th. Ann. Meet. Geol. Soc. Japan*, 351.

Okudaira, T., Hara, I., Sakurai, Y. and Hayasaka, Y., 1993: Tectono-metamorphic processes of the Ryoke belt in the Iwakuni-Yanai district, southwest Japan. *Mem. Geol. Soc. Japan*, **No. 42**, 91-120.

Ord, A. and Christie, J. M., 1984: Flow stresses from microstructures in mylonitic quartzite of the Moine Thrust zone, Assynt area, Scotland. *Jour. Struct. Geol.*, **6**, 639-654.

Otsuki, K., 1992: Uplifting and shear deformation of high-P metamorphic belt by oblique subduction of plate: and investigation by quasi-3-dimensional lubricant model. *Jour. Geol. Soc. Japan*, **98**, 435-444.

Passchier, C. W., 1984: Mylonite dominated footwall geometry in a shear zone, central Pyrenees. *Geol. Mag.*, **121**, 429-436.

Passchier, C. W., 1985: Water-deficient mylonite zones-An example from the Pyrenees. *Lithos*, **18**, 115-127.

Passchier, C. W., 1986: Mylonite in the continental crust and their role as seismic reflectors. *Geologie en Mijnbouw*, **65**, 167-176.

Passchier, C. W. and Simpson, C. 1986: Porphyroclast systems: a kinematic indicators. *Jour. Struct. Geol.*, **8**, 831-843.

Paterson, S. R., Tobisch, O. T. and Bhattacharyya, T., 1989: Regional, structural and strain analyses of terranes in the Western Metamorphic Belt, Central Sierra Nevada, California. *Jour. Struct. Geol.*, **11**, 255-273.

Paterson, S. R., Vernon, R. H. and Tobisch, O. T., 1989: A review of criteria for the identification of magmatic and tectonic foliation in granitoids. *Jour. Struct. Geol.*, **11**, 349-363.

Platt, J. P. and Behrmann, J. H., 1986: Structures and fabrics in a crustal scale shear zone, Betic Cordieras, SE Spain. *Jour. Struct. Geol.*, **8**, 15-34.

Platt, J. P. and Vissers, R. L. M., 1980: Extensional structure in anisotropic rocks. *Jour. Struct. Geol.*, **2**, 397-410.

Plutonism Research Group of the Hokkaido University, 1964: Tectonics of the metamorphics and granites near the Lake Sakuma, Nagano Prefecture: Tectonics of the Ryoke Metamorphic Belt in the Central Japan — part I. *Jour. Geol. Soc. Japan*, **70**, 446-459.

Poirier, J. P., 1980: Shear localization and shear instability in materials in the ductile field. *Jour. Struct. Geol.*, **2**, 135-142.

Poirier, J. P., 1985: *"Creep of Crystals"*. Cambridge University Press, Cambridge.

Poirier, J. P. and Guillopé, M. 1979: Deformation induced recrystallization of minerals. *Bull. Mineral.*, **102**, 67-74.

Powell, M. and Powell, R., 1977: Plagioclase-alkali feldspar geothermometer revisited. *Mineralogist Mag.*, **41**, 253-256.

Price, G. P., 1985: Preferred orientations in quartzites. In "Preferred *Orientation in Deformed Metals and Rocks*", ed. by Wenk, H.-R., 385-406, Academic Press, Inc., Orland.

Pryer, L. L., 1993: Microstructures in feldspars from a major crustal thrust zone: the Grenville Front, Ontario, Canada. *Jour. Struct. Geol.*, **15**, 21-36.

Rasse, P., 1974: Al and Ti contents of hornblende, indicators of pressure and temperature of regional metamorphism. *Cont. Min. Pet.*, **45**, 231-236.

Ramsay, J. G., 1980: Shear zone geometry: a review. *Jour. Struct. Geol.*, **2**, 83-99.

Ratschbacher, L., 1986: Kinematics of Austro-Alpine Cover Nappes: changing translation path due to transpression. *Tectonophysics*, **125**, 335-356.

Ratschbacher, L., Frisch, W., Neubauer, F., Schmid, S. M. and Neugebauer, J., 1989: Extension in compressional orogenic belts: The eastern Alps. *Geology*, **17**, 404-407.

Ratschbacher, L., Wenk, H.-R. and Sintubin, M., 1991: Calcite textures: examples from nappes with strain-path partitioning. *Jour. Struct, Geol.*, **13**, 369-384.

Ring, U., 1992: The kinematic history of the Pennine Nappes east of the Lepontine Dome: implications for the tectonic evolution of the Central Alps. *Tectonics*, **11**, 1139-1158.

Ruppel, C. and Hodges, K. V. 1994: Pressure-temperature-time paths from two-dimensional thermal models: Prograde, retrograde, and inverted metamorphism. *Tectonics*, **13**, 17-44.

Rutter, E. H., 1972: The influence of interstitial water on the rheological behavior of calcite rocks. *Tectonophysics*, **14**, 13-33.

Rutter, M. J., Van der Laan, S. R. and Wyllie, P. J., 1989: Experimental data for a empirical igneous geobarometer: Aluminum in hornblende at 10 kbar pressure. *Geology*, **17**, 897-900.

Sakakibara, N., 1993: Geological structures of the shear zones developed in the inner area of the Ryoke belt, Kinki, Province. *Abst. 100th Ann. Meet. Geol. Soc. Japan*, 467.

Sakakibara, N. and Hara, I., 1992: Mylonites of the Sakawa granite. *Abst. 99h Ann. Meet. Geol. Soc. Japan*, 334.

Sakakibara, N., Hara, I., Shiota, T., Kanai, K., Kaikiri, K., Hide, K. and Paulitsch, P., 1992: Quartz Microtextures of the Sambagawa schists and their implications in convergent margin processes. *Island Arc*, **1**, 186-197.

Sakakibara, N., Ohtomo, Y. and Hara, I., 1989: Deformation of granitic rocks in the Ryoke belt (I) Deformation styles of quartz. *DELP publication*, **No. 28**, 47-51.

Sakurai, Y. and Hara, I., 1979: Studies on microfabric of granites, with special reference to quartz fabric. *Mem. Geol. Soc. Japan*, **No. 17**, 287-294.

Sakurai, Y. and Hara, I., 1990: Deformation style of the Ryoke granitic rocks and their tectonics. (II) Deformation style of K-feldspar. *Chikyu Monthly*, **12**, 461-465.

Sanderson, D. J., 1982: Models of strain variation in nappes and thrust sheets: a review. *Tectonophysics*, **88**, 201-233.

Schmeling, H., Cruden, A. R. and Marquart, G., 1988: Finite deformation in and around a fluid sphere moving through a viscous medium: implications for diapiric ascent. *Tectonophysics*, **149**, 17-34.

Schmid, S. M., Boland, J. N. & Paterson, M. S., 1977: Superplastic flow in fine grained limestone. *Tectonophysics*, **44**, 233-261.

Schmid, S. M. and Casey, M., 1986: Complete fabric analysis of some commonly observed quartz c-axis patterns. In "*Mineral and rocks deformation: Laboratory studies*" (The Paterson volume), ed. by Hobbs, B. E. and Heard, H. C., AGU, Washington D. C., Geophys. Monogr. Ser., **36**, 263-286.

Schmid, S. M. and Casey, M. and Starkey, J. 1981: An illustration of the advantages of a complete texture analysis described by the orientation distribution function (ODF) using quartz pole figure data. *Tectonophysics*, **78**, 101-117.

Schmid, S. M. and Hass, R., 1989: Transition from near-surface thrusting to intrabasement decollement, Schlinig Thrust, eastern Alps. *Tectonics*, **8**, 697-718.

Schmid, S. M., Panozzo, R. and Bauer, S., 1987: Simple shear experiments on calcite rocks: rheology and microfabric. *Jour. Struct. Geol.*, **9**, 747-778.

Schmid, S. M., Ruck, Ph. and Schreurs, G., 1988: The significance of the Schams nappes for a better understanding of the Paleotectonic and orogenic evolution of the crust along the Earstern Swiss Traverse (abstr.). In: Deep Structure of the Alps. Meet., Paris.

Schmidt, M. W., 1992: Amphibole composition in tonalite as a function of pressure: an experimental calibration of the Al-in hornblende barometer. *Cont. Min. Petrol.*, **110**, 304-310.

Schultz-Era, D. D. and Hudleston, P. J. 1991: Strain in an Archean greenstone belt of Minnesota. *Tectonophysics*, **190**, 233-268.

Sellars, C. M., 1978: Recrystallization of metals during hot deformation. *Phil. Trans. R. Soc.*, **135**, 513-516.

Seo, T. 1985: The study of the Ryoke metamorphism in view of metamorphic history and conditions - as illustrated in the metamorphic terrain of the southwestern part of Mikawa Plateau, Central Japan. *Jour. Sci. Hiroshima Univ. Ser. C*, **25**, 93-155.

Seo, T. and Hara, I. 1980: The development of the schistosity in biotite schists from southwestern part of Mikawa Plateau. *Jour. Geol. Soc. Japan*, **86**, 817-826.

Shi, Y. and Wang, C.-Y., 1987: Two-dimensional modeling of the P-T-t paths of regional metamorphism in simple overthrust terrains. *Geology*, **15**, 1048-1051.

Shimamoto, T., 1989: The origin of S-C mylonites and a new fault-zone model. *Jour. Struct. Geol.*, **11**, 51-64.

Shimizu, I., 1991: Crystal size distribution by dynamic recrystallization. *Abst. 98th. Ann. Meet. Geol. Soc. Japan*, 413.

Shoji, K., Honda, Y., Ohara, S., Otaguro, K. and Ogura, Y., 1992: Discovery of meta-pyroclastics from the eastern part of Kii Peninsula, southwest Honshu. *Japan. Jour. Educ. Mie Univ.*, **43**, 19-31.

Siddans, A. W. B., 1983: Finite strain patterns in some alpine nappes. *Jour. Struct. Geol.*, **5**, 441-445.

Simpson, C., 1980: Oblique girdle orientation patterns of quartz C-axes from a shear zone in the basement core of the Maggia Nappe Ticino, Switzerland. Jour. Struct. Geol., **2**, 243-247.

Simpson, C., 1985: Deformation of granitic rocks across the brittle-ductile transition. *Jour. Struct., Geol.*, **7**, 503-511.

Simpson, C. and Schmid, S. M. 1983: An evaluation of criteria to deduce the sense of movement in sheared rocks. *Geol. Soc. Am. Bull.*, **94**, 1281-1288.

Simpson, C. and Wintsch, R. P., 1989: Evidence for deformation-induced K-feldspar replacement by myrmekite. *Jour. Metamorphic Geol.*, **7**, 261-275.

Stefanick, M. and Jurdy, D., 1992: Stress observations and driving force models for the South American plate. *Jour. Geophys. Res.*, **97**, 11905-11913.

Stormer, J. C., Jr., 1975: A practical geothermometer. *Am. Mineralogist*, **60**, 677-674.

Sugiyama, R. 1939: Studies on the Rocks developed along the So-Called "Median Tectonic Line" Part I. *Jour. Geol. Soc. Japan*, **46**, 169-187.

Takagi, H., 1984: Mylonitic rocks along the Median Tectonic line in Takato-Ichinose area, Nagano Prefecture. *Jour. Geol. Soc. Japan*, **91**, 637-651.

Takagi, H., 1985: Mylonitic rocks of the Ryoke belt in the Kayumi area, eastern part of the Kii Peninsula. *Jour. Geol. Soc. Japan*, **91**, 637.-651.

Takagi, H., 1986: Implications of mylonitic microstructures for the geotectonic evolution of the

Median Tectonic Line, central Japan. *Jour. Struct. Geol.*, **8**, 3-14.

Takagi, H. and Ito, M., 1988: The use of asymmetric pressure shadows in mylonites to determine the sense of shear. *Jour Struct. Geol.*, **10**, 347-360.

Takagi, H., Mizutani, T. and Hirooka, K., 1988: Deformation of quartz in an shear zone of the Ryoke belt —an example in the Kishiwada area Osaka Prefecture—. *Jour. Geol. Soc. Japan*, **94**, 869-886.

Takagi, H. and Nagahama, H., 1987: The Ryoke Belt in the Hiki Hills, northeastern marginal area of the Kanto Mountains. *Jour. Geol. Soc. Japan*, **93**, 201-215.

Takagi, H., Shibata, K., Sugiyama, Y., Uchiumi, S. and Matsumoto, T., 1989: Isotopic ages of rocks along the Median Tectonic Line in the Kayumi area, Mie Prefecture. *Jour. Min. Petrol. Econ. Geol.*, **84**, 75-88.

Takahashi, Y., 1992: K-Ar ages of the granitic rocks in Awaji Island - with an emphasis on timing of mylonitization. *Jour. assoc. Min. Pet. Econ. Geol.*, **87**, 291-299.

Takahashi, Y. and Hattori, H., 1992: Granitic rocks in Awaji Island —with an emphasis on the foliated granites—. *Bull. Geol. Surv. Japan*, **43** (5), 335-357.

Takeshita, T., 1993: Deformation of the forearc region and along the Median Tectonic Line in Southwest Japan during the opening of the Japan Sea: A preliminary report. *Mem. Geol. Soc. Japan*, **No. 42**, 225-244.

Takeshita, T. and Karato, S., 1989: Anisotropy in the Earth formed by plastic flow in rocks. *Jishin*, **42**, 255-269.

Takeshita, T. and Wenk, H.-R., 1988: Plastic anisotropy and geometrical hardening in quartzites. *Tectonophysics*, **149**, 345-361.

Toriumi, M. 1985: Two types of ductile deformation/ regional metamorphic belt. *Tectonophysics*, **133**, 307-326.

Toriumi, M. and Kuwahara, H., 1988: Inhomogeneous progressive deformation during low P/T type Ryoke regional metamorphism in central Japan. *Lithos*, **21**, 109-116.

Toriumi, M. and Masui, M., 1986: Strain in the Sanbagawa and Ryoke paired Metamorphic belts, Japan. *Geol. Soc. Am. Mem.*, **164**, 387-394.

Toriumi, M., Teruya, J., Matsui, M. and Kuwahara, H., 1986: Microstructures and flow mechanisms in regional metamorphic rocks of Japan. *Contrib. Mineral. Petrol.*, **94**, 54-62.

Tsukahara, H. and Ikeda, R., 1991: Crustal stress orientation pattern in the central part of Honshu, Japan —stress province and their origins—. *Jour. Geol. Soc. Japan*, **97**, 461-474.

Tsuneishi, Y., 1970: Geological structure in and around the Matsuzaka area, Mie Prefecture. *Bull. Earthq. Res. Inst.*, **48**, 637-651.

Tullis, J., Christie, J. M. and Griggs, D. T., 1973: Microstructure and preferred orientations of experimentally deformed quartzites. *Bull. Geol. Soc. Am.*, **84**, 297-314.

Tullis, J. and Yund, 1977: Experimental deformation of dry Westly granite. *Jour. Geophys . Res.*, **82**, 5705-5718.

Tungatt, P. D. and Humphreys, F. J., 1981: An in-situ optical investigation of the deformation behavior of sodium nitrate — An analogue for calcite. *Tectonophysics*, **78**, 661-675.

Turner, F. J. 1953: Nature and dynamic interpretation of deformation lamellae in calcite of three marbles. *Am. Jour. Sci.*, **251**, 276-298.

Twiss, R. J., 1977: Theory and applicability of a recrystallized grain size paleopiezometer. *Pure Appl. Geophys.*, **115**, 227-244.

Urai, J. L., Means, W. D. and Lister, G. S., 1986: Dynamic recrystallization of minerals. *Am. Geophys. Union Monogr. Ser.*, **36**, 161-200.

van der Pluijm, B. A., 1991: Marble mylonites in the Bancroft shear zone, Ontario, Canada: microstructures and deformation mechanisms. *Jour. Struct. Geol.*, **13**, 1125-1135.

Vauchez, A., 1987: The development of discrete shear zone in a granite: Stress, strain and changes in deformation mechanisms. *Tectonophysics*, **133**, 137-156.

Weijermars, R., 1991: The role of stress in ductile deformation. *Jour. Struct. Geol.*, **13**, 1061-1078.

Weijermars, R., 1992: Progressive deformation in anisotropic rocks. *Jour. Struct. Geol.*, **14**, 723-742.

Weijermars, R., 1993: Estimation of paleostress orientation within deformation zones between two mobile plates. *Geol. Soc. Am. Bull.*, **105**, 1491-1510.

Wenk, H.-R., Canova, G., Molinari, A. and Kock, U. F., 1989: Viscoplastic modeling of texture development in quartzite. *Jour. Geophys. Res.*, **94**, 17895-17906.

Wilson, C. J. L., 1975: Preferred orientation in quartz ribbon mylonite. *Geol. Soc. Am. Bull.*, **86**, 968-974.

White, S., 1976: The effects of strain on the microtextures, fabrics, and deformation mechanisms in quartzites. *Phil. Trans. R. Soc. Lond.*, **A283**, 69-86.

White, S. H., Burrows, S. E., Carreras, J., Shaw, N. D. and Humphreys, F. J., 1980: On mylonites in ductile shear zones. *Jour. Struct. Geol.*, **2**, 175-187.

White, S. H. & Knipe, R. J., 1978: Transformation- and reaction-enhanced ductility in rocks. *J. geol. Soc. London*, **135**, 513-516.

Wintsch, R. P. and Dunning, J., 1985: The effect of dislocation density on aqueous solubility of quartz and some geological implications. *Jour. Geophys. Res.*, **90**, 3649-3657.

Wyllie, P. J., 1977: Crustal anatexis: an experimental review. *Tectonophysics*, **43**, 41-71.

Yamada, T., Hayama, Y., Kagami, H., Kutsukake, T., Maeno, S., Masaoka, K., Nakai, Y. and Yoshida, M., 1979: Geology of the Ryoke belt in the Sennan district, Osaka Prefecture, Japan. *Mem. Geol. Soc. Japan*, **No. 17**, 209-220.

Yamagishi, H., 1992: Microstructures in Granite S-C mylonites. *Abstract 99th Ann. Meet. Geol. Soc. Japan*, 360.

Yamamoto, H. and Masuda, T., 1987: Horizontal ductile shearing in mylonites of the Ryoke Belt in the Misakubo district, northwest Shizuoka Prefecture. *Abstract 94th Ann. Meet. Geol. Soc. Japan*, 452.

Yamamoto, H. and Masuda, T., 1990: Horizontal ductile shearing in mylonites of the Ryoke Belt in the Misakubo district, northwest Shizuoka Prefecture. *Geosci. Repts. Shizuoka Univ.*, **16**, 25-47.

Yamamoto, H. 1994: Kinematics of mylonitic rocks along the Median Tectonic Line, Akaishi Range, central Japan. *Jour. Struct. Geol.*, **16**, 61-70.

Yokoyama, S., 1979: Distribution patterns of dyke swarms in the Setonaikai region. *Mem. Geol. Soc. Japan*, no.. **17**, 295-302.

Yokoyama, S., 1983: Late Mesozoic to Early Tertiary basic-acidic dyke swarms in the Chugoku-setouchi district. *Jour. Sci. Hiroshima Univ. Ser. C*, **8**, 165-188.

Yoshida, M. and Masaoka, K., 1973: Mylonitic rocks around the Median Tectonic Line in Kinki district, Japan. Part 1. The lithology of mylonitic rocks and their geological situation. In "*The Median Tectonic Line*", ed. by Sugiyama, R., 149-178, Tokai Univ. Press.

Yoshizawa, H., Nakajima, W. and Ishizaka, K., 1966: The Ryoke metamorphic zone of Kinki district, Southwest Japan. Accomplishment of regional geological map. *Mem. Coll. Sci. Univ. Kyoto*, Ser. B, **22**, 437-454.

Nobuo SAKAKIBARA
Department of Earth and Planetary Systems Science, Hiroshima University, Higashi-hiroshima, 724, Japan.